1988

Preparation and characterization of Staphylococcal protein A adsorbents for high performance affinity chromatography

Samuel C. Crowley
Iowa State University

Order Number 8825383

Preparation and characterization of *Staphylococcal* Protein A adsorbents for high performance affinity chromatography

Crowley, Samuel C., Ph.D.

Iowa State University, 1988

U·M·I
300 N. Zeeb Rd.
Ann Arbor, MI 48106

Preparation and characterization of Staphylococcal Protein A adsorbents for high performance affinity chromatography

by

Samuel C. Crowley

A Dissertation Submitted to the

Graduate Faculty in Partial Fulfillment of the

Requirements for the Degree of

DOCTOR OF PHILOSOPHY

Department: Chemistry
Major: Analytical Chemistry

Approved:

Signature was redacted for privacy.

In Charge of Major Work

Signature was redacted for privacy.

For the Major Department

Signature was redacted for privacy.

For the Graduate College

Iowa State University
Ames, Iowa

1988

TABLE OF CONTENTS

GENERAL INTRODUCTION

Introduction

The separation of biomolecules such as proteins, carbohydrates and lipids has classically depended upon differences in their physiochemical properties (1,2,3). Examples of such properties are solubility of the biomolecules in salt solutions and organic solvents, density, size, and the charge-to-mass ratio of the biomolecule (3). Techniques based on these properties include the various precipitation schemes, gel permeation chromatography (GPC), ultrafiltration, electrophoresis and centrifugation (3).

The gross separation of these general classes of biomolecules is relatively simple since they are quite different in their physiochemical characteristics (1). Typically, single contact techniques such as precipitation or liquid extraction are capable of selecting the desired family of biomolecules (3). Within a class, however, physiochemical differences are much smaller, requiring more rigorous schemes to separate the desired components (3). Usually biochemists have approached these situations with multi-dimensional separation schemes involving a variety of mechanisms (2). One disadvantage of this multi-dimensional approach is that it still requires fairly significant differences between physiochemical properties of the desired biomolecules and the other molecules of the matrix (3). Since such differences may not be present, these techniques are not always suitable for the separation of very similar biomolecules.

An alternate approach is the use of a single separation mechanism in a multiple contact process such as high performance liquid chromatography (HPLC) (1,4,5). In addition to the hydrophobic separation mechanisms usually considered, ion-exchange, surface adsorption, size exclusion and mixed mode retention mechanisms are available. These various retention mechanisms allow the application of these single mechanism separations to a wide variety of bioanalytical separations. An example of the selectivity possible with this process is the ability to resolve peptides differing by only one amino acid (6). Unfortunately, in the majority of cases a multi-dimensional pre-separation must first be performed to narrow the range of components in the sample and to simplify optimization of the separation for the analyte (6,7). Such schemes can be tedious and low in sample recovery (2,6,7).

A more selective separation mechanism would simplify biochemical analysis. Biological recognition, or the innate ability of biomolecules to form specific non-covalent complexes with other molecules, is one of the most selective processes known (3). Examples of this type of interaction include antigen-antibody interactions, nucleic acid interactions, lectin-carbohydrate interactions, and enzyme-substrate interactions (2,3). The use of biological recognition as an analytical tool for the quantitation of biomolecules is an accepted practice. Examples of methods based on bioactivity are the various enzyme (8) and immunological assays (9). Typically, these procedures rely on the high selectivity of the bioreagent to bind with the analyte in the sample without a prior separation. Unfortunately, these techniques still

require that the product of the biorecognition reaction be differentiated from the sample matrix in some manner. This is required so that the extent of the biorecognition reaction can be measured without a separation. An example of this differentiation is the formation of a uniquely colored product as a result of the enzyme reaction. This requirement limits the broad application of biorecognition techniques to the relatively few biomolecules in which nature has fortuitously provided such a feature.

To overcome this problem, a more versatile approach is required. The coupling of a selective separation technique based on bioactivity with a general detection method such as UV absorbance has proven quite useful. Examples of this combination of selective separation and universal detection are affinity chromatography, affinity electrophoresis, and affinity ultrafiltration (2). The term "affinity" is used with these techniques to designate that bioactivity is the basis of the separation mechanism (10). As with any separation method, these techniques depend upon the partitioning of the analyte between two phases with the relative enrichment of the analyte in one of the phases (3). In these methods, the bioreagent, referred to as the affinity ligand, is fixed in one of the phases. The analyte is then applied and allowed to partition between the phases. The analyte is preferentially taken up in the ligand phase by virtue of the formation of the affinity complex. This permits the very selective separation of the analyte from the sample and the quantitation of the analyte with a nonspecific technique.

Principles and practice of affinity chromatography

Of the various techniques based on biorecognition, the differential migration processes, specifically affinity chromatography, have been the most popular. The general scheme of an affinity chromatographic separation is presented in Figure 1. In this scheme, the affinity ligand is covalently bound to the stationary phase and a multi-component sample containing the analyte is applied to the column under conditions favoring the formation of the analyte-ligand complex. As this sample flows through the column bed, the affinity ligands bind with the analyte. The nonretained components then elute from the column at the void volume. After the nonretained components have been washed from the column, the eluent conditions are changed so that the analyte-ligand complex dissociates and the analyte elutes from the column. As so described, all affinity chromatograms are fundamentally similar. An initial band containing the nonretained components elutes at the column void volume and is followed by the analyte band eluted as the strong eluent is applied to the column.

The initial step in the development of an affinity chromatographic technique is the selection of an appropriate affinity ligand. This is usually dictated by the bioactivity of the analyte. The possible candidates for an affinity ligand are limited to the relatively few molecules capable of forming noncovalent complexes with the analyte. Once the possible ligands have been selected, the characteristics of the analyte-ligand complex as well as the cost, availability and stability of the proposed affinity ligand must be considered (2).

Figure 1. Separation scheme for affinity chromatography with biospecific elution

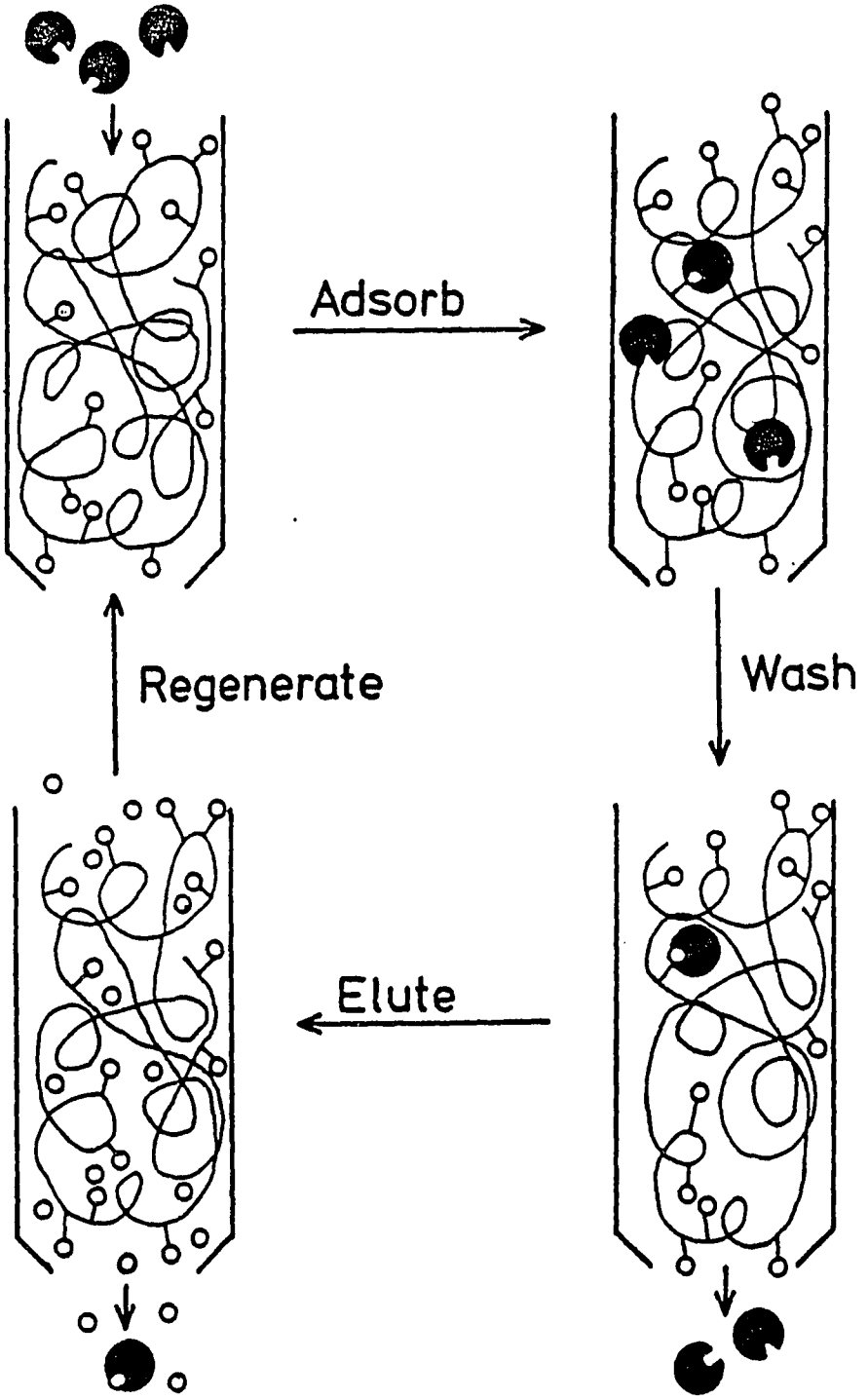
Adsorb
Wash
Elute
Regenerate

Examples of commonly used affinity ligands are enzyme cofactors and inhibitors, sugars, proteins and nucleic acids.

Affinity ligands can usually be divided into two types: general and specific (2,11). The general ligands exhibit an affinity for an entire class of biomolecules. Examples of these ligands include enzyme cofactors, such as NAD, and lectins, such as Concanavallin A. Synthetic dyes have proven useful as general ligands with some analytes (12). These general ligands retain all components of the sample with an affinity for the ligand and will coelute these components. The second type, the specific affinity ligands, exhibit an affinity for a single analyte molecule, eluting the analyte in a highly purified form (13,14). Good examples of such specific affinity ligands are antibodies. These are immunoglobulin (Ig) proteins produced by many animals in response to the presence of a foreign species, or antigen. These Ig proteins are capable of complexing the antigen to which they were prepared to facilitate the removal of the antigen from the body. As such, these Ig proteins can be used as affinity ligands for many analytes for which suitable affinity ligands are not available (13-15).

After the affinity ligand has been selected, the next step is to choose the support to be used. Several criteria for an affinity support have been described (2,16). As with any chromatographic support, the mechanical rigidity must be sufficient to withstand the eluent pressure and flow requirements. The support should also be inert, with the affinity interaction being the only retention mechanism operating in the column. To meet this requirement, nonionic and

hydrophilic materials with sufficient pore size to minimize size exclusion phenomena are used. It must be possible to "activate" this support so that the affinity ligand may be immobilized on it.

The chromatographic efficiency required by the separation must also be considered. Generally, the specificity of the retention mechanism is sufficient so that resolution is not a problem. Rather, the efficiency is required to obtain the desired separation speed and band volume. Preparative techniques require high sample loadings, but speed and bandwidth may be compromised to permit the use of a less costly support material in a "low performance" chromatographic technique. These requirements are met with polysaccharide supports. Examples of such supports are cellulose, dextran and agarose, which have typically been used in preparative affinity chromatography techniques (2,13).

In some experimental situations, greater chromatographic efficiency and speed are required than can be provided with these low performance supports (17). To meet these requirements, dual composition supports have been prepared. These supports are a combination of two phases, one providing mechanical rigidity and the other minimizing nonspecific adsorption and providing sites for the attachment of affinity ligands. Silica supports have been modified to meet these criteria (18). These materials are made nonadsorptive by forming a covalently bound hydrophilic coating over the silica base. To form this coating, the silica surface is first derivatized with glycidoxypropyltrimethoxysilane (GOPS) and the epoxy group opened to

form a glycerol layer over the silica. This glycerol layer is similar to the polysaccharide materials with respect to reactivity and adsorptive characteristics. Typically, these supports have been used for analytical studies and mechanistic studies of the affinity chromatographic process (17,19,20) where the separation efficiency must be high.

The third step in the design of an affinity separation is the immobilization of affinity ligands onto the solid support (2,17). The most common immobilization chemistries use an activation reagent to couple an amine group from the ligand to a hydroxyl group of the solid support. The cyanogen bromide activation of the support linking the ligand through an isourea group has been the most popular technique (11,17). However, this group is relatively unstable, allowing ligand to "leak" from the support. Also, the isourea group is charged and introduces an ionic site to the support and, thus, the possibility of a nonspecific retention mechanism (2,11). To overcome these problems, several alternatives to the cyanogen bromide method have been developed. Some of these immobilization reagents are 1,1'-carbonyl-diimidazole (CDI) (21), tresyl chloride (22), and Schiff's base intermediate (23). In each case the covalent bond formed between ligand and support is stable, retaining the ligand on the support and presenting minimal nonspecific adsorption problems. Generally, the activation of a support with any of these methods is a simple procedure.

The availability of these various immobilization chemistries is important. The immobilization method used can have a dramatic effect

on the activity of the affinity ligand. For example, the activity of immobilized Protein A has been observed to vary greatly with the immobilization chemistry (24,25). At present this effect is not well understood. This requires that the optimum immobilization method for an affinity ligand be determined empirically.

Once the immobilization chemistry has been chosen and the affinity support prepared, the support can then be packed in a suitable column and prepared for use. This requires the determination of proper sample application and elution conditions. The sample must be applied to the column under eluent conditions favoring the formation of the affinity complex. This requires that the eluent pH and ionic strength be proper to maintain activity of the analyte and ligand and that any cofactors needed for activity be included in the eluent. Finally, the chromatograph must be operated so that sufficient time is permitted for the affinity interaction to occur (24).

Two general schemes have been developed for elution of the analyte from the column (2,17). The use of a denaturing reagent in the eluent to disrupt the affinity complex and elute the analyte is the most common elution technique (2,14). Examples of denaturing eluents are low pH buffers, chaotropic salt solutions and organic solvents. In using these eluents care must be taken not to irreversibly denature the affinity ligand (14). Biospecific elution is the second general elution technique. In this case, illustrated in Figure 1, a second biomolecule having an affinity for either the affinity ligand or analyte is added to the eluent. This second biomolecule is referred to

as the inhibitor. As this eluent is applied to the column, a complex equilibrium is established as both the analyte and inhibitor compete for available affinity ligand sites (19,20,26). With this situation, the analyte is displaced from the stationary phase and eluted from the column. Limitations of this type of elution include the lack of availability of a suitable inhibitor for many affinity systems and isolation and detection problems caused by coelution of the analyte and inhibitor (2).

History and development of affinity chromatography

One of the first reports of an affinity chromatographic separation was the purification of α-amylase (27) This work, in which insoluble starch served as both the affinity ligand and the solid support, was reported by Starkenstein in 1910. The first rationally designed affinity chromatographic separation was reported in 1951 by Campbell et al. (28). In this work, antibody was recovered from blood serum with an immobilized antigen column. The affinity support was prepared specifically for this work by covalently bonding the antigen ligand to the cellulose matrix.

In 1953 the concepts and application of affinity chromatographic procedures were extended by Lerman (29). He proposed the use of both specific affinity ligands, such as antigens, antibodies, enzyme substrates or enzyme cofactors, and general affinity ligands, such as azo-dyes. Additionally, he proposed the use of both biospecific elution and nonspecific elution techniques to recover analyte from the

column. Unfortunately, the cellulose supports available at the time had poor chromatographic properties. Also, the ligand immobilization chemistry was not sufficiently developed (2) to permit the simple covalent attachment of a wide range of ligands while maintaining the inert nature of the support.

The development of beaded agarose supports for GPC (30) and the introduction of the cyanogen bromide immobilization method (31) during the mid-1960s overcame most of the experimental limitations. In 1968 Cuatrecasas used these advances to produce methods for the affinity chromatographic preparation of staphyloccal nuclease, α-chymotrypsin, and carboxypeptidase from their respective biological sources (16). Also in this study he proposed the term "affinity chromatography" to describe this technique. This report marked the advent of the modern era of affinity chromatographic separations. By 1971 over 100 applications of the technique had been reported, most using the technique as a preparative tool.

The first text devoted to affinity chromatographic techniques was written by Dean and Lowe and appeared in 1974 (32). As the scope of the field enlarged, several variations of the technique developed and nomenclature soon became troublesome. To address this problem, a section of the 1975 Enzyme Engineering Conference suggested that the general term "affinity chromatography" be used to describe the technique (10). Interest in affinity chromatography continues today with several suppliers offering ready-to-use affinity supports for a number of applications.

The purification of biochemicals remains the most common application of affinity chromatography at present. Using affinity chromatography, dramatic purifications of biochemicals have been reported with relatively simple experimental procedures. In addition to preparative uses, affinity chromatography has also been used to quantify analytes from biological matrices. Glycosylated hemoglobin in serum (11), proteins in urine (17), and IgG in serum (33) have been determined with affinity techniques. These applications are characterized by minimal sample preparation prior to chromatographic analysis and relatively clean chromatograms. A variation of these uses is an affinity-based sample preparation where both removal of sample components and concentration of the analyte are possible. An example of this type has been described for the determination of aflatoxins (34). An antibody specific for aflatoxins B(1) and B(2) was prepared and immobilized. This affinity support was then packed in a short column. With this type of column a large sample volume may be applied and eluted in a small volume of strong eluent, in this example, methanol. The analyte, once recovered, is then assayed with the standard protocol for aflatoxins. The affinity pre-separation resulted in cleaner chromatograms as well as enhanced sample recovery and limit of detection for aflatoxin.

The development of high performance supports has produced dramatic advances in liquid chromatographic techniques in the last two decades. The improvements in chromatographic speed and efficiency have resulted in better resolution of analyte from sample components and enhanced

sensitivity of detection with shorter analysis times. Additionally, these techniques have proven to be easily automated with small computers, greatly simplifying chromatographic analysis.

The application of these high performance supports to affinity chromatography was limited by the adsorptivity of these supports. The development of glycidoxypropyltrimethoxysilane derivatization of silica supports by Regnier to produce a nonadsorptive hydroxyl surface for size exclusion chromatography ameliorated the nonspecific adsorption problem (18). The initial report of the combination of an affinity-based separation with HPLC equipment was by Ohlson in 1978 (35). In this work, horse liver alcohol dehydrogenase and soybean trypsin inhibitor were separated from the respective sample matrix with analysis times under five minutes.

To designate this combination of affinity separation mechanism and HPLC equipment, the term High Performance Affinity Chromatography (HPAC) has been used (36). Applications of HPAC have been described for the determination of both albumin and immunoglobulin G in human serum (33). This work demonstrated the analytical application of very short columns (less than one cm) for HPAC separations based on the tremendous selectivity of the affinity mechanism (36). HPAC has also been used for the fundamental study of biochemical interactions (19,24,37,38). The improved chromatographic efficiency of HPAC compared to regular affinity chromatography has allowed the chromatographic estimation of kinetic as well as thermodynamic parameters, which had not been possible with the low performance supports (19).

As currently developed, affinity chromatographic techniques have been applied to many aspects of biochemistry. The preparative use of affinity chromatography remains the most commonly encountered form of the technique. Although fundamentally similar, analytical applications generally require the use of high performance supports. The analytical applications allow for more rigorous elution than is possible with preparative applications since the retention of activity by the analyte is not important. Limiting this is the need to maintain the activity of the affinity ligand. Antibody ligands are excellent candidates for this type of elution as they can be successfully renatured many times (39). In addition, affinity chromatography can be used for the study of fundamental biochemical interactions. Here the unique properties of the chromatographic approach may simplify the design of the desired experiment (37).

The Protein A-Immunoglobulin affinity interaction

Protein A is a bacterial cell wall protein isolated from Staphylococcal aureas (40). This protein is capable of forming non-covalent affinity complexes with many immunoglobulin proteins (40,41). The unique properties of both Protein A and the immunoglobulins have generated much interest in the use of these proteins as analytical (33) and preparative reagents (42). Examples of applications involving these proteins include such diverse areas as preparative chromatographic techniques (43) and immunoassay techniques (44-46). The following is a brief description of both Protein A and the immuno-

globulins and the resulting affinity complex formed between these proteins.

Protein A is found in many strains of the staphylococcus bacterium, although the Cowen I strain has been the most commonly used source (45). The coverage of Protein A on the cell surface of the bacterium has been estimated to be 80,000 molecules Protein A per cell (47). Assuming a bacterial cell diameter of two micrometers, or a surface area of 3.1 square micrometers per cell, this represents 25,700 Protein A molecules per square micrometer. Protein A is recovered from S. aureus with a heat extraction process and purified with size exclusion and ion exchange chromatography (40). Protein A is a very rugged molecule capable of retaining activity through treatments as extreme as pH 2, urea, thiocyanate, guanidinium HCl, heat and aqueous ethylene glycol (48).

Protein A has a molecular weight of 42 kD, an isoelectric point of 5.1 (49), and a diffusion coefficient of 4.3×10^{-7} cm^2/sec. The hydrodynamic data are a Svedberg constant of 2.1 S, a Stokes radius of 5.0 nm, and a specific volume of 29 mL/g. These values are indicative of a larger protein than indicated by the molecular weight (50). Protein A is also known to have an f/f_{min} ratio of 2.1, indicating an extended or rodlike shape, which would explain the apparently anomalous data regarding molecular size (51).

The structure of Protein A is composed of five subunits arranged in a linear fashion. The C terminal subunit is a cell wall anchoring

unit and the four remaining subunits are approximately homologous and are each capable of complexing or binding one immunoglobulin molecule (52). The intact protein molecule, however, binds less than the optimal four immunoglobulin molecules. This reduced binding capacity is probably due to steric hindrance (53).

The immunoglobulin (Ig) proteins or antibodies are produced by the humoral immune systems of many animals in response to the presence of a foreign species and are responsible for eliminating foreign species from the body. Examples of the foreign bodies (or antigens) which can initiate the production of antibodies are peptides and proteins from phylogenetically different organisms.

The ability of modern immunization techniques to prompt the immune system to produce a protein capable of specifically binding another molecule is a valuable tool. This type of methodology potentially allows for the custom biosynthesis of a bioreagent for virtually any analyte of a biological origin. Once a sufficient quantity of analyte (usually a few milligrams) has been prepared, it is possible to induce antibody production. With this approach, the analyte becomes the antigen responsible for inducing the production of the antibody. Macromolecular analytes are naturally antigenic. Smaller analytes may be made antigenic through coupling with a naturally antigenic carrier molecule. As antibodies bind to only a small region, or epitope, of the antigen, some of the antibodies induced by this hybrid antigen will be capable of binding the native analyte. The immune system will prepare several unique antibodies against a single antigen. This is

referred to as the avidity of the antibody and such preparations are referred to as polyclonal (54). By using current cell culture techniques, it is possible to select for the production of just one of these immunoglobulins, allowing for more homogeneous properties of the antibody reagent (55). Mammals may produce up to five general classes of immunoglobulins: IgG, IgA, IgM, IgD and IgE (41). Of these, IgG is the most often produced and used as an antibody reagent (41).

The physiochemical properties of the IgG immunoglobulin class have been reported. These include a molecular weight of about 153 kD, a diffusion constant of approximately 4 x 10^{-7} cm^2/sec, a Svedberg constant of 6.6 to 7.2 S, an intrinsic viscosity of approximately 0.06, a partial specific volume of about 0.739 mL/g, an f/f_{min} ratio of about 1.38 and an isoelectric point between 5.8 and 7.3 (56). These values are characteristic of a large globular protein (50). The wide range of isoelectric points and other physiochemical properties given is indicative of the heterogeneity of the primary structure of these proteins. This heterogeneity arises from small regions of the Ig molecule which are variable in their amino acid sequence, allowing for the production of antibodies capable of binding to a wide variety of different antigens.

Structurally, the IgG molecule can be divided into three major regions. Two of these are the Fab regions, where the actual antigen binding occurs. Both of these regions are identical, and the native antibody is bivalent with respect to antigen binding. The actual binding occurs at the amino terminal end of the Fab regions where the

amino acid sequences of each individual type of antibody are variable (54). The third region of the IgG protein is the Fc region; this region is the home of the site which interacts with the complement system to effect removal of the antigen from the body. The Fc region is also where Protein A binds with the immunoglobulin protein (52).

The interaction of Protein A and immunoglobulin proteins to form a noncovalently bound complex has been widely studied. Protein A was initially reported to bind exclusively with IgG (43), but further studies have demonstrated that it also binds with various mammalian and avian IgM (57), IgA (58) and IgE (59) proteins. Often a species may exhibit distinct types or subclasses of each of these immunoglobulin proteins through variations in the Fc region which can affect the formation of Protein A-IgG. In humans four such IgG subclasses have been demonstrated (54). Of these, IgG3 is the only one which does not complex with Protein A (41,43,60). This subclass represents only seven to ten percent of the total amount of human IgG protein (60). Rabbit IgG has not been shown to demonstrate such subclass variation with Protein A binding (41). This makes rabbit IgG a good selection for fundamental studies of the Protein A-IgG interaction (24,37). Regardless of the type of immunoglobulin protein used to complex with the Protein A, the complex forms readily in solutions of pH 7-7.4 and dissociates readily in an acidic solution (40,41,43). However, the pH at which dissociation occurs tends to be unique to each immunoglobulin. This has been used to separate subclasses of human IgG and guinea pig IgG with a pH gradient (60,61). Dissociation of the Protein A-IgG

complex is also possible with urea, guandinium HCl, high molarity neutral salts, ethylene glycol and lithium diiodosalicylate (55).

The formation of the Protein A-IgG complex at neutral pH values is highly favored. Affinity or equilibrium constants (K_{eq}) of this reaction have been variously reported to be 3×10^6 to 1×10^{10} M^{-1} (55). Experimental observations have indicated that the intact Protein A molecule is bivalent with respect to IgG (53). The affinity constant for each of the two IgG binding sites has been reported as 2.3×10^8 M^{-1} and 6.4×10^6 M^{-1} (62). This difference in K_{eq} for the two sites demonstrates a negative cooperativity in the binding of IgG to Protein A. The overall K_{eq} for both adsorption steps has been determined experimentally as 4.1×10^8 M^{-1} (62).

The kinetics of the association process have been studied. Usually, such studies involve the complexation of immobilized Protein A with radioactively labeled IgG. A study of the association of IgG onto killed S. aureau bacteria with an excess of active Protein A on the cell surface has reported very fast initial binding of 74 and 81% of initially free IgG at 10 and 30 sec, respectively. Maximum uptake was attained in two minutes (45). Similar data have been obtained for IgG covalently bound to paper disc and Protein A adsorbing from solution. At an excess of IgG ligand sites, the adsorption was found to be greater than 90% complete in three minutes, with a maximum yield attained in 15 minutes (62). In such experiments, as smaller excesses of ligand are used, the time required for equilibration increases to several hours (62). Conversely, the adsorption of IgG by immobilized

Protein A in an affinity chromatographic configuration has been observed to be rapid, probably due to the large excess of ligand used with this technique (63).

When sufficient IgG is used to saturate the Protein A column, incomplete adsorption of IgG results. Incomplete adsorption has also been observed when high eluent flow rates are used even with an excess of ligand (24,38). In this phenomenon an injection of pure analyte results in two peaks, one that is retained on the column and one that is not. It has been shown that this is a kinetic adsorption problem, or that the column residence time was too short for all of the applied IgG to interact with the ligands on the column. It has also been shown that the relative size of the retained fraction is proportional to the residence time and that this relationshp can be used to study the adsorption kinetics of the system. Using this approach, known as "split-peak" chromatography, the association rate for the binding of rabbit IgG to Protein A has been estimated as 2.4×10^5 M^{-1} sec^{-1} (24).

The dissociation of the Protein A-IgG complex has been similarly studied using killed Staphylococcus a bacteria. In this study, Protein A sites on the bacterium were saturated with labeled IgG and the progress of the dissociation of the affinity complex was followed as label was lost from the bacteria. In neutral pH solutions, at equlibrium less than five percent of the IgG was in solution at 90 minutes at 37°C (44). In another set of studies, the same workers found the complex dissociation rate to be 4.8×10^{-5} sec^{-1}, thus demonstrating the dynamic nature of the Protein A-IgG complex. It has

also been shown that when an acidic solution (pH 5) is applied to the complex, 75% of the bound IgG is dissociated in one hour. This demonstrates the ability of acidic conditions to dissociate the Protein A-IgG complex. The bioselective dissociation of IgG has been similarly studied. The presence of free solution IgG, in excess, has been shown to result in the dissociation of 85% of bound labeled IgG in one hour (43). In this situation, once a dissociation of labeled ligand occurs, mass action favors the adsorption of unlabeled IgG over the readsorption of labeled IgG. These results indicate that the stability of the complex is at least partially due to the rapid readsorption of dissociated IgG onto the Protein A ligand.

Outline of the Experimental Sections

The main goal of this work is to study the application and optimization of HPAC techniques. Both experimental and theoretical aspects of the design of an affinity separation will be examined with respect to the use of protein affinity ligands. Immobilized Protein A is used throughout the work as an example of such a macromolecular affinity ligand. The Protein A-IgG affinity interaction has been previously proposed as a model system for the study of protein-protein non-covalent complex formation (24,37,48) and is used here to demonstrate the suitability of HPAC for use with macromolecular ligands and analytes.

The application of HPAC techniques to the analysis of biological samples would combine the selectivity of the bioactivity methods with

the simple, direct quantitation offered by spectrophotometry. The affinity separation mechanism promises a minimum of preseparation sample preparation coupled with the simplicity of an HPLC apparatus, eliminating many manipulations and permitting shorter analysis times. An example of one HPAC quantitative method is given in Section I, where the IgG protein is separated from a human serum matrix with an immobilized Protein A ligand.

The preparation and properties of immobilized protein ligands in high performance affinity chromatography is an important aspect of the development of any HPAC separation. A few of the various immobilization chemistries are presented in Section II with emphasis on the use of 1,1'-carbonyldiimidazole (CDI) for the covalent attachment of protein ligands to diol-bonded silica suppports. Experimental conditions for the optimal yield of several immobilized protein ligands are also described. Additionally, the ability to control the yield of protein immobilization so that an affinity support can have defined characteristics is demonstrated. The effect of immobilization conditions on the properties of the resulting immobilized protein were also examined.

The kinetics of analyte dissociation from an affinity support are an important characteristic of an affinity separation (17). The complex must be sufficiently stable to be retained on the support while capable of being eluted in some manner. Thus, not only are the kinetics of the native dissociation processes important, the kinetics of the denaturing dissociation processes are similarly important

(44,45). The Peak Decay (PD) model is a special case of the more general affinity chromatographic models and was designed specifically for the study of biocomplex dissociation processes (37). The PD model is designed to negate any readsorption of the analyte once dissociation has occurred so that the elution is strictly a function of the affinity complex dissociation. This model is amenable to the study of both the naturing and denaturing dissociation processes, and has been successfully applied to the study of the Con-A sugar interaction (64). The application of the PD model to the study of the Protein A-IgG interaction is described in Section III and the kinetic parameters of both biospecific and low pH elution are reported for this affinity system.

SECTION I.

DETERMINATION OF IMMUNOGLOBULINS IN BLOOD SERUM BY HIGH PERFORMANCE AFFINITY CHROMATOGRAPHY

SUMMARY

High performance affinity chromatography columns were prepared by immobilizing Protein A from Staphylococcus aureus on 10 μm diol-bonded silica. Immunoglobulin-containing samples were injected into the column at pH 7 and the nonretained components eluted. The retained immunoglobulins were then eluted by a step change to pH 3. The retention characteristics of the Protein A column were studied with the chromatography of immunoglobulin G, A, and M standards as well as electrophoresis and Ouchterlony double diffusion immunoassay of both retained and nonretained serum fractions. Retention of IgG1, IgG2 and some IgA was shown. IgM, some IgA and albumin were not retained indicating that nonspecific adsorption was not a significant problem. Analysis of 3 μL samples of reference blood sera without pretreatment was performed using immunoglobulin G standards. Good agreement was observed between the immunoglobulin G concentrations measured by this method and by radial immunodiffusion. Chromatographic analysis times were 4 min or less.

INTRODUCTION

High performance affinity chromatography (HPAC) is potentially useful for the analysis of complex samples such as biological fluids with a minimum of sample pretreatment. Relatively nonspecific detection methods, such as UV absorbance, can be used if the selectivity of the affinity chromatography column is sufficient.

One application of clinical interest is the determination of immunoglobulins in blood serum. There are five known classes of immunoglobulins: immunoglobulin G, A, M, D and E (IgG, IgA, IgM, IgD, IgE). Of these five, only the first three are usually found in significant concentrations in blood serum (Table I). The concentrations of the immunoglobulins are altered by many diseases (1). Common methods for measuring immunoglobulins include electrophoresis, radial immunodiffusion (RID), immunoelectrophoresis, nephelometry and radioimmunoassay (1-3). HPAC methods for quantitating immunoglobulins should be inexpensive, since the immobilized ligand is reused, as well as simple and rapid.

Immobilized antibodies specific for certain classes or subclasses of the immunoglobulins could be used as the affinity ligand for HPAC determinations. We have chosen to immobilize a more general ligand, Protein A from Staphylococcus aureus, for the determination. Protein A is known to bind with the Fc region of IgG1, IgG2 and IgG4 (4,5). IgG3, a subclass which normally constitutes 7-9% of the total IgG (6,7), does not react with Protein A (4-6). The subclasses of IgG have

Table I. Immunoglobulin concentrations in blood serum

Immunoglobulin	Molecular weight	Normal concentration (mg/mL)
IgG	150,000	7.1-15.3
IgA	160,000	0.6- 4.9
IgM	900,000	0.4- 2.1

been partially separated by Protein A affinity chromatography using a pH gradient (6). It initially was believed that Protein A only bound to IgG (5), but more recent studies have shown that it also binds to at least some subclasses of IgA (4,8), IgM (8,9) and IgE (10).

Table I lists the concentrations of several immunoglobulins in blood serum (2). Since Protein A binds to most of these immunoglobulins, immobilized Protein A should be useful for the determination of the immunoglobulin content of blood serum. Immunoglobulins retained by the Protein A ligand can be eluted by a change in buffer from neutral to acidic pH (5,6,9).

EXPERIMENTAL

Reagents

Antihuman IgA, antihuman IgM and antihuman serum albumin antisera as well as Protein A, human serum albumin (HSA) and human immunoglobulin G were obtained from Sigma (St. Louis, MO). Agarose was from Bio-Rad (Richmond, CA). Reference blood sera were obtained from Hyland (Deerfield, IL). Human immunoglobulin A (98%) and human polyclonal immunoglobulin M (98%) came from Calbiochem-Behring (San Diego, CA). HPLC-grade phosphoric acid, 85%, was obtained from Fisher (St. Louis, MO). Antiserum to human IgG1, IgG2, IgG3, and IgG4 were from Miles Laboratories (Elkhart, IN).

Apparatus

The chromatographic system was described previously (11). A Bio-Rad 1420B power supply and 155 tube gel cell were used for electrophoresis.

Methods

LiChrospher SI4000 diol-bonded silica was synthesized and activated with 1,1'-carbonyldiimidazole as described previously (11) with the following modification: 0.050 mL (3-glycidoxypropyl)trimethoxysilane were used per gram of silica.

Activated silica (0.6 g) was shaken at 4°C with 1.1 mg Protein A in 50.0 mL 0.1 M sodium phosphate buffer, pH 8.0. After 24 h, 33 µL ethanolamine were added and the mixture shaken for an additional 24 h to remove any remaining active groups. The immobilized Protein A was

washed with 2 M NaCl and water and then was slurry-packed into a 5.0 cm x 4.6 mm i.d. column at 2700 psi using 0.1 M potassium phosphate buffer, pH 7.0.

Chromatography was performed at room temperature. Reference blood sera were injected without pretreatment using 3 µL or 10 µL sample loops. Immunoglobulin G standards were prepared in the pH 7.0 buffer described below. The weak mobile phase was 0.1 M potassium phosphate buffer, pH 7.0, prepared using HPLC-grade H_3PO_4 and reagent grade KOH. The strong mobile phase was 0.1 M potassium phosphate, pH 3.0, prepared using reagent grade KH_2PO_4 and KOH. Detection was by UV absorbance at 280 nm. All separations were performed at a flow rate of 1.0 mL/min. Samples were injected into the pH 7.0 mobile phase. Retained proteins were eluted by a step change to the pH 3.0 buffer.

Retained and nonretained peaks were collected from repeated injections and concentrated using an Amicon 12 ultrafiltration chamber and PM 30 membranes (Lexington, MA). The concentrated fractions were resuspended in pH 7.0 buffer and concentrated a second time. Samples of the concentrated fractions (20-100 µL) were examined by electrophoresis and qualitative immunoassay studies.

Sodium dodecyl sulfate polyacrylamide gel electrophoresis (SDS-PAGE) was performed using 7% discontinuous gels at pH 8.9 according to a published procedure (12) which was modified to include 0.1% SDS in solution #1 and the electrode buffer solution. Gel tubes of 10 cm x 5 mm i.d. were used. The gels were stained with Coomassie Brilliant Blue

R-250 (Eastman Kodak, Rochester, NY). Bovine serum albumin, IgG, IgA and conjugated BSA molecular weight standards (66,000-264,000D) (all from Sigma) were used as reference standards.

The immunological characterization of the fractions was performed by the method of Ouchterlony double diffusion (13). To improve adhesion of the agarose gel, the slides were pre-coated with 0.1% agarose and dried. A 1% agarose solution made up in 0.1 M phosphate, pH 7, and 0.9% sodium chloride was applied to a depth of 2 mm over these slides and allowed to set. A circular pattern of six wells about a central well was chosen. Both retained and nonretained fractions were assayed for the presence of IgG1, IgG2, IgG3, IgG4, IgM, IgA and HSA. Aliquots of the eluent fractions (20-200 µL) were placed in the central well with the various antisera in the perimeter wells. The gels were placed in a humidity chamber where the diffusion process and precipitation reaction were allowed to progress for four to six days. The gels were washed three times with 0.9% sodium chloride to remove nonprecipitated proteins. The precipitated proteins were stained with Coomassie Brilliant Blue and the gels preserved by drying.

RESULTS AND DISCUSSION

To utilize Protein A for clinical analysis, it clearly is important to know its specificity of binding. We examined this by testing the retention of several immunoglobulin classes on our HPAC columns with fractions collected for qualitative electrophoretic and immunological study.

Figure 1(a) shows that IgA was only partially retained by the HPAC column. This is in agreement with other work which showed that Protein A binds to IgA2 but not to IgA1 (8). Figure 1(b) shows that only an insignificant fraction of IgM was retained by the column.

Quantitative results for immunoglobulin analysis could be adversely affected by the nonspecific adsorption of other serum components if these components were co-eluted by the pH change. Since albumin is the only protein present in greater concentration in blood serum than the immunoglobulins (2), it is most likely to cause such a nonspecific interference. Figure 2(a) shows that no measurable amount of albumin was retained by the HPAC column.

Figure 2(b) is a chromatogram of a pure IgG standard solution. Very little IgG eluted unretained. Since Protein A does not bind IgG3, the unretained peak should have been slightly larger based on the usual fraction of IgG3 present in IgG (6,7). Perhaps the IgG sample used here had a lower than normal percentage of IgG3. Figure 2(c) shows the analysis of a reference blood serum sample without any dilution or pretreatment.

Figure 1. Analysis of 10 µL injections of 2 mg/mL human IgA (a) and IgM (b). Approximately 30% of the IgA was retained, while only a trace of IgM was retained. The nonretained fractions eluted at 0.7 min, while the retained protein was eluted at approximately 3 min by the step change in mobile phase pH. Most of the baseline disturbance at 3 min for the IgM sample was caused by the solvent change

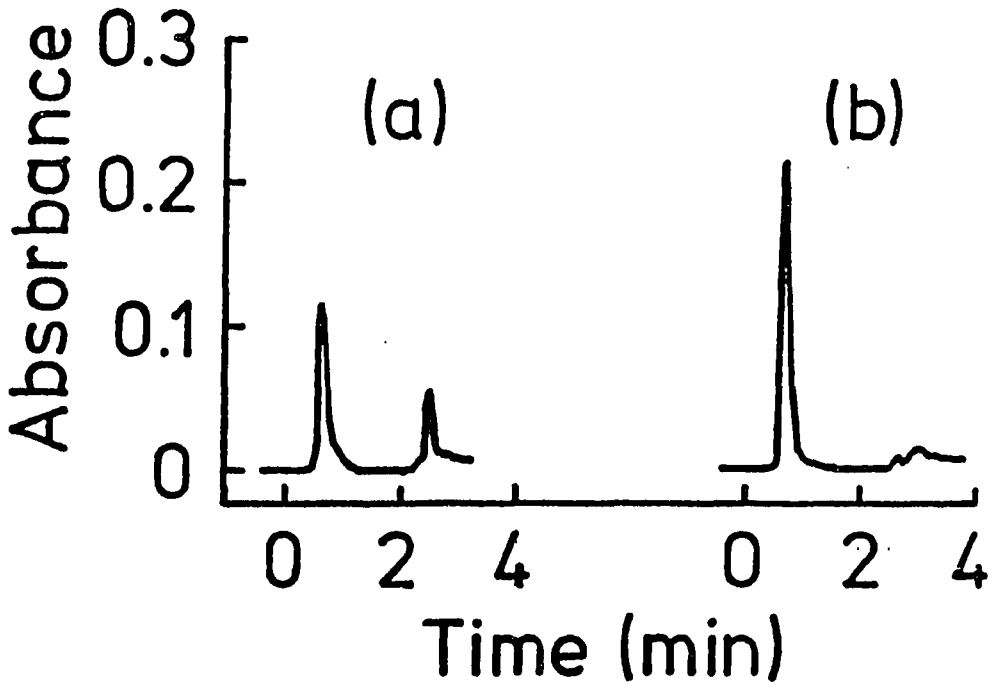
Absorbance
0.3
0.2
0.1
0
(a)
(b)
0 2 4
0 2 4
Time (min)

Figure 2. Analysis of 3 µL injections of 50 mg/mL human albumin (a), 11 mg/mL human IgG (b), and an undiluted reference serum sample containing 8.8 mg/mL IgG (c). The nonretained peak from the IgG sample is about 3% of the total absorbance of the sample

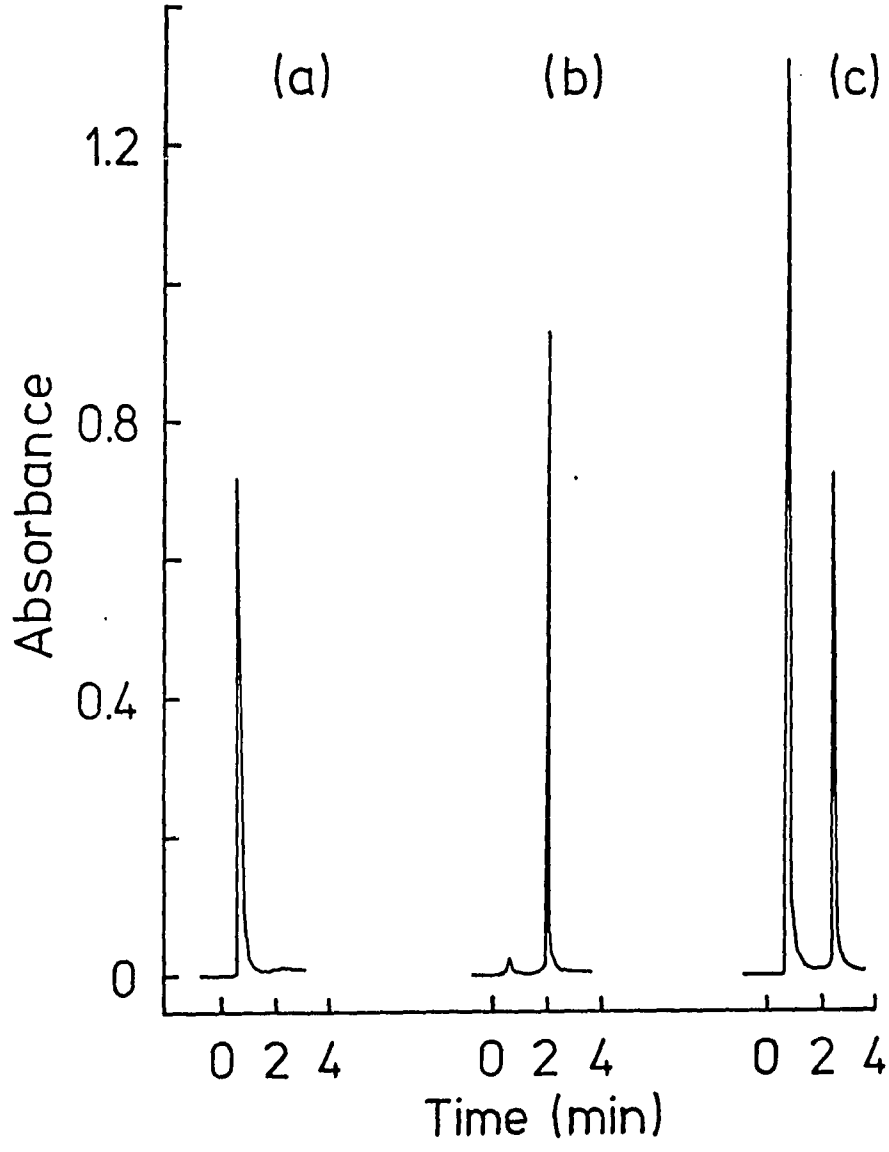
(a)
(b)
(c)
1.2
0.8
0.4
0
Absorbance
0 2 4
0 2 4
0 2 4
Time (min)

Electrophoresis was performed on pooled, concentrated fractions collected from the HPAC columns. Using the retained fraction from the pure IgG standards, one major electrophoretic band and several very faint bands were observed. The faint bands may be fragments of IgG (14). The major band of the nonretained fractions from the IgG standards migrated the same distance as the IgG band in the retained fraction. This band was probably IgG3. A few faint bands were also observed.

The major band from the retained blood serum fractions corresponded to IgG. IgA, since it has almost the same molecular weight as IgG (Table I), could not be resolved from the IgG with this technique. A few faint bands were also observed. A band corresponding to IgM was not observed.

Similarly, the eluent fractions were qualitatively profiled with an immunological assay. The nonretained fraction was found to have IgA, IgM and HSA. The retained fraction was found to contain IgG1, IgG2, IgA and HSA. Qualitatively, IgA and HSA were observed to be trace components of the retained fractions. Neither IgG3 nor IgG4 was found in either the retained or the nonretained fractions. These subclasses are minor components of total IgG and could be below the detection limit of the Ouchterlony technique.

The results of these studies may be summarized to qualitatively describe the absorptive properties of the Protein A support. All of these studies indicated that IgM was not retained by the column. This is a surprising result since Protein A columns have been used for the

purification of IgM from blood serum (9). This discrepancy needs to be examined further.

IgA was found in both retained and nonretained fractions. Qualitatively, the immunological assays indicated that the majority of the IgA was nonretained as was indicated by the HPAC studies. This distribution of IgA in both the retained and nonretained fractions was expected as there are two IgA subclasses, only one of which is reported to bind with Protein A (4,8). Similarly, IgG would be present in both of these fractions. This was indicated by the HPAC and electrophoretic studies. Both IgG1 and IgG2 were retained as indicated by the immunoassay technique. A trace quantity of HSA was found in the retained fraction. This is probably due to some type of nonspecific retention mechanism.

Figure 3 shows a calibration curve of peak height vs. IgG concentration prepared using the pure human IgG standards. Table II compares the IgG concentrations for three standard reference sera analyzed by the manufacturer by RID with the concentrations determined by HPAC using the calibration curve of Figure 3. There is good agreement between the two sets of values.

A common practice in clinical chemistry is to use reference sera as standards. The reference sera AI-AIII of Table II were used to prepare the calibration curve shown in Figure 4. A second set of reference sera, BI-BVI, was quantitated using this curve. The results are shown in Table III. Again, the results were in good agreement with the RID values, even for the two samples (BI and BII) which were not within the range of the calibration curve.

Figure 3. Calibration curve prepared using human IgG as standard. The heights of the retained peaks are plotted

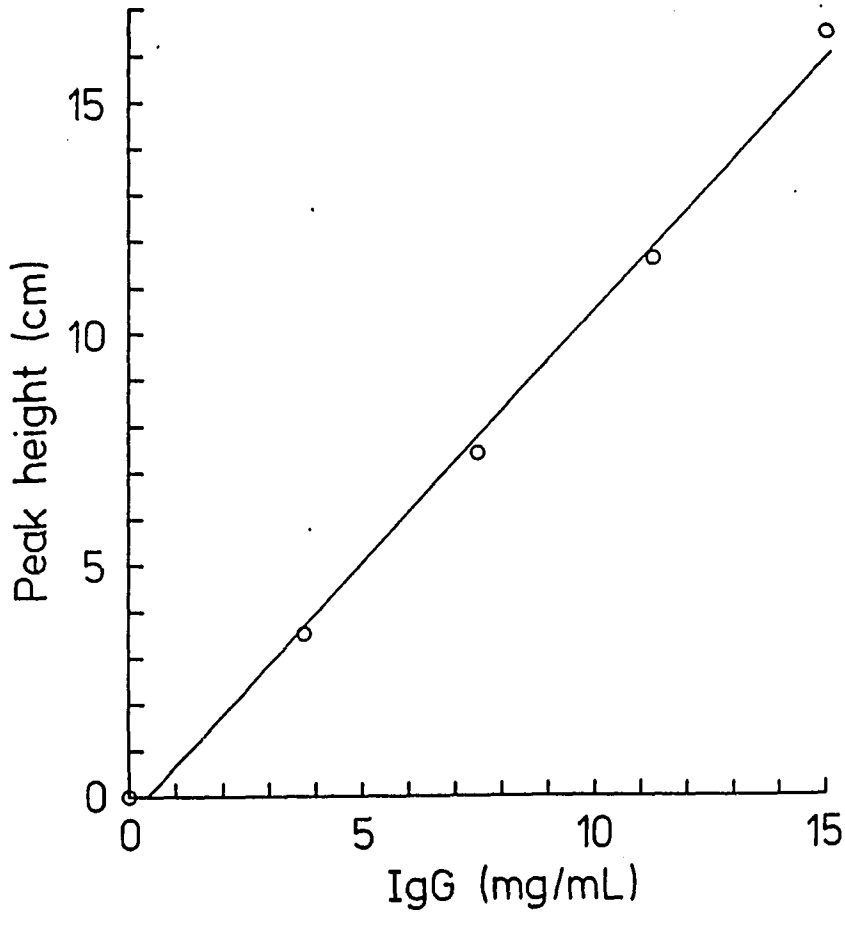
Peak height (cm)
0
5
10
15
0
5
10
15
IgG (mg/mL)

Table II. Comparison of reference sera analyzed by RID and by HPAC with IgG as standards

Serum sample	[IgG] (mg/mL)	
	RID	HPAC
AI[a]	17.50	17.2
AII	8.75	8.9
AIII	2.92	3.6

[a]This sample only was diluted 1:1 with buffer.

Figure 4. Calibration curve prepared using reference serum samples as standards

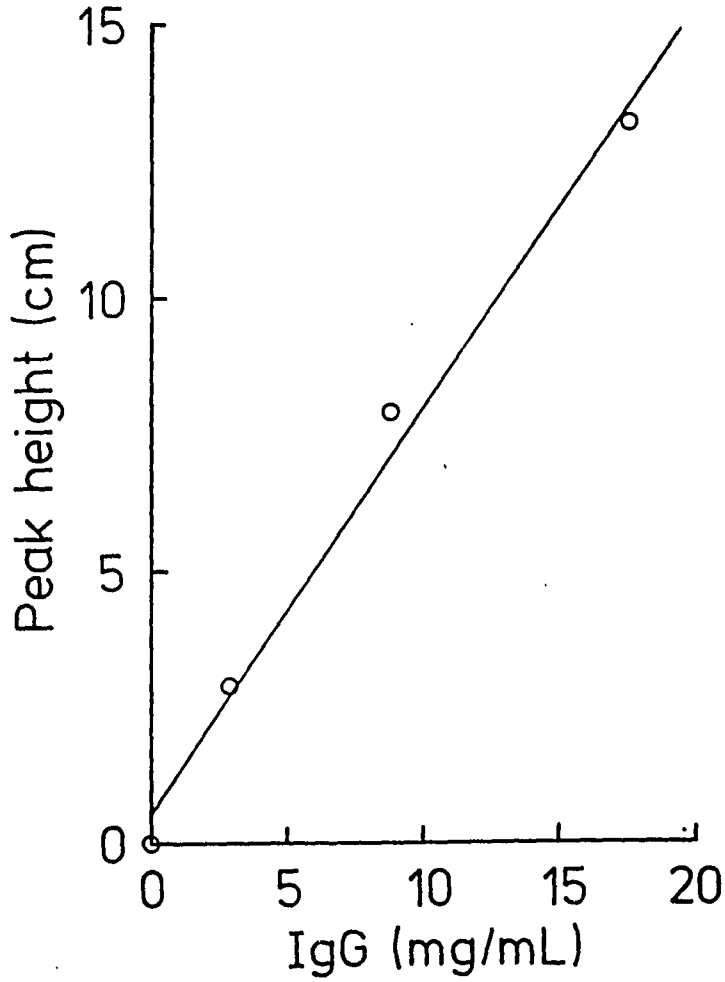
15
10
5
0
Peak height (cm)
0
5
10
15
20
IgG (mg/mL)

Table III. Comparison of reference sera analyzed by RID and by HPAC with other reference sera as standards

Serum Sample	[IgG] (mg/mL)	
	RID	HPAC
BI	28.15	28.3
BII	22.55	25.7
BIII	16.90	17.0
BIV	11.25	10.7
BV	5.65	6.1
BVI	1.69	1.3

CONCLUSIONS

The data presented suggest that this HPAC method measures the IgG concentration of blood serum. The reference serum samples all contained nearly the same relative concentrations of the major immunoglobulins (74% IgG, 15% IgA, 11% IgM). The agreement shown in Table III would be expected to be good no matter which immunoglobulins were retained by the column. The good agreement of sera and IgG standards shown in Table II could have resulted if IgG3 was not retained, but this difference could have been corrected by the expected partial retention of IgA.

In spite of these uncertainties, it is clear that this HPAC method may be very useful as a rapid screening procedure for the determination of immunoglobulins in blood serum. Very small samples were needed--3 μL or less of undiluted serum. Analysis times were on the order of 4 min. The columns have long lifetimes--one column which contains 1.1 mg of Protein A has been used in our laboratory for approximately 1000 separations over a period of two years.

ACKNOWLEDGMENTS

This research was suppported by the Research Corporation and PHS/NIH Grant No. 2S07 PR07034-15.

REFERENCES

1. Cochrum, K. R. In "Review of Physiological Chemistry"; Harper, H. A.; Rodwell, V. W.; Mayes, P. A., Eds.; Lange: Los Altos, CA, 1979, pp. 596-608.
2. Kaplan, A.; Szabo, L. L. "Clinical Chemistry"; Lea and Febiger: Philadelphia, 1979, pp. 383, 418.
3. Alper, C. A.; Ritchie, R. F. Clin. Biochem. Anal. 1978, 7, 139.
4. Goding, J. W. J. Immunol. Methods 1978, 20, 241.
5. Hjelm, H.; Hjelm, K.; Sjoquist, J. FEBS Lett. 1972, 28, 73.
6. Duhamel, R. C.; Schur, P. H.; Brendel, K.; Meezan, E. J. Immunol. Methods, 1979, 31, 211.
7. Fasman, G. D., Ed., "Handbook of Biochemistry and Molecular Biology"; Vol. II, 3rd ed., CRC Press: Cleveland, 1976, p. 528.
8. Saltvedt, E.; Harboe, M. Scand. J. Immunol. 1976, 5, 1103.
9. Vidal, M. A.; Conde, F. P. J. Biochem. Biophys. Meth. 1981, 4, 155.
10. Johansson, S. G. O.; Inganas, M. Immunol. Rev. 1978, 41, 248.
11. Walters, R. R. J. Chromatogr. 1982, 19, 249.
12. Maurer, H. R. "Disc Electrophoresis"; DeGruyter: Berlin, 1971, back flap.
13. Barret, J. T. "Textbook of Immunology"; C. V. Mosby: St. Louis, MO, 1970, Chap. 5.
14. Miller, T. J.; Stone, H. O. J. Immunol. Methods 1978, 24, 111.

SECTION II.

OPTIMIZATION OF PROTEIN IMMOBILIZATION ON 1,1'-CARBONYLDIIMIDAZOLE-ACTIVATED DIOL-BONDED SILICA SUPPORTS

SUMMARY

The activation of diol-bonded silica with 1,1'-carbonyldiimidazole and the coupling of protein ligands were examined as a function of activation conditions, coupling time, buffer, salt and pH. It was found that extensive sonication and vacuum-degassing during the activation step significantly increased the amount of ligand coupled. In the coupling step, it was found that a subpopulation of active groups was resistant to hydrolysis and resulted in increased coupling yields of ligand over a six day reaction time. The coupling and hydrolysis reactions were faster in carbonate buffer than in phosphate buffer, but the overall yields were similar. Coupling yields of several proteins were found to be relatively insensitive to pH over the range 4 to 8.

INTRODUCTION

The reagent most often used in the preparation of an affinity adsorbent is cyanogen bromide. This method was developed by Axen and Porath (1) and is illustrated in Figure 1. The initial step is the formation of reactive sites on the support. The CNBr reagent forms imido carbonate and cyanate intermediates with vicinal diol groups of the support. These reactive groups are capable of reacting with a primary amine of the ligand, forming a covalent isourea link between the ligand and the support. The selection of proper pH for the ligand coupling step is dependent upon the pK_a of the ligand amine. Coupling pH should be chosen to maximize the amount of neutral ligand amine. A wide variety of ligands has been attached by this method. These range from enzyme cofactors such as NAD to antibodies and other proteins (2,3).

Though the cyanogen bromide method is the most popular, it has several limitations (4). The isourea coupling group has a pK_a of 10.4. An anionic exchange site is thus introduced at typically used pHs of 2-8 (3). Another problem in using cyanogen bromide lies with the stability of the isourea group. The reactivity of the bond is enhanced by pHs greater than 5 and elevated temperatures (3,4). Affinity ligands are thus lost from the column as the unstable isourea linkage breaks.

High performance affinity chromatography (HPAC) requires a high performance solid support. Porous silica is the most common example of

Figure 1. Activation of polysaccharide chromatographic supports with the cyanogen bromide reagent. The exact nature of the reactive intermediate is uncertain

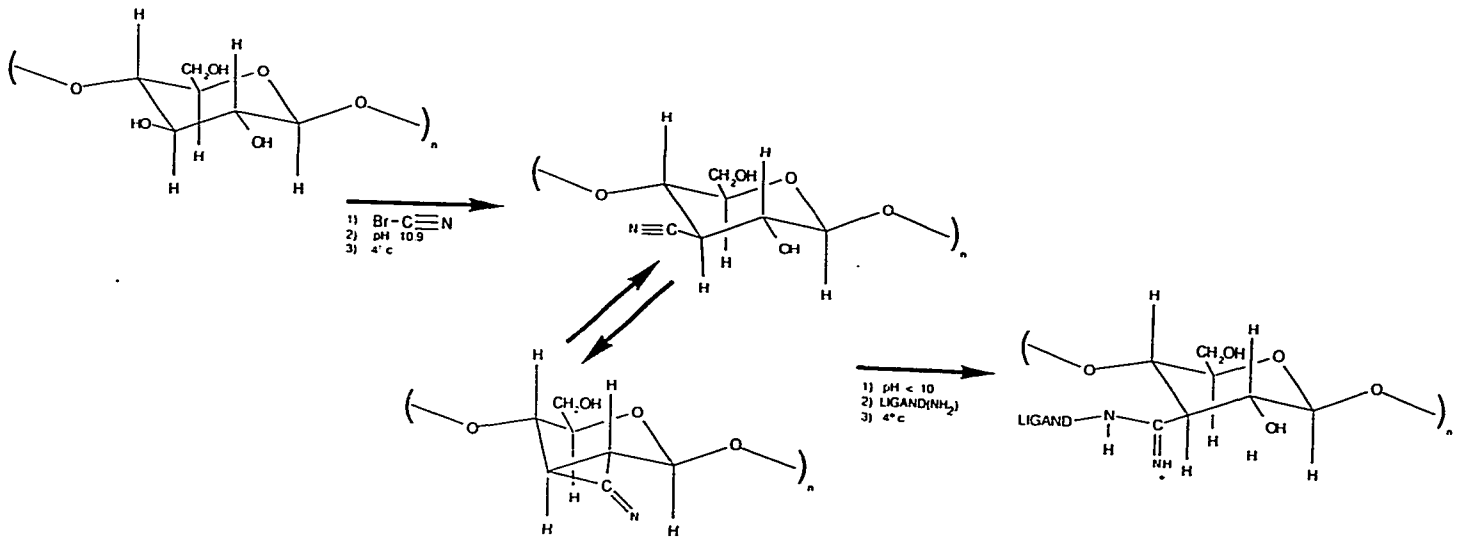
1) Br-C≡N
2) pH 10.9
3) 4°c
1) pH < 10
2) LIGAND(NH2)
3) 4°c
LIGAND

such a support (5). Silicas are limited in this use by the irreversible nonspecific surface adsorption of biopolymers. This adsorption phenomenon can be minimized by derivatizing the silica surface. Glycidoxypropyltrimethoxysilane (GOPS) is the most common such derivatization reagent (6). GOPS covers the silica surface, minimizing nonspecific adsorption and provides epoxy groups capable of further reactions for ligand immobilization (5) as illustrated in Figure 2.

Epoxy silica can either be used for the direct immobilization of ligands or further modified for the indirect immobilization of the ligand. The epoxide group is subject to nucleophilic attack. Ligands with amine, thiol or hydroxy groups can be easily attached by the direct method (5) as shown for amines in Figure 3. N^6[N-(6-aminohexyl)carbamoylmethyl]NAD (5), 3-aminobenzeneboronic acid (7), and Cibacron Blue dye (8,9) are examples of ligands attached by this method.

The direct method, although the simplest approach, has disadvantages. The reaction is very slow, often requiring 5 days under optimum conditions. To speed the reaction, high concentrations of expensive affinity ligands are used. Also, the high pH and temperatures may have undesirable effects (4). Unreacted epoxy groups must be eliminated after ligand immobilization. The common method for this is acid hydrolysis (pH 2, 3 hrs, 50°C). The addition of 2-mercaptoethanol is a milder method for use with delicate ligands (5), though ligand activity may be compromised.

Figure 2. Derivatization of the silica support with GOPS. The reaction is done under aqueous conditions to promote polymerization of GOPS and maximize the coverage of the silica support

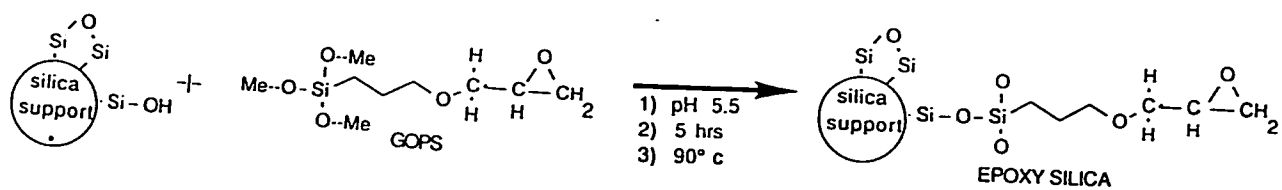
silica support
Si – OH
Me--O-Si
O--Me
O--Me
GOPS
1) pH 5.5
2) 5 hrs
3) 90° c
silica support
Si – O – Si
EPOXY SILICA

Figure 3. The immobilization of primary amine-containing ligands on epoxy-silica supports

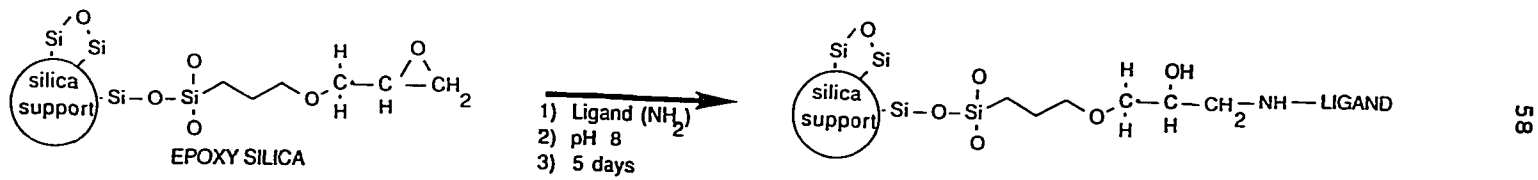
silica support
Si – O – Si
EPOXY SILICA
1) Ligand (NH_2)
2) pH 8
3) 5 days
silica support
Si – O – Si
NH — LIGAND

The indirect coupling approaches share a common first step, the acid hydrolysis of the epoxy group. This produces a vicinal diol group capable of further functionalization as illustrated in Figure 4. Essentially, the indirect approaches "activate" the support by introducing a good leaving group onto the derivatized silica. This active intermediate thus simplifies the actual ligand immobilization.

The Schiff's base or aldehyde method presented in Figure 5 has been used to immobilize N^6(6-aminohexyl)-AMP, anti-HSA (10), insulin (11) and Concanavalin A (12) to derivatized silica. The production of aldehyde silica is the first step in this synthesis. Sodium periodate is added to oxidize the vicinal diol to an aldehyde group. In the second or ligand coupling step, the ligand with a free primary amine is added to the suspension of aldehyde silica. This primary amine forms a Schiff's base with the derivatized silica, which is finally reduced to a secondary amine with sodium cyanoborohydride (5,12). This method is faster than the direct ligand coupling and much better suited for proteins. Any unreacted aldehyde groups may be reduced to alcohols with $NaBH_4$ (5).

Reactive sulfonyl chlorides are known to be good leaving groups (13). One of the indirect methods uses tresyl chloride, a sulfonyl chloride, as the leaving group and is illustrated in Figure 6. The tresyl chloride is easily reacted with the diol silica in the activation process (13,14). The degree of activation is easily controlled and can be determined by elemental analysis (14). The immobilization reaction is much faster than the direct coupling of ligand. It is also

Figure 4. Acid hydrolysis of the epoxy group to form a diol or glycerol hydrophilic layer over the support

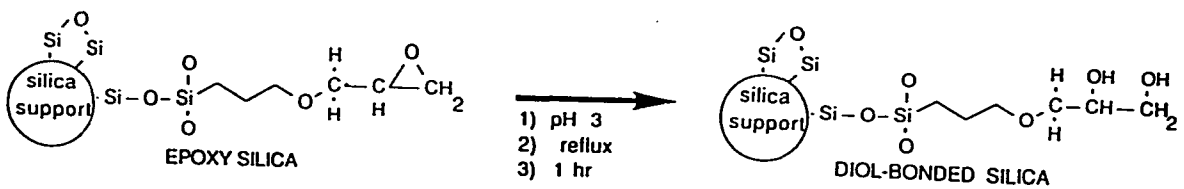
silica support
EPOXY SILICA
1) pH 3
2) reflux
3) 1 hr
silica support
DIOL-BONDED SILICA

Figure 5. Preparation of aldehyde-silica and coupling of a primary amine-containing ligand to the aldehyde-silica

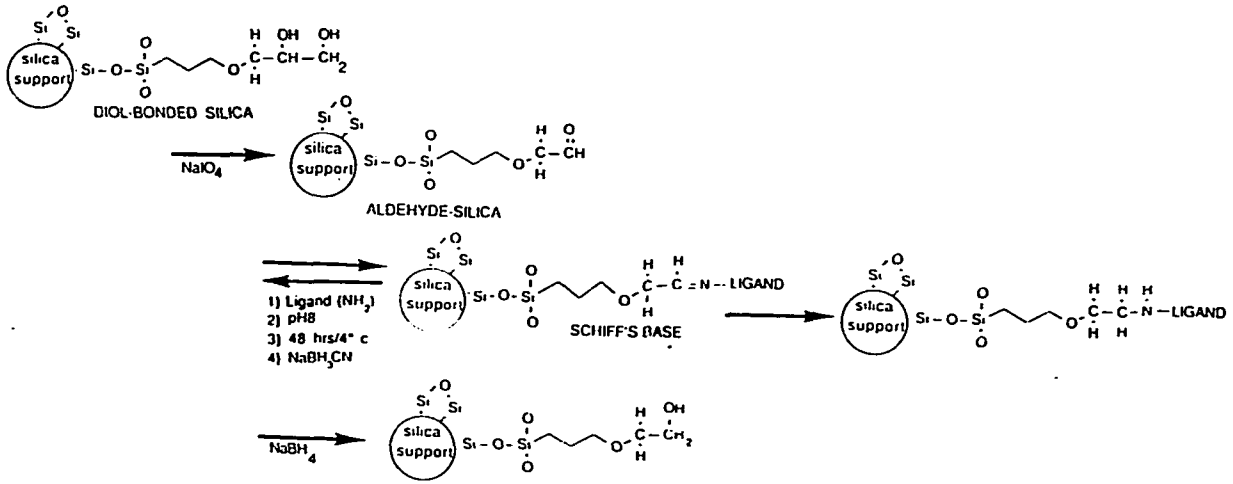
silica support
DIOL-BONDED SILICA
NaIO4
ALDEHYDE-SILICA
1) Ligand (NH3)
2) pH8
3) 48 hrs/4° c
4) NaBH3CN
SCHIFF'S BASE
LIGAND
NaBH4

Figure 6. Activation of the diol-silica with tresyl chloride and coupling of a primary amine-containing ligand to the tresyl silica

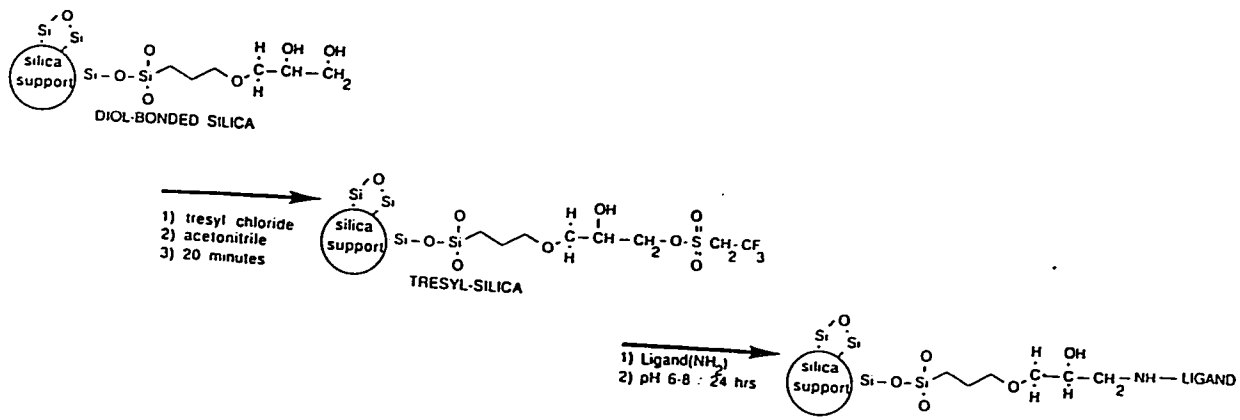
silica support
DIOL-BONDED SILICA
1) tresyl chloride
2) acetonitrile
3) 20 minutes
TRESYL-SILICA
1) Ligand(NH2)
2) pH 6-8 ; 24 hrs
LIGAND

more versatile than direct coupling, with a wider pH range (6-8) and lower coupling temperatures may be used to enhance ligand activity. Examples of ligands so attached are soybean trypsin inhibitor (STI) and N^6-(6-aminohexyl)AMP (13,14).

Another activation reagent used with HPAC applications is 1,1'-carbonyldiimidazole (CDI). The use of CDI as an activating agent for affinity chromatographic matrices is illustrated in Figure 7. It was first demonstrated by Bethell and coworkers in a series of papers (15-19) and more recently by other workers (20-25). CDI has also been used for the coupling of proteins to polyethylene glycol (26), and is well known as a synthetic reagent (27).

The great advantage of CDI for affinity adsorbent preparation is that the alkyl carbamate linkage formed between a hyroxylic support and an amine-containing ligand is neutral (15). This is in contrast to other immobilization methods such as the cyanogen bromide (28,29), tresyl chloride (30), epoxide (30) and Schiff's base (30) methods, in which basic groups may be introduced when amine-containing ligands are coupled and which can cause nonspecific adsorption by ion exchange (29).

Bethell et al. primarily examined ligand immobilization on agarose matrices (15-19). They found high pH to be optimal (typically pH 8.5-10) and that the immobilization of ligands and hydrolysis of reactive groups took place within approximately one day (16). Silica and glass matrices, such as are used in high-performance affinity chromatography (5,30), cannot tolerate such alkaline conditions. However, CDI-

Figure 7. Activation of diol-silica with CDI and immobilization of a primary amine-containing ligand to supports so activated

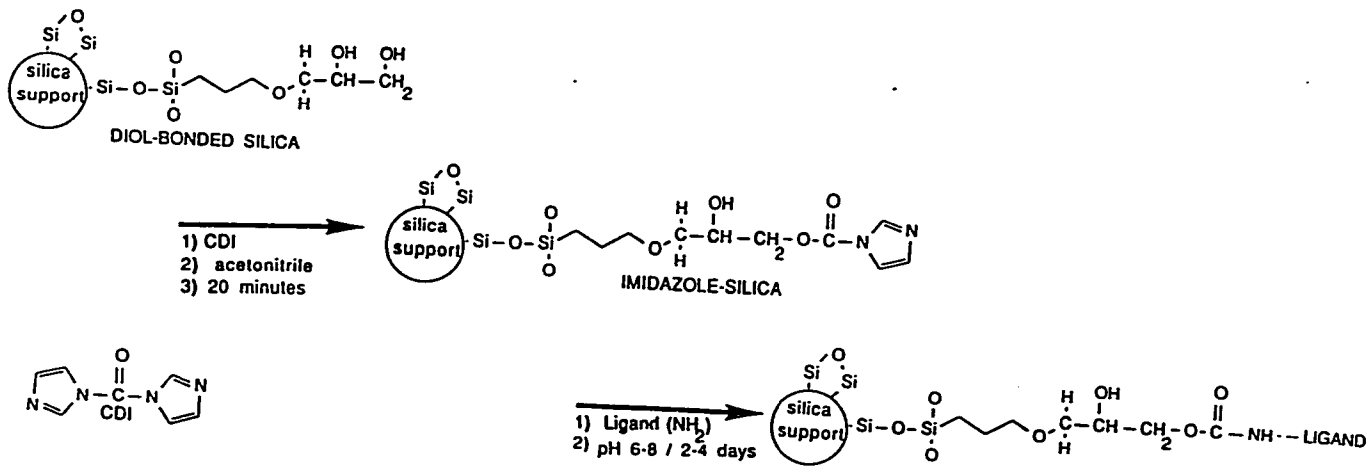
silica support
DIOL-BONDED SILICA
1) CDI
2) acetonitrile
3) 20 minutes
IMIDAZOLE-SILICA
CDI
1) Ligand (NH2)
2) pH 6-8 / 2-4 days
LIGAND

activated silica and glass matrices successfully coupled amine ligands when used at a pH of 8.5 and below (20-25), and CDI-activated glass matrices are commercially available from Pierce Chemical Co. (Rockford, IL).

In this paper, the CDI activation reaction in an organic solvent of diol-bonded silica (prepared by the reaction of silica with GOPS (6)) and the coupling of an amine-containing ligand to the CDI-activated support in aqueous solution are examined and optimized. It is shown that the optimum conditions for CDI-immobilization are significantly different when diol-bonded silica is used as the matrix rather than agarose.

EXPERIMENTAL

Reagents

Bovine serum albumin (BSA), soybean trypsin inhibitor (STI), rabbit immunoglobulin G (IgG), Protein A, eel acetylcholinesterase, bovine trypsin, glucosamine hydrochloride, and acetylthiocholine iodide were from Sigma (St. Louis, MO). Horse liver alcohol dehydrogenase (HLADH) and β-nicotinamide adenine dinucleotides (NAD and NADH) were from Boehringer Mannheim (Indianapolis, IN). The HLADH was further purified according to a published procedure (31). Reagents for the bicinchoninic acid (BCA) protein assay were from Pierce (Rockford, IL). LiChrospher SI500, SI1000 and SI4000 silicas were from Rainin (Woburn, MA).

Methods

Diol-bonded LiChrospher SI500, SI1000 and SI4000 were prepared as described previously (16). The optimized CDI-activation and ligand coupling conditions for LiChrospher SI500 diol-bonded silica were scaled to a uniform set of conditions as follows: 1.0 g of diol-bonded silica was suspended in 1.0 mL of acetonitrile (dried over molecular sieves) containing a tenfold molar excess of CDI relative to the diol groups in the silica. The suspension was degassed by sonication under aspirator vacuum for 15 min and then shaken at room temperature for an additional 30 min. The activated silica was filtered, washed with acetonitrile, and sucked dry on a medium-porosity sintered-glass filter. The activated matrix was suspended in 10 mL of the coupling

buffer (0.1 M phosphate or carbonate of the desired pH) and degassed for 5 min. The affinity ligand was then added (10-100 mg protein), and the volume was adjusted to 20 mL with deionized water. The suspension was shaken at 4°C in a water bath for six days. The support was washed with buffer or water and collected by filtration or centrifugation.

A spectrophotometric assay was used to determine the degree of CDI activation of the diol-bonded silica. Imidazole standards, CDI-activated silicas and diol-bonded silica blanks (1-3 mg) were suspended in 1 mL of 3 mM phosphate buffer (pH 10), sonicated and degassed, then boiled for 30 min to hydrolyze the imidazoyl carbonate reactive intermediate. The silica was removed by centrifugation, and the imidazole concentration of the supernatant was determined by absorbance at 210 nm.

Immobilized glucosamine was determined by the alkaline ferricyanide assay (32). Immobilized protein was determined by either the Lowry protein assay (33) or the Pierce Chemical Co. bicinchoninic acid protein assay. In all of these assays, blank values were determined using diol-bonded silica samples. The silica was removed by centrifugation prior to absorbance measurement.

The activities of immobilized HLADH (31) and acetylcholinesterase (34) were determined by enzyme assays. The activities of immobilized STI and Protein A were determined from chromatographic breakthrough curves (35) of trypsin and IgG, respectively.

RESULTS AND DISCUSSION

Activation Step

The CDI-activation of agarose has typically been performed for 15-30 min in dioxane (15-19), acetone (15,19,23) or dimethylformamide (19,26) at room temperature. In our work, acetonitrile was used as the solvent, since better coupling yields were obtained than with dioxane, dimethylformamide, dimethylsulfoxide and chloroform (36). In addition, sonication and vacuum degassing of the suspension were used to help remove air from the pores of the matrix. Table I indicates the effect of varying the activation parameters on the amount of protein coupled. From Experiment 1, it was apparent that increasing the duration of the sonication/degassing step significantly increased the amount of ligand coupled. Increasing the total activation time, Expt. 2, gave a smaller relative increase in yield. It thus appeared that the sonication/degassing process helped to facilitate the reaction between the diol-bonded phase and the CDI.

Since the acetonitrile evaporated as the degassing time increased, Expt. 3 was performed to see whether the change in CDI concentration was important. The results indicated no effect of changing activation volume and CDI concentration.

Further experiments were performed to determine whether extensive sonication fractured the silica. Such fracturing could lead to non-specific adsorption of protein on the newly exposed bare silica surface. Treatment of several types of diol-bonded silica under conditions identical to the usual activation and coupling conditions,

Table I. Activation of 0.1 g of Licrospher S1500 diol

Expt.	Sonication/degassing duration (min)	Total activation time (min)	Activation solution volume (mL)	Coupling time (d)	BSA coupled (mg/g silica)
1	1	31	1.0[a]	2	2.4
	3	33	1.0[a]	2	2.9
	10	40	1.0[a]	2	3.8
2	15	15	1.0[a]	6	7.1
	15	45	1.0[a]	6	7.0
3	15	45	0.25-paste	6	7.0
	15	45	0.5-0.25	6	7.0
	15	45	1.0-0.75	6	7.3

[a]Initial volume.

but without CDI, led to the immobilization of 0.15 ± 0.05 mg BSA/g silica. Thus, no significant damage to the silica was indicated.

The imidazole assay was used to assess the degree of activation of diol-bonded silica as a function of the surface area of the support. Using diol-bonded silica matrices with a surface area of 6, 20 and 50 m^2/g and a diol coverage of 17, 72 and 190 μmol/g, respectively, with a tenfold excess of CDI yielded approximately one imidazole per diol group (13, 72 and 156 μmol imidazolyl carbonate/g silica, respectively, as shown in Fig. 8). In terms of surface coverage, the diol content averaged 3.6 $\mu mol/m^2$ (roughly equivalent to 1.5 monolayers (37)), while the imidazolyl carbonate coverage was 3.2 $\mu mol/m^2$. This activation level can be compared to 1.6 $\mu mol/m^2$ obtained with diol-bonded controlled-pore glass (CPG) (22), 0.4 $\mu mol/m^2$ with the CDI-activated CPG sold by Pierce, and 1.6-3.0 $\mu mol/m^2$ obtained with tresyl chloride-activated diol-bonded silica (31).

To prevent multipoint attachment of macromolecules and a consequent decrease in ligand specific activity (38), it is sometimes necessary to use low activation levels. Figure 9 shows that low levels of activation were achieved by decreasing the amount of CDI used. In general, the appropriate amount of CDI to use must be determined empirically, since the yield of the activation step was low (11%). The activation levels of cellulose and agarose have also been varied; however, the yields were higher (35-70%) (15,16,19).

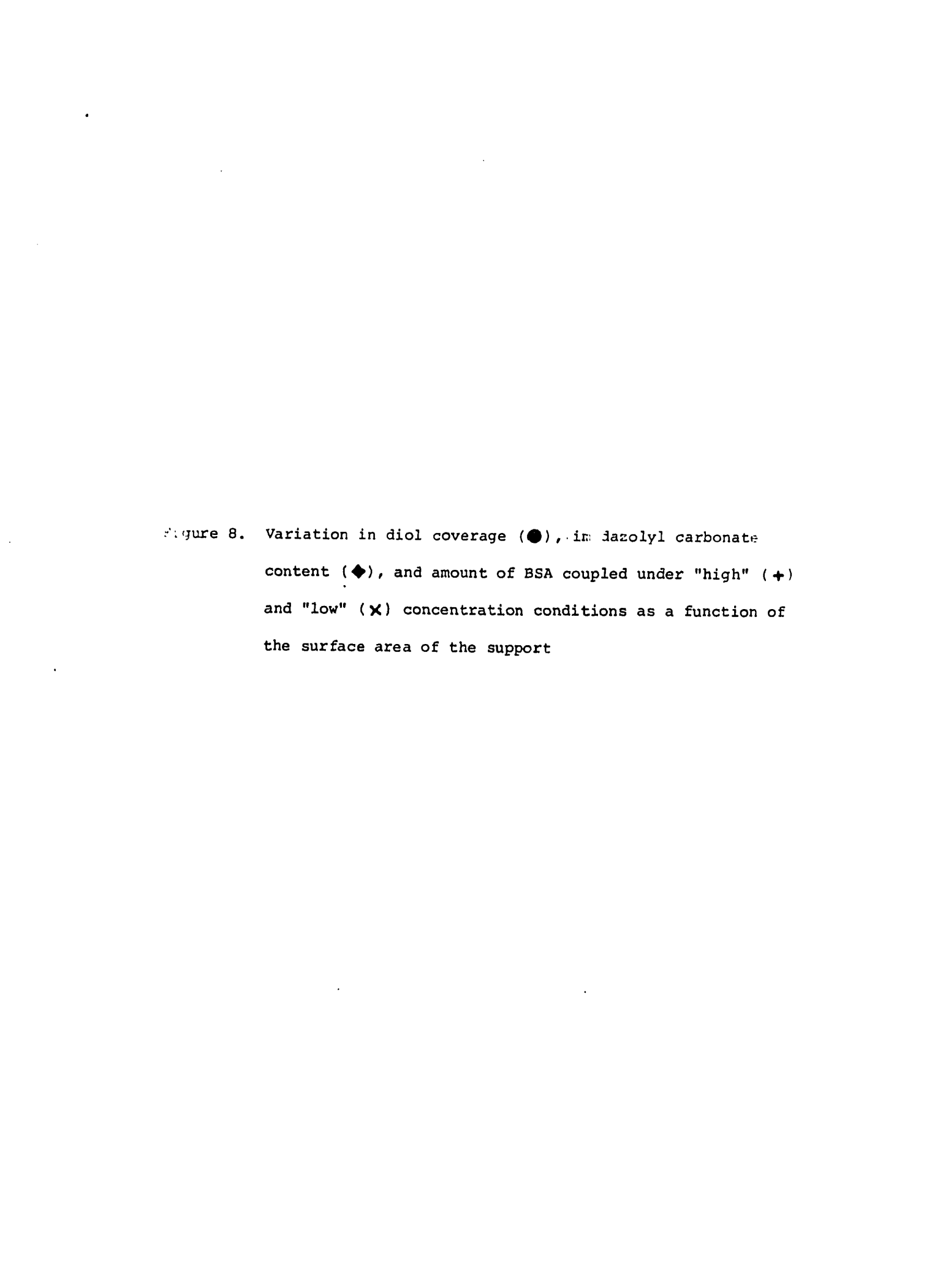

Figure 8. Variation in diol coverage (●), imidazolyl carbonate content (◆), and amount of BSA coupled under "high" (+) and "low" (×) concentration conditions as a function of the surface area of the support

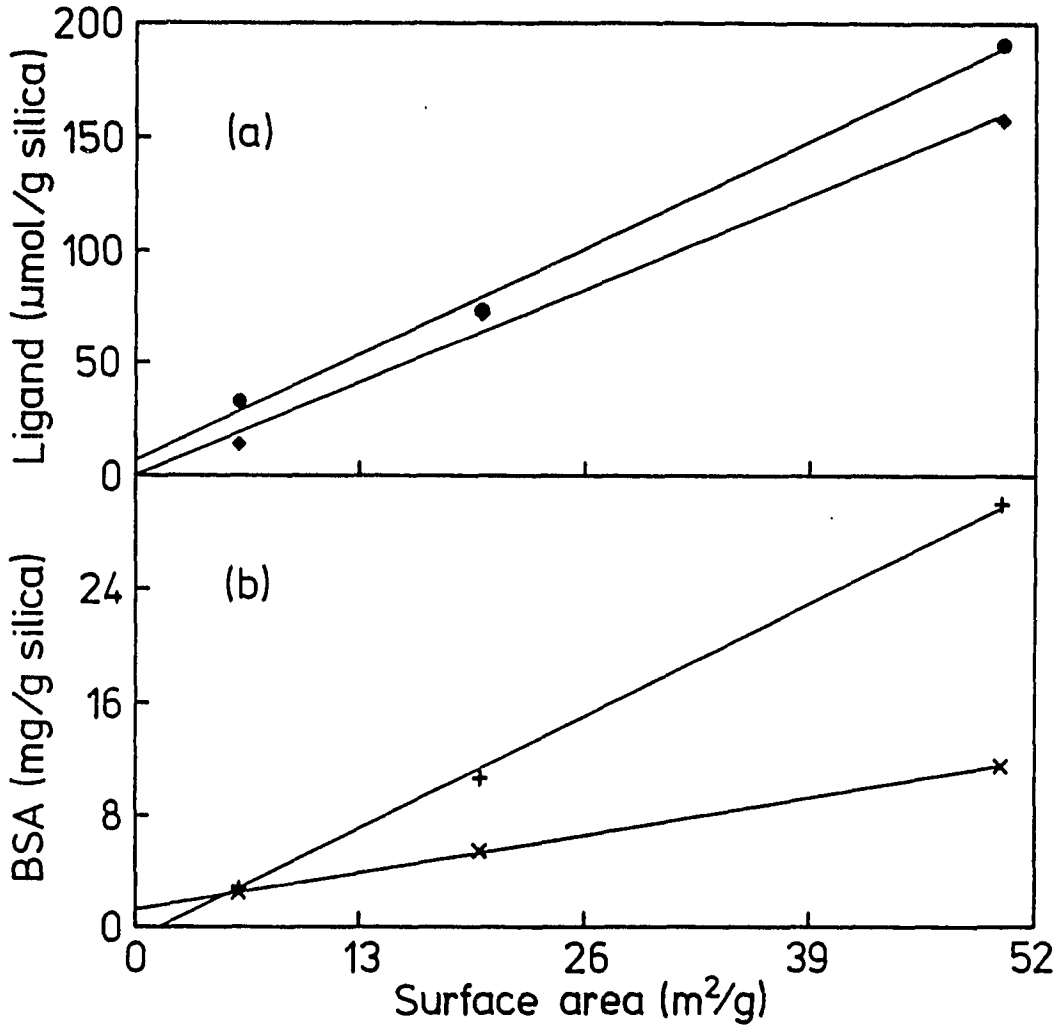
200
150
100
50
0
Ligand (μmol/g silica)
(a)
24
16
8
0
BSA (mg/g silica)
(b)
0
13
26
39
52
Surface area (m²/g)

Figure 9. Imidazoyl carbonate content as a function of the mole ratio of CDI to diol in the activation mixture

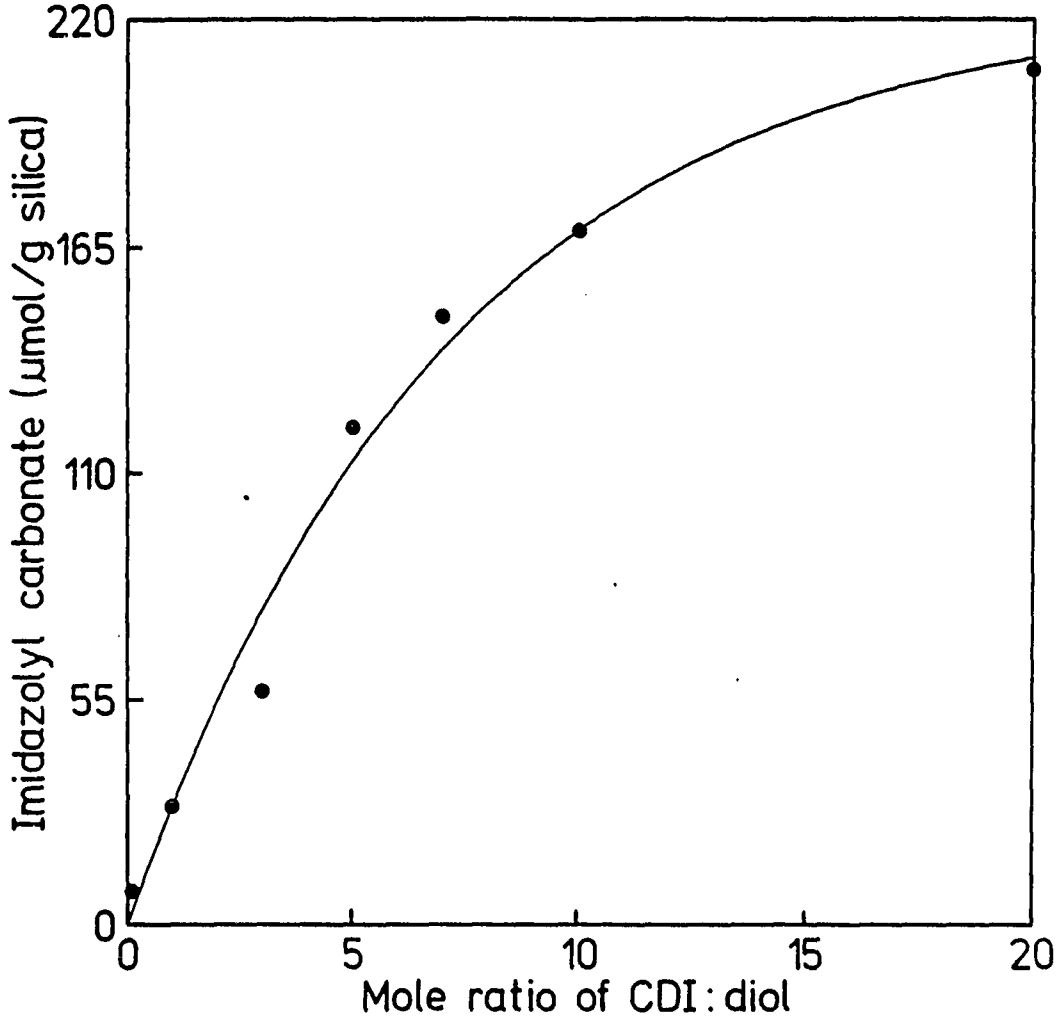
220
165
110
55
0
Imidazolyl carbonate (μmol/g silica)
0
5
10
15
20
Mole ratio of CDI : diol

Hydrolysis of Active Groups

Bethell et al. found that the imidazolyl carbonate groups were lost by hydrolysis in water at room temperature during reaction times ranging from 1.5 h at pH 11 to 30 h at pH 5 (18). Studies of diol-bonded silica were performed in which buffer and pH were varied and the imidazole assay was used to measure the loss of imidazole. The results were imprecise, but the general trend was that hydrolysis was very slow in water and phosphate buffer (6 d at pH 6 and 8) and moderately slow in carbonate buffer (2-4 d at pH 8). It appeared that there might be two subpopulations of active groups present, one of which was hydrolyzed immediately upon contact with water and one which was more stable, and the rate of hydrolysis depended on the buffer salt and the pH.

Coupling of Glucosamine

The monovalent ligand glucosamine was used to determine which subpopulation of active groups was primarily responsible for coupling ligands. As shown in Table II, the immobilization rates paralleled the loss of the more stable sites. At pH 8 in carbonate buffer, coupling was complete after 2 days. In phosphate buffer the reaction was complete after approximately 4 days. It is interesting that the same amount of glucosamine was immobilized in both carbonate and phosphate buffers. Apparently, both immobilization and hydrolysis reactions were faster in carbonate buffers.

The yield of the coupling reaction was only about 11% relative to the initial number of active sites. The most ligand attached in this

Table II. Immobilization of Glucosamine

		Glucosamine coupled (μmol/g)				
Buffer	pH	0.5 d	1 d	2 d	4 d	6 d
phosphate	6	7	10	17	19	17
phosphate	8	3	16	12	18	15
carbonate	8	5	16	18	20	18

laboratory by the CDI method was 1.0 μmol/m^2, or ca. 30% relative to the number of diol groups. It thus appears that rapid hydrolysis of many of the active groups ultimately limits the maximum density of immobilized ligands. Using CDI-activated agarose, Hearn et al. coupled several monovalent ligands at pH 9-11 with yields of 20-70% relative to the initial number of active groups (16).

Coupling of Albumin and Immunoglobulin G

BSA and IgG were chosen to study the immobilization of proteins. Replicate immobilization of BSA yielded a relative standard deviation of 13%. This figure is probably representative of the precision of the immobilized protein data presented below.

The effects of several buffer salts on the immobilization of BSA were examined at pH 8.0 in 0.05 M buffers. The concentrations of BSA attached were: phosphate buffer, 31 mg/g; carbonate, 34 mg/g; borate, 31 mg/g; acetate, 28 mg/g; and trishydroxymethylaminomethane (TRIS), 22 mg/g. Thus, all of the buffers, except TRIS, yielded similar results. TRIS and other amine-containing buffers should not be used for coupling.

Ionic strength effects were briefly examined. When 0.005 M phosphate (pH 8) was used, one-half as much BSA was immobilized as when the buffer concentration was 0.05 M. Increasing the ionic strength with NaCl slightly increased coupling. Similar effects have been observed with other activating agents (39). However, increasing the ionic strength with phosphate sometimes led to decreased coupling yields.

Carbonate and phosphate buffers were selected for further study. Two concentrations of IgG and BSA were used in these studies. "High" concentration will refer to the use of 5 mg/mL protein concentrations with a maximum immobilization level of 100 mg/g. "Low" will refer to one-tenth of these concentrations.

Figure 10 shows the immobilization of BSA over a pH range of 3 to 9. There was a broad maximum centered at pH 4-5. Previous workers utilized high pH for coupling to agarose because monovalent ligands coupled best near the pK_a of the amine group (16,24). It was thus somewhat surprising to find such a low optimum pH for the BSA. This is very advantageous, since silica matrices are not stable above pH 8.

The time-dependence of immobilization was further examined at pH 6 and 8 (Table III). The data exhibited the same trends as the glucosamine data in Table II. Reaction was more rapid in carbonate than phosphate buffer, but the total amount of protein coupled was similar for both buffers. For BSA, yields were higher at pH 6 than at pH 8, in agreement with Figure 10. The yields reached about 90% under "low" conditions and 50% under "high" conditions. IgG appeared to be significantly more reactive than BSA; 100% immobiliztion was observed under most conditions. It should be noted that 100 mg IgG/g LiChrospher SI500 was close to monolayer coverage. Similar coverages have been obtained for tresyl chloride-activated diol-bonded silica (31).

Immobilization experiments were performed on matrices of variable surface area. Just as in the activation step, the amount of protein

Figure 10. The pH dependence of BSA coupling using phosphate buffer

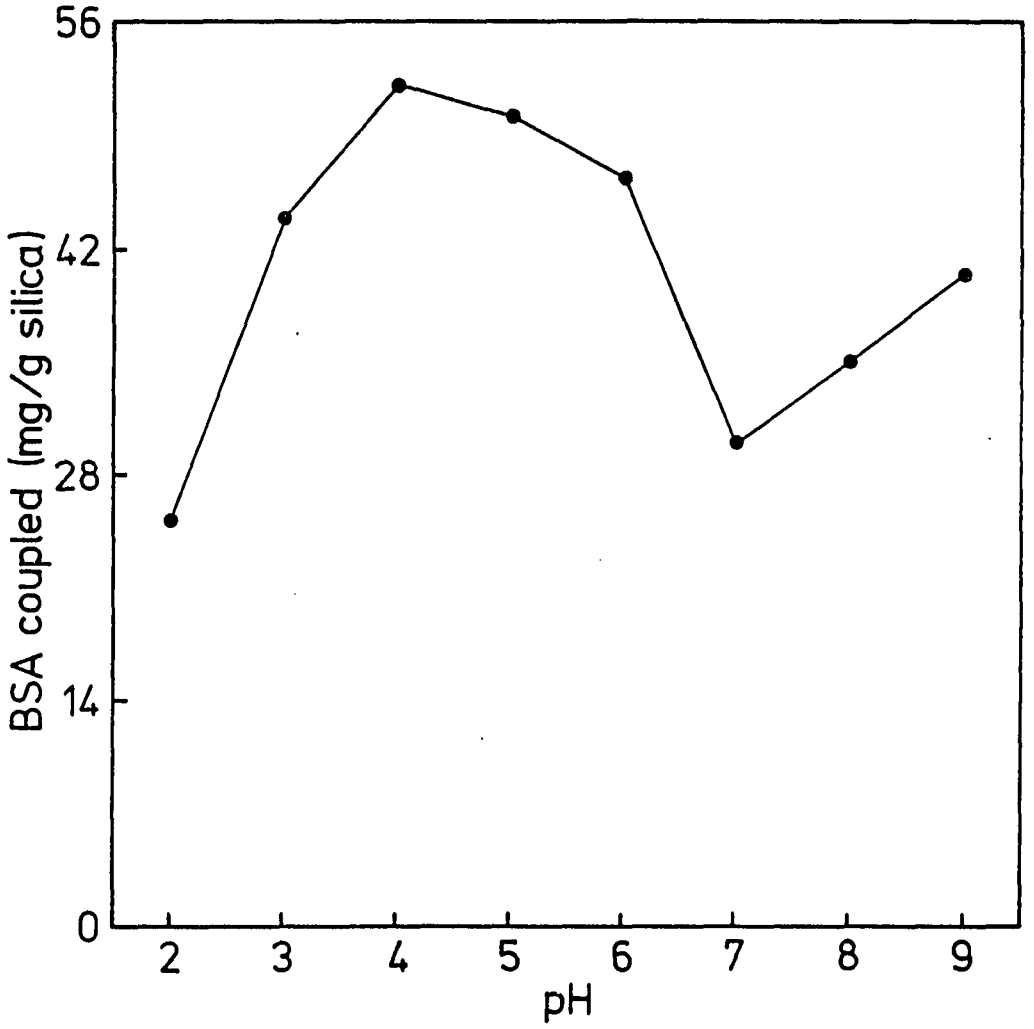
56
42
28
14
0
BSA coupled (mg/g silica)
2
3
4
5
6
7
8
9
pH

Table III. Immobilization of BSA and IgG

Protein	Concentration	Buffer	pH	Protein coupled (mg/g) 1 d	2 d	4 d	6 d
BSA	low	phosphate	6	8	8	8	8
	high	phosphate	6	31	45	48	57
	low	phosphate	8	6	6	6	6
	high	phosphate	8	28	29	37	42
	low	carbonate	6	11	12	12	13
	high	carbonate	6	43	47	47	52
	low	carbonate	8	8	7	7	9
	high	carbonate	8	26	30	34	34
IgG	high	phosphate	6	97	100	101	108
	high	phosphate	8	82	100	103	118
	low	carbonate	6	10	10	11	12
	high	carbonate	6	118	109	111	111
	high	carbonate	8	61	63	63	63

Table IV. Effect of the amount of CDI on protein coupling

	Protein coupled (mg/g)		
mol CDI/mol diol	BSA-low	BSA-high	IgG-low
10.	5.3	19.6	7.1
1.	1.0	1.1	3.1
0.1	0.4	0.7	2.1

attached increased linearly with the surface area of the matrix. Using the same matrices described earlier, "low" and "high" BSA concentrations yielded surface coverages of 0.2 and 0.6 mg BSA/m^2, respectively.

BSA was immobilized with decreased amounts of CDI (Table IV). As expected from the activation study (Fig. 9), the coupling yields dropped rapidly as the amount of CDI decreased. Immobilized IgG yields were less affected than BSA yields. In general, the high sensitivity of the yield to the amount of CDI made it difficult to control coverage by this means.

Deactivation of Excess Reactive Groups

Active groups remaining after ligand immobilization are frequently removed by reaction with ethanolamine. To test the effectiveness of ethanolamine in removing imidazolyl carbonate active groups, a solution of 0.08 M ethanolamine in 0.05 M phosphate buffer (pH 8) was allowed to react with CDI-activated diol-bonded silica for various lengths of time. The ethanolamine solution was then removed by filtration, replaced with a glucosamine solution, and allowed to react with any remaining active sites for an additional 6 days. The amount of glucosamine coupled is listed in Table V. It is apparent that ethanolamine was not much more effective at removing active groups than simple hydrolysis in buffer. This may be due to the high pK_a of ethanolamine (9.5, vs. 7.7 for glucosamine and the near neutral buffer pH values used). A better alternative for ensuring removal of active groups would be to perform the coupling in carbonate buffer or to treat the matrix with carbonate after coupling of ligand is complete.

Table V. Removal of active groups with ethanolamine

Duration of reaction in ethanolamine (d)	Glucosamine coupled (μmol/g)
0	18
1	7
2	8
4	2
6	2
control[a]	5

[a]6 d hydrolysis in buffer.

Immobilization of Various Proteins

STI, Protein A, acetylcholinesterase and HLADH were immobilized at several pH values in phosphate buffer. The matrices were then assayed for protein content and biospecific activity. It should be noted in these experiments that the amount of protein attached could be increased by increasing the concentration and amount of protein used in the coupling step. However, the percentage yields declined. This same trend can be seen in Table III for the BSA data and has been observed for CDI-activated cellulose (23).

Both the yield and activity of immobilized STI (Table VI) were moderately insensitive to pH in the range of 5-8. The yield was highest at pH 5 and the specific activity, based on the binding of trypsin, was almost constant over the pH range 5-7. The manufacturer indicated a specific activity of 1-3 mg trypsin/mg STI for the STI; thus, almost all of the activity was preserved during immobilization.

Protein A from Staphylococcus aureus, which binds to the F_c region of several classes of immunoglobulins, was immobilized at pH 4-8 (Table VI). Both the yield and specific activity for binding IgG increased slightly as the pH decreased from 8 to 4. However, the specific activity was much lower than the manufacturer's value of 13 mg IgG/mg Protein A. A comparative study of three coupling methods has shown that CDI is a poor reagent for the immobilization of Protein A (25).

Acetylcholinesterase appeared to be immobilized in highest yield at pH 4 (Table VII). However, in a second experiment, the highest yield was at pH 8. In either case, pH 4 proved unsuitable because the

Table VI. Immobilization of STI and Protein A

Ligand	pH	Protein coupled (mg/g)	Test solute	Specific activity (mg test solute/mg ligand)
STI[a]	5	19.9	trypsin	2.7
	6	18.5		2.6
	7	17.3		2.8
	8	17.6		2.1
Protein[b]	4	10.2	IgG	0.7
	6	8.6		0.6
	8	9.0		0.5

[a]STI applied: 200 mg/g silica.

[b]Protein A applied: 10 mg/g silica.

Table VII. Immobiliztion of acetylcholinesterase and HLADH

Ligand	pH	Protein coupled (mg/g)	Specific activity (immobilized/native)
Acetylcholinesterase[a]	4	3.8	0.4
	6	2.7	1.1
	8	2.6	1.0
HLADH[b]	5.1	15.5	0.
	6.5	11.7	1.0
	8.0	10.7	1.0

[a]Acetylcholinesterase applied: 11 mg/g silica.

[b]HLADH applied: 19.4 mg/g silica.

specific activity was significantly less than at pH 6 and 8, where 100% of the initial activity was retained during immobilization.

HLADH, immobilized in the presence of NADH, $ZnSO_4$ and isobutyramide (31), was coupled in highest yield at pH 5.1, but was found to be totally inactive (Table VII). HLADH is known to be denatured in buffers of pH <5 (40), and this situation occurred briefly during pH adjustment of the protein solution. However, at pH 6.5 and 8.0, the HLADH was immobilized with 100% retention of activity. Both the yields and activities were comparable to those obtained with tresyl chloride (31).

ACKNOWLEDGMENT

The authors gratefully acknowledge the support of the National Science Foundation under Grant No. CHE-8305057.

REFERENCES

1. Axen, R.; Porath, J.; Ernbach, S. Nature 1967, 214, 1302.
2. Turkova, J. "Affinity Chromatography"; Elsevier: Amsterdam, 1978.
3. Lowe, C. R. In "Laboratory Techniques in Biochemistry and Molecular Biology"; Work, T. S.; Work, E., Eds.; North-Holland: Amsterdam, 1979, pp.
4. Matsumoto J. Chromatogr. 1982, 239, 747.
5. Larsson, P.-O.; Glad, M.; Hansson, L.; Mansson, M. O.; Ohlson, S.; Mosbach, K. Adv. Chromatogr. 1983, 21, 41.
6. Regnier, F. E.; Noel, R. J. Chromatogr. Sci. 1976, 14, 316.
7. Glad, M.; Ohlson, S.; Hansson, L.; Mansson, M. O.; Mosbach, K. J. Chromatogr. 1980, 200, 254.
8. Lowe, C. R.; Glad, M.; Larsson, P.-O.; Ohlson, S.; Small, D.; Atkinson, T.; Mosbach, K. J. Chromatogr. 1981, 215, 303.
9. Small, D.; Atkinson, T.; Lowe, C. R. J. Chromatogr. 1981, 216, 175.
10. Ohlson, S.; Hansson, L.; Larsson, P.-O.; Mosbach, K. FEBS Lett. 1978, 93, 5.
11. Sportsman, J. R.; Wilson, G. S. Anal. Chem. 1980, 52, 2013.
12. Borchert, A.; Larsson, P.-O.; Mosbach, K. J. Chromatogr. 1982, 244, 49.
13. Nilsson, K.; Mosbach, K. Biochem. Biophys. Res. Commun. 1981, 102, 449.
14. Nilsson, K.; Mosbach, K. Methods Enzymol. 1984, 104, 56.

15. Bethell, G. S.; Ayers, J. S.; Hancock, W. S.; Hearn, M. T. W. J. Biol. Chem. 1979, 254, 2572.

16. Hearn, M. T. W.; Bethell, G. S.; Ayers, J. S.; Hancock, W. S. J. Chromatogr. 1979, 185, 463.

17. Hearn, M. T. W.; Harris, E. L.; Bethell, G. S.; Hancock, W. S.; Ayers, J. A. J. Chromatogr. 1981, 218, 509.

18. Bethell, G. S.; Ayers, J. S.; Hearn, M. T. W.; Hancock, W. S. J. Chromatogr. 1981, 219, 353.

19. Bethell, G. S.; Ayers, J. S.; Hearn, M. T. W.; Hancock, W. S. J. Chromatogr. 1981, 219, 361.

20. Crowley, S. C.; Walters, R. R. J. Chromatogr. 1983, 266, 157.

21. Walters, R. R. J. Chromatogr. 1982, 249, 19.

22. Walters, R. R. Anal. Chem. 1983, 55, 1395.

23. Chapman, R. S.; Ratcliffe, J. G. Clin. Chim. Acta 1981, 118, 129.

24. Anderson, D. J.; Walters, R. R. J. Chromatogr. 1985, 331, 1.

25. Hage, D. S.; Walters, R. R.; Hethcote, H. W. Anal. Chem. 1986, 58, 224.

26. Beauchamp, C. O.; Gonias, S. L.; Menapace, D. P.; Pizzo, S. V. Anal. Chem. 1983, 131, 25.

27. Staab, H. A. Angew. Chem. Int. Ed. Eng. 1962, 1, 351.

28. Axen, R.; Myrin, P.-A.; Janson, J.-C. Biopolymers 1970, 9, 401.

29. Jost, R.; Miron, T.; Wilchek, M. Biochim. Biophys. Acta 1974, 362, 75.

30. Larsson, P.-O. Methods Enzymol. 1984, 104, 212.

31. Nilsson, K.; Larsson, P.-O. Anal. Biochem. 1983, 134, 60.

32. Robyt, J. F.; Ackerman, R. J.; Keng, J. G. Anal. Biochem. 1972, 45, 517.

33. Lowry, O. H.; Rosebrough, N. J.; Farr, A. L.; Randall, R. J. J. Biol. Chem. 1951, 193, 265.

34. Ellman, G. L.; Courtney, K. D.; Andres, V.; Featherstone, R. M. Biochem. Pharm. 1961, 7, 88.

35. Lund, U. J. Liq. Chromatogr. 1981, 4, 1933.

36. Moore, R. M., Department of Chemistry, Iowa State University, Ames, IA, personal communication.

37. Becker, N.; Unger, K. K. Chromatographia 1979, 12, 539.

38. Koch-Schmidt, A.-C.; Mosbach, K. Biochemistry 1977, 16, 2105.

39. Zemanova, I.; Turkova, J.; Capka, M.; Nakhapetyan, L. A.; Svec, F.; Kalal, J. Enzyme Microb. Technol. 1981, 3, 229.

40. Branden, C.-I.; Jornvall, H.; Eklund, H.; Furugren, B. In "The Enzymes"; Boyer, P.D., Ed.; Vol. XI; Academic Press: New York, 3rd ed., 1975, p. 147.

SECTION III.

STUDIES ON THE DESORPTION OF IgG FROM IMMOBILIZED PROTEIN A USING THE PEAK DECAY MODEL: A GENERAL METHOD FOR QUANTITATIVELY DESCRIBING THE ELUTION OF ANALYTE FROM AN AFFINITY SUPPORT

SUMMARY

The dissociation of IgG from immobilized Protein A was studied. For this work the Peak Decay (PD) kinetic model was used. The derivation of this model as well as a computer simulation of this model are reviewed. The application of the computer simulation for the estimation of the chromatographic parameters required to produce the PD effect is demonstrated. Using the PD model, the dissociation kinetic rate at 25°C was found to be 0.008 sec^{-1}. This value is in reasonable agreement with literature values for the native dissociation of the Protein A-IgG complex. Additionally, the kinetics of low pH denaturing elution were studied with the PD model. An IgG dissociation rate of 1.2 sec^{-1} was observed with this type of elution. The activation parameters of both the naturing and denaturing dissociation processes were determined and found to be in reasonable agreement with literature values. The suitability of the PD model for the study of protein-protein interactions as well as high affinity biocomplexes ($K_{eq} >> 10^6$) is demonstrated.

INTRODUCTION

Solid phase techniques have become popular alternatives for biochemical analysis because of the stability and reusability they impart to the immobilized biochemical reagent or ligand. Enzyme electrodes (1), Enzyme linked Immunosorbent assay (ELISA) assays (2) and affinity chromatography (3) are examples of techniques using immobilized biochemicals. Since these applications are often operated in the nonequilibrium mode, the biocomplex association and dissociation kinetic rates as well as the affinity or equilibrium constants are important considerations in experimental design (4,5,6). Unfortunately, the extrapolation of these parameters as determined in free solution to the solid phase is often not valid. The presence of the solid support and the immobilization chemistry used can alter the microenvironment of the bioligand (1). Additionally, the immobilization of the ligand and the presence of the solid support impede the free diffusion of the analyte and eliminate diffusion of the ligand. This is significant since free diffusion has often been observed to be the rate-limiting step for free solution reactions (1).

The determination of biocomplex dissociation kinetics with affinity chromatographic techniques has been previously described (4,7). These approaches have typically used a general model for affinity chromatography with biospecific elution. This model is presented in Figure 1A and is descriptive of "reversed-role" affinity chromatography where both the analyte (A) and the inhibitor (I) bind

Figure 1. Models used to describe the affinity chromatographic process

A) The general model for retention of analyte (A) on an affinity ligand (L) with biospecific elution using inhibitor (I). Both I and A bind with the same site on the ligand with this binding competition for ligand represented as (X). Subscripts m and p represent the moving and stagnant mobile phase, respectively

B) The Peak Decay model. This model is a special case of the general model (see Fig. 1A) where all adsorptive processes have been eliminated during desorption through the use of large [I] and rapid flow rates

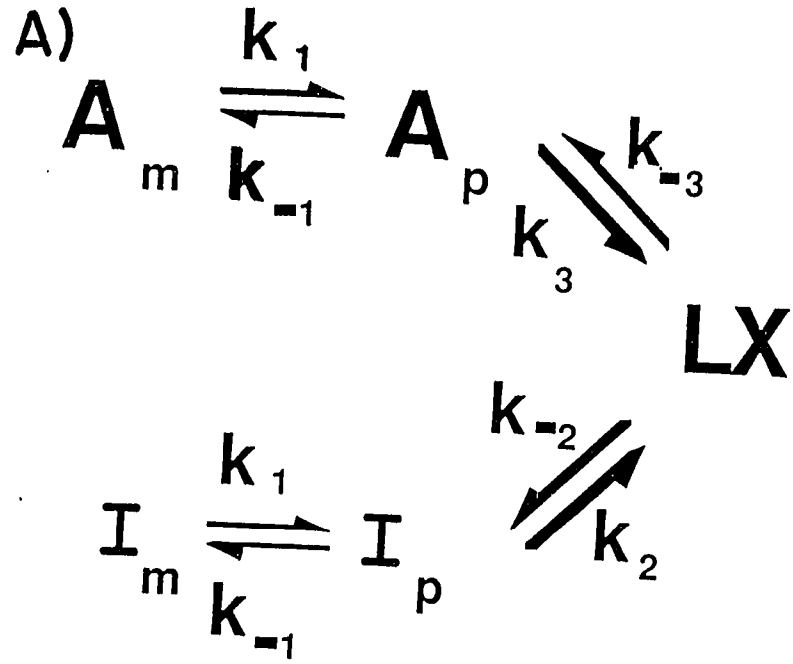
A)
k 1
A m
k -1
A p
k -3
k 3
LX
k -2
k 1
I m
k -1
I p
k 2

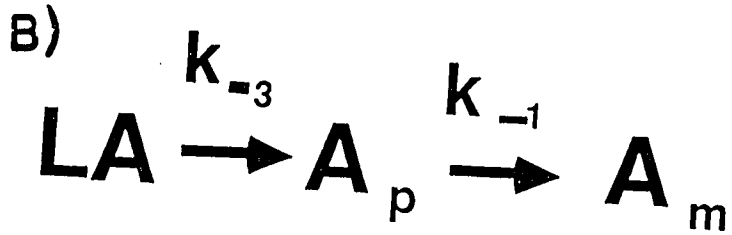
B)
k -3
k -1
LA
A p
A m

with the same site on the affinity ligand (L) (8). Thus, both the inhibitor and the analyte compete for available ligand sites. In this work all inhibitors will be assumed to be of the competitive type. The inclusion of the diffusion-controlled mass transfer processes between the intra-pore stagnant mobile phase and the inter-pore moving mobile phase is more descriptive of a macromolecular chromatographic behavior (9). Additional parameters of this model are:

K_3 - equilibrium constant for formation of the analyte affinity ligand complex

k_3 - association rate constant for the analyte and affinity ligand complex

k_{-3} - dissociation rate constant describing dissociation of the analyte-affinity ligand complex

K_2 - equilibrium constant for affinity ligand-inhibitor complex

k_2 - rate constant for the formation of the affinity ligand-inhibitor complex

k_{-2} - rate constant for the dissociation of the affinity ligand-inhibitor complex

k_1 - rate of diffusion-controlled mass transfer of analyte and inhibitor from the moving mobile phase to the stagnant mobile phase

k_{-1} - rate of diffusion-controlled mass transfer of analyte and inhibitor from the stagnant mobile phase to the moving mobile phase

Each of these kinetic processes and the chromatographic system contribute to the broadening of the analyte band. This broadening is quantitatively described by the Height Equivalent of a Theoretical Plate (HETP) for the analyte band. The contributions of each of these broadening processes are summed in the HETP term. It is possible to independently estimate the contribution to broadening from each of these nonabsorptive processes and obtain the biocomplex kinetic broadening (absorptive processes) contribution by difference. Equations have been derived relating the HETP contribution to the actual kinetic rates of analyte-ligand complexation. These procedures are, however, quite complex and significant errors may be introduced (10).

The biocomplex dissociation rate may be easily determined by modifying the design of the affinity chromatographic experiment. The Peak Decay (PD) model is one special case of the general model designed specifically for the estimation of biocomplex dissociation kinetics. It is presented in Figure 1B (8). The PD model is a consecutive reaction sequence or a biphasic process (11). The actual dissociation is followed by the diffusion of the analyte from the pore and into the moving mobile phase followed by the elution of analyte from the column. The adsorptive processes are negated experimentally with high inhibitor concentrations to favor formation of the inhibitor-ligand biocomplex (once a ligand site has become available) and rapid eluent flow rates to elute the dissociated A from the column before it can diffuse back into the pores of the support.

As this system is designed to operate in a nonequilibrium manner, very poor band shapes are produced. The initial response is a rapid rise with a tail slowly decaying to baseline. An example of such a peak is presented in Figure 2 and illustrates the origin of the peak decay nomenclature. Ideally, the rate of decay is indicative of the dissociation of analyte from the ligand.

Unique to the design of the PD model is the ability to apply the model for the estimation of the dissociation kinetics of nonspecific elution methods (8). These nonspecific elution techniques, such as change of eluent pH or the addition of organic solvent or chaotropic ion to the eluent, involve some type of biocomplex denaturation leading to the dissociation of the biocomplex and elution of the analyte. This situation is analogous to the use of inhibitor with biospecific elution technique. Used in this manner the PD method could measure the rate of denaturation of the biomolecules. The various nonspecific elution techniques have been shown to dissociate and denature the affinity complexes in specific mechanisms (12). The PD method should be suitable for the study of these various nonspecific elution techniques (8).

This model has been successfully applied to the study of Concanavalin A sugar biocomplexes ($K_{eq} = 10^5$) (13). The PD model should also be useful for the study of higher affinity systems which have proven difficult for the classical chromatographic kinetic techniques. The Protein A IgG affinity complex should be useful as a

Figure 2. Peak decay profiles calculated from Equation 1a for the conditions $k_{-1}/k_{-3} = 10$. Taken from Ref. 8

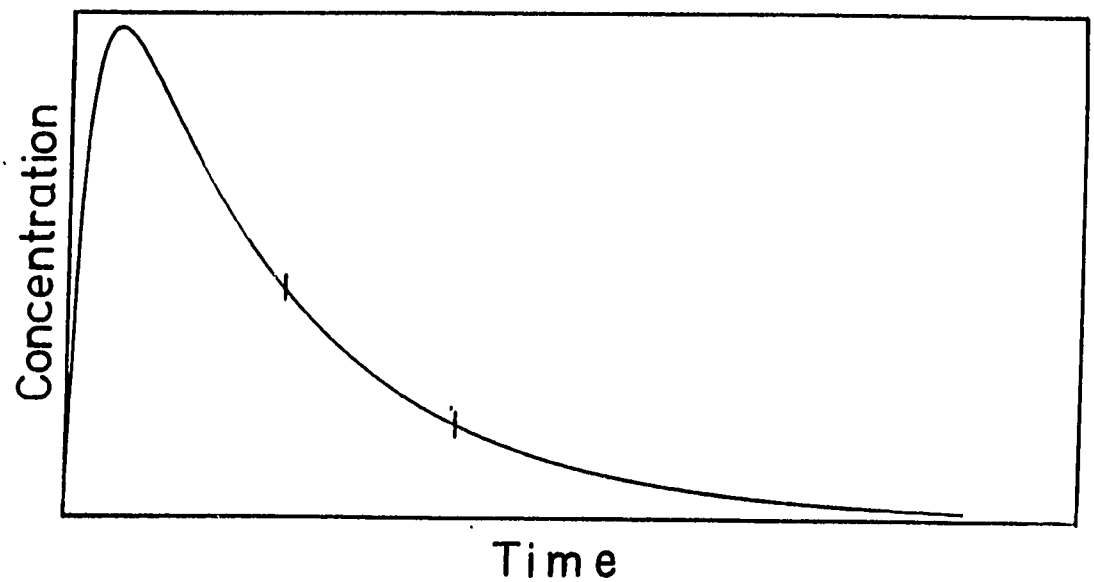
Concentration
Time

model for higher affinity ($K_{eq} > 10^6$) protein complexes (9).

Protein A is a cell wall protein isolated from the Staphylococcus aureus bacteria. Structurally, protein A is composed of five subunits arranged in a linear form with a molecular weight of 42 kD. Four of these subunits are homologous and capable of binding with the Fc region of many mammalian immunoglobulin proteins (14) while the fifth is located at the C-terminal and anchors the native protein to the bacteria cell wall (15).

In these studies, Protein A was immobilized and used as the affinity ligand. Rabbit IgG was used as the analyte. Rabbit IgG protein has been reported to be homogeneous with respect to Protein A or not to exhibit subclasses which could have varying kinetic properties (9,16), and is readily available. The Protein A IgG complex forms readily at neutral pH values and rapidly dissociates at acidic pH values (17).

Protein A is bivalent with respect to the binding of IgG (18). This is less than the optimal tetravalency and has been explained by steric hindrance (19). Lindmark has studied the adsorption of IgG to Protein A and demonstrated cooperativity between the primary and secondary adsorptions of IgG, with the affinity constants presented in Table I (20). This cooperativity results in a 40-fold decrease in the affinity constant of the secondary adsorption with respect to the primary adsorption. Sufficient IgG must be available to saturate the primary adsorption site before the second site fills. Secondary adsorption of IgG is a real complication in present experiments, since

Table I. Estimation of the chromatographic parameters required to produce the peak decay effect with various combinations of thermodynamic and kinetic data

mole IgG / mole Protein A	primary adsorption 1		secondary adsorption 1	
K_3[a] (M^{-1})	4.1 E 08		6.4 E 06	
	calculated k_{-3}[b]	experimental k_{-3}[c]	calculated k_{-3}[b]	experimental k_{-3}[d]
k_{-3} (sec^{-1})	6.1 E -04	2.3 E -05	3.75 E -02	5.5 E -04
rate ratio				
k_{-1}[e]/k_{-3}	3.9 E 03	10.4 E 04	64	4.4 E 03
estimated k'	10	10	1	10
peak decay parameters tm (sec)	4.9 E 02	1.3 E 04	8.0	5.5 E 02

[a] k_{-3} calculated using K_3 and k_3. A k_3 value of 2.5 x 10^5 M^{-1} sec^{-1} as determined by split peak kinetics (9).

[b] k_{-1} calculated as 2.4 sec^{-1} for the diffusion-limited case (8,9).

[c] k_{-3} experimentally determined using heat killed Staph A with limiting IgG by Mayhre and Kronvall (6).

[d] k_{-3} experimentally determined using heat killed Staph A with excess IgG by O'Keefe and Bennett (5).

[e] Ref. 20.

high IgG inhibitor concentrations are required. This could introduce heterogeneities into the PD dissociation, as some might have a mix of 1° and 2° desorption events.

The study of the Protein A IgG interaction is complicated by the lack of a suitable competitive inhibitor (8,17,21). IgG must be used as both the analyte and inhibitor. A fluorescent label covalently attached to the analyte IgG has been proposed to distinguish between the analyte IgG and the inhibitor IgG (8). Dandliker and Levison have used a fluorescein label attached to IgG antibody for the study of antibody antigen kinetics (22-24). These reports and work by Goding indicate a minimal effect on the macromolecular interaction with the presence of the fluorescent label.

In the theory section a brief description of the Peak Decay kinetic model and the derivation of the defining equations are presented. Additionally, a computer simulation of the PD model is described to allow for estimation of the suitability of the PD model to a particular affinity system and to estimate the experimental parameters required to produce the PD effect. Fundamental elution studies were undertaken to compare the dissociation rates under both naturing and denaturing conditions. Additionally, the activation parameters of the various elution schemes were studied for comparison of the elution methodology. The energetics of the PD desorption were studied by determining the effect of temperature on the measured PD rate.

THEORY

Derivation of Defining Equations

An equation describing the PD model can be derived and is presented as Equation 1a where $m(A_o)$ and $m(A_t)$ are the total moles of analyte retained at t = 0 and at time t, respectively. The diffusive and dissociation rates are k_{-1} and k_{-3}, respectively. This equation can be simplified with the assumption that $k_{-3} << k_{-1}$ and by making a logarithmic transformation, leading to Equation 1b. A theoretical elution profile is presented in Figure 2 (8).

$$\frac{d\, m(A_t)}{dt} = \frac{k_{-1}k_{-3}m(A_o)}{k_{-1} - k_{-3}} \left(e^{-(k_{-3}t)} - e^{-(k_{-1}t)}\right) \qquad (1a)$$

$$\ln \left(\frac{d\, m(A_t)}{dt} \right) = \ln \left(m(A_o)\, k_{-3}\right) - k_{-3}\, t \qquad (1b)$$

As with any biphasic process, the estimation of a kinetic rate constant for either step of the process is most easily made if it is significantly smaller than the rate constant of the other step (8,11). If the rates are similar, the PD treatment, as based on Eq. 1b, would fail to properly describe the system. Hence, the fundamental limitation in applying the PD model is the k_{-1}/k_{-3} rate ratio of a given biocomplex.

Estimation of the k_{-1}/k_{-3} ratio of the experimental affinity system is the initial step in the application of the PD model. As described above, k_{-1} is the rate of mass transport from the stagnant

mobile phase to the moving mobile phase. This is a diffusion-controlled process and is affected by interactions between the support and the analyte. This diffusion of the analyte is restricted by the geometry of the pore and support. This is expressed in Eq. 2 (25), where D, dp and (γ) are the analyte diffusion coefficient, particle diameter and tortuosity of the support, respectively. Tortuosity quantifies the degree of restriction of free diffusion by analyte as defined by Giddings and can be assumed to be 0.1 for large proteins and high performance silica supports.

The k_{-1} and k_1 rates are not equivalent as described by Eq. 2 where V_p and V_e are the column pore volume and the column excluded volume, respectively.

$$(V_e/V_p)k_1 = k_{-1} = \frac{60\ (\gamma)\ Dm}{dp^2} \qquad (2)$$

If available, the best estimate of k_{-3} is one obtained from free solution experiments. Typically, k_{-3} must be inferred from the free solution affinity or equilibrium constant (K_{eq}) and association rate (k_3) data. Finally, data from similar affinity systems may also be used as an approximation.

The experimental parameters affecting the generation of a PD profile are ligand density (moles ligand (m_L)/column void volume (V_m)), inhibitor concentration, and eluent flow rate. Unlike the fundamental rate ratio limitations, these parameters can be controlled to produce the PD effect. The relationship between the flow rate and inhibitor concentrations and the resulting experimental PD rate can be quite

complex. When the assumptions used to define the PD model are met, the measured PD rate is independent of these experimental parameters, as predicted by Equations 1a and 1b. Rather than attempt a rigorous derivation of the effect of these experimental parameters upon the resulting PD rate, a more satisfactory approach is a computer simulation of the experiment. This simulation may also be used to estimate the chromatographic parameters required to produce the PD effect (8).

Computer Simulation of the Peak Decay Effect

The computer simulation divides the column lengthwise into a series of segments. These segments are further divided into three subsegments representing the moving mobile phase, the stagnant mobile phase and the affinity ligand. The chromatographic process is approximated by introducing the analyte into the initial segment and distributing the analyte between the phases. Elution is approximated by transferring the moving mobile phase to the next segment and re-equilibrating the analyte in each segment. This is diagrammed in Figure 3 where the equilibration and transfer steps are demonstrated. This type of approach is analogous to the plate theory of chromatography (8,9).

As with the design of the actual experiment, it is possible to configure the simulation to describe the Peak Decay Model (8,13). Rather than eliminating the k_3 and k_1 steps as in the derivation of the PD model, these adsorptive kinetic processes are included in the simulation. The simulation assumes that initially all of the ligand

Figure 3. Illustration of the model used for computer simulations. From top to bottom, the rows represent the moving phase, stagnant mobile phase, and stationary phase. The flow is from left to right, along the length of the column. Taken from Ref. 8

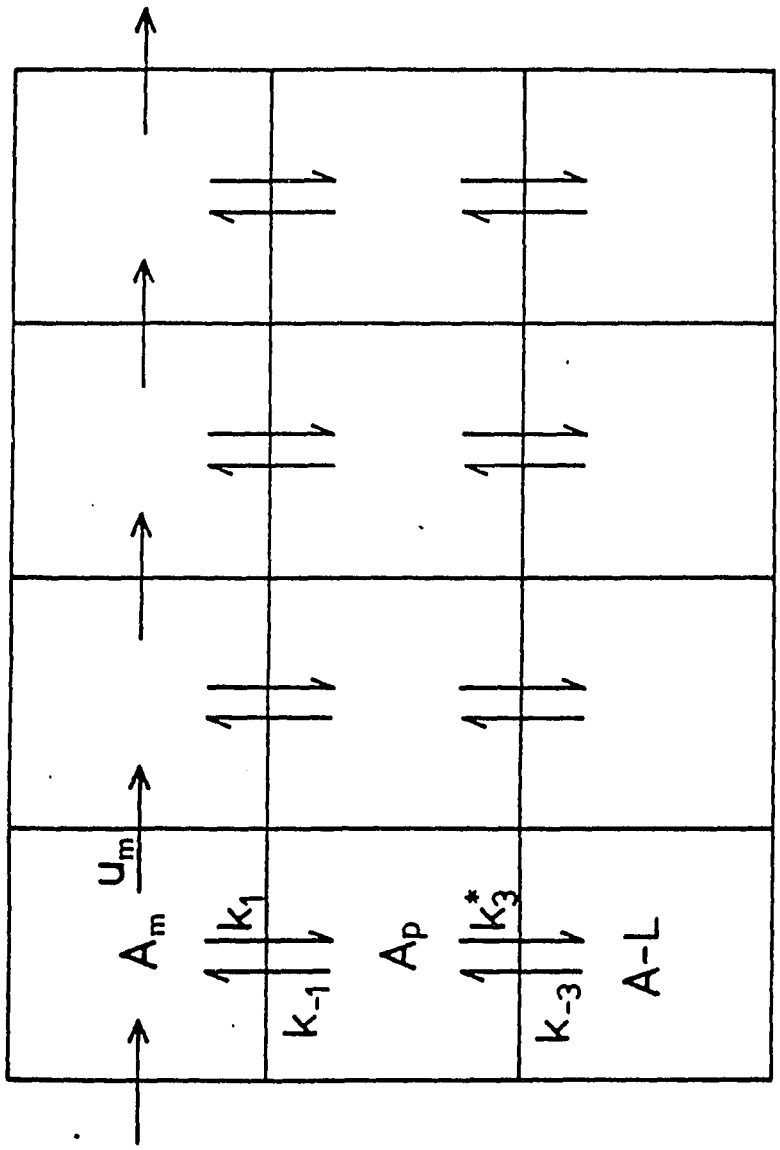
U_m
A_m
k_1
k_{-1}
A_p
k_3^*
k_{-3}
A-L

sites are saturated with analyte and competitive inhibitor is continuously applied to the column with the moving mobile phase. The inhibitor is equilibrated in the initial segment with dissociated A. Both I and A in the moving mobile phase are then transferred to the next segment. Eventually, the analyte exits the column, describing the simulated elution profile. From this simulated profile the overall desorption rate may be calculated. This simulated rate will be referred to as the "apparent" Peak Decay rate. Similarly, the k_{-3} rate used with the simulation is defined as the "true" Peak Decay rate. If the assumptions of the PD model have been met and the adsorptive processes minimized, the "apparent" PD rate should equal the "true" PD rate. Using this simulation, various flow rates and inhibitor concentrations have been studied, and their effect on the "apparent" PD rate described.

The computer simulation is designed to use reduced parameters of capacity factor (k') and column residence time (t_m) to represent the inhibitor concentration and the flow rate, respectively. The relationship between inhibitor concentration and k' is presented in Eq. 3,

$$k' = \frac{m_L}{V_m} \left(\frac{K_3}{1 + K_2[I]} \right) \qquad (3)$$

where m_L and V_m represent the total number of ligand sites and the column void volume. The residence time may be calculated from the column volume, the volumetric flow rate and the porosity of the support. For high performance supports a porosity of 0.8 is typical

(9). Similarly, the "apparent" PD rate is normalized by division by the "true" PD rate. This value is referred to as the "normalized slope" and is unity when the "apparent" PD rate and the "true" PD rate are equal. Using these techniques, the effect of various inhibitor concentrations and flow rates on the simulated "apparent" PD rate have been studied.

The k_{-1}/k_{-3} rate ratio can affect the accuracy of the "apparent" PD rate. The relationship of normalized PD rate with the rate ratio at different inhibitor concentrations is depicted in Figure 4 (8). Some important considerations for the application of the PD model are illustrated by Figure 4. The most obvious characteristic is the failure of the PD model to accurately estimate the PD rate at rate ratios between 0.1 and 10. This is a fundamental limitation of the biphasic process. For a given affinity system and, hence, rate ratio, the use of lower k' (higher concentration of I) results in a better approximation of the "true" PD kinetic rate. Similarly, more accurate apparent PD kinetic rates at a given k' strength are obtained with higher rate ratios. This is because at high rate ratios there is faster diffusion of the free A from the pore relative to the dissociation of analyte from the ligand, thus allowing for accurate determination of kinetic rates by Equation 1b.

In contrast to the above cases, the "apparent" PD rate is not accurate at rate ratios less than one. This, too, is a fundamental limitation of the PD model. When the rate ratio is less than one, the diffusion step is slower than the dissociation step and free A

Figure 4. Plot of the normalized slope from computer simulations of peak decay profiles as a function of k_{-1}/k_{-3} and k' for the conditions $V_p = V_e$ and $\dot{L}_{col} = 0$. Taken from Ref. 8

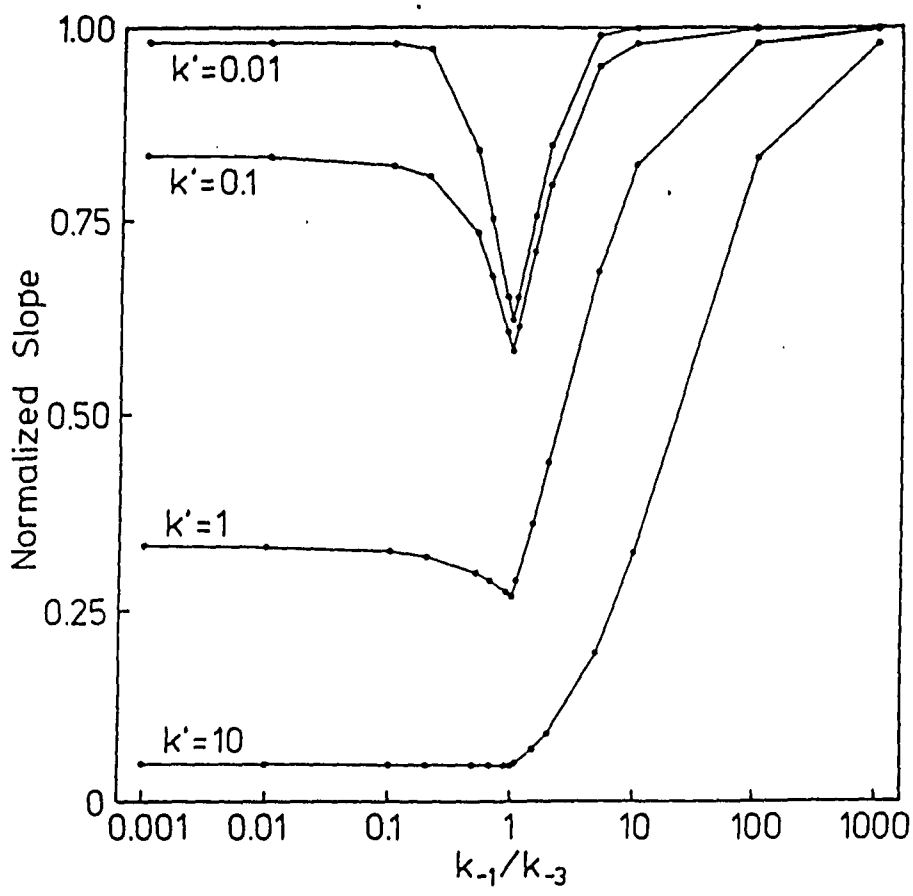
1.00
0.75
0.50
0.25
0
Normalized Slope
k'=0.01
k'=0.1
k'=1
k'=10
0.001
0.01
0.1
1
10
100
1000
k-1/k-3

accumulates in the pore. Unfortunately, at low inhibitor concentration (high k') free A may readsorb onto available ligand sites requiring strong inhibitors to sufficiently reduct k'.

As with the inhibitor concentation study, the effect of flow rate on the "apparent" PD kinetic rate may be studied with the simulation. If too slow a flow rate is used, analyte diffusing from the pore accumulates in the moving mobile phase and elute as a band rather than being swept from the column immediately after exiting from the pore. Thus, the possibility of reentry of desorbed A into a second pore is introduced. A graphical representation of the effect of flow rate on the "apparent" PD rate is presented in Figure 5. The unitless value(s) of (tm x k) is the independent variable and the normalized slope is the dependent variable. The relationships of these parameters at k' values equal to 0.01, 0.1, 1.0 and 10 are presented. These various inhibitor concentrations are included so that the eluent strength selected previously from Figure 4 may be included in the estimation of residence time. Figure 5 is a grouping of several of these types of plots. The columns represent kinetic rate ratios of 0.1, 1 and 10. The rows represent V_p/V_e ratios of 1.0 and 0.1, descriptive of totally porous silica and nonporous chromatographic supports, respectively. These combinations of support and affinity systems were chosen to represent a wide range of possibilities for the design of the experiment (8).

The inclusion of the eluent strength lines restates many of the conclusions from Figure 4. When $k_{-1} = k_{-3}$, the model will fail to

Figure 5. Plots of normalized slope from computer simulations of peak decay profiles as a function of void time multiplied by the smaller of k_{-1} or k_{-3}. $V_p/V_e = 1$ in (a-c), $V_p/V_e = 0.1$ in (d-f). In (a) and (d), $k_{-1}/k_{-3} = 0.1$. In (b) and (e), $k_{-1} = k_{-3}$. In (c) and (f), $k_{-1}/k_{-3} = 10$. $k' = 0.001$ (□), 0.01 (●), 0.1 (■), 1.0 (◆), and 10.0 (○). Taken from Ref. 8

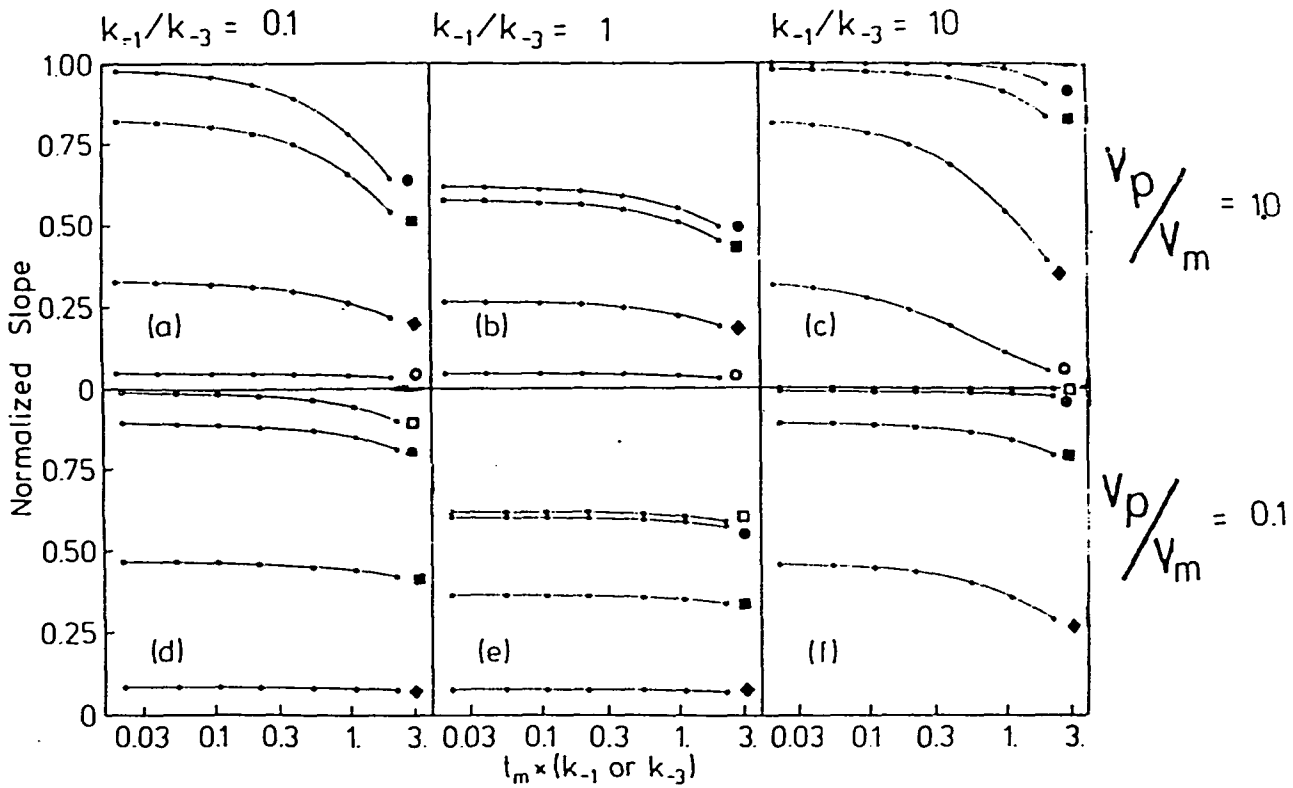
k_{-1}/k_{-3} = 0.1
k_{-1}/k_{-3} = 1
k_{-1}/k_{-3} = 10
Normalized Slope
1.00
0.75
0.50
0.25
0
(a)
(b)
(c)
(d)
(e)
(f)
v_p/v_m = 1.0
v_p/v_m = 0.1
0.03 0.1 0.3 1. 3.
$t_m \times (k_{-1}$ or $k_{-3})$

accurately describe the "true" PD rate no matter how high the inhibitor concentration. As in Figure 4, inhibitor concentration has a dramatic effect on the "apparent" PD rate at a rate ratio of 10. If higher rate ratio plots were available, the k' lines would begin to converge at a normalized slope close to unity as was seen in Figure 4. The shape of the eluent strength curve is also important. For each of the plots at low values of (t_m x k_{-3}), the "apparent" rate is independent of residence time. As t_m is increased, this independence is lost as the plot "breaks" to lower values of normalized slope. The t_m corresponding to this break increases with increasing inhibitor concentration, indicating that some readsorption is occurring at low inhibitor concentrations. The results of Figure 4 indicate that this should be less significant at higher values of the rate ratio. Generally, the "apparent" PD rate is independent of t_m or flow rate at (t_m x k) values smaller than 0.3. From these simulations, then, the inhibitor concentration and flow rate necessary to produce the PD effect for a given support may be estimated.

In summary, not all affinity systems will be amenable to the PD model. The fundamental limitation is the rate ratio, which must be greater than 10. Additionally, the analyte-saturated ligand site must be sufficiently stable to allow washing of nonsorbed analyte from the column without elution of the sorbed analyte. This restriction would eliminate many low affinity ($K_{eq} < 10^4$) systems. The lack of a suitable competitive inhibitor would seem to be such a fundamental limitation. For such systems the use of a "tagged" analyte to saturate the

system and untagged analyte as competitive inhibitor has been proposed (8). In addition to these fundamental limitations, more practical problems may arise. For the particular affinity support and column dimensions the required inhibitor concentration and flow rate may be impractical. This can be addressed by using a support of appropriate ligand density, as calculated from Eq. 3 and Figure 4, in a column of proper size for the practical flow rates, as estimated from Figure 5. This process could result in low ligand loadings and small column dimensions. Under these conditions, only a very small amount of analyte would be retained and detection could become a problem. This illustrates the careful balance of these parameters that must be struck to produce an accurate estimate of the PD rate.

MATERIALS AND METHODS

Reagents

Fluorescein isothiocyanate (FITC), adsorbed on celite, immunoglobulin G (rabbit), Protein A, DEAE cellulose, and Sephadex G-20 were obtained from Sigma (St. Louis, MO). LiChrospher SI4000 was from Merck (Rahway, NJ). All other chemicals were of reagent grade and were obtained from Fisher Scientific (Pittsburgh, PA).

Instrumental

The chromatographic system was a quaternary system and is illustrated schematically in Figure 6. The solvent delivery system was a Beckman (Berkeley, CA) 334 ternary system with the injection valve modified to act as a switching valve between the ternary system and a Rainin (Woburn, MA) Rabbit pump equipped with a 5 mL/min pump head. This switching valve configuration minimized the precolumn system volume so that changes in the eluent strength applied to the column were very sharp. This produced an essentially plug flow profile of eluent strength as the column was eluted. Additionally, this allowed for rapid changes in eluent strength and minimal pressure pulsation upon switching of the valve.

The columns used for this work were of a type described previously and prepared from 4.6 mm ID stainless steel tubing blanks (13,26). For biospecific elution and pH elution, 25 mm and 6.4 mm length columns were used. For this work the eluent reservoirs as well as the columns

Figure 6. Illustration of the quaternary HPLC system used in the peak decay studies. The injection valve has been modified to act as a switching valve to select from either the Rainin pump or the Beckman system. Strong eluent was delivered by the Rainin pump. The syringe eluent reservoirs allowed the use of small volumes of the IgG eluent in a convenient manner. When saturating the column with FITC-IgG, the waste was recycled

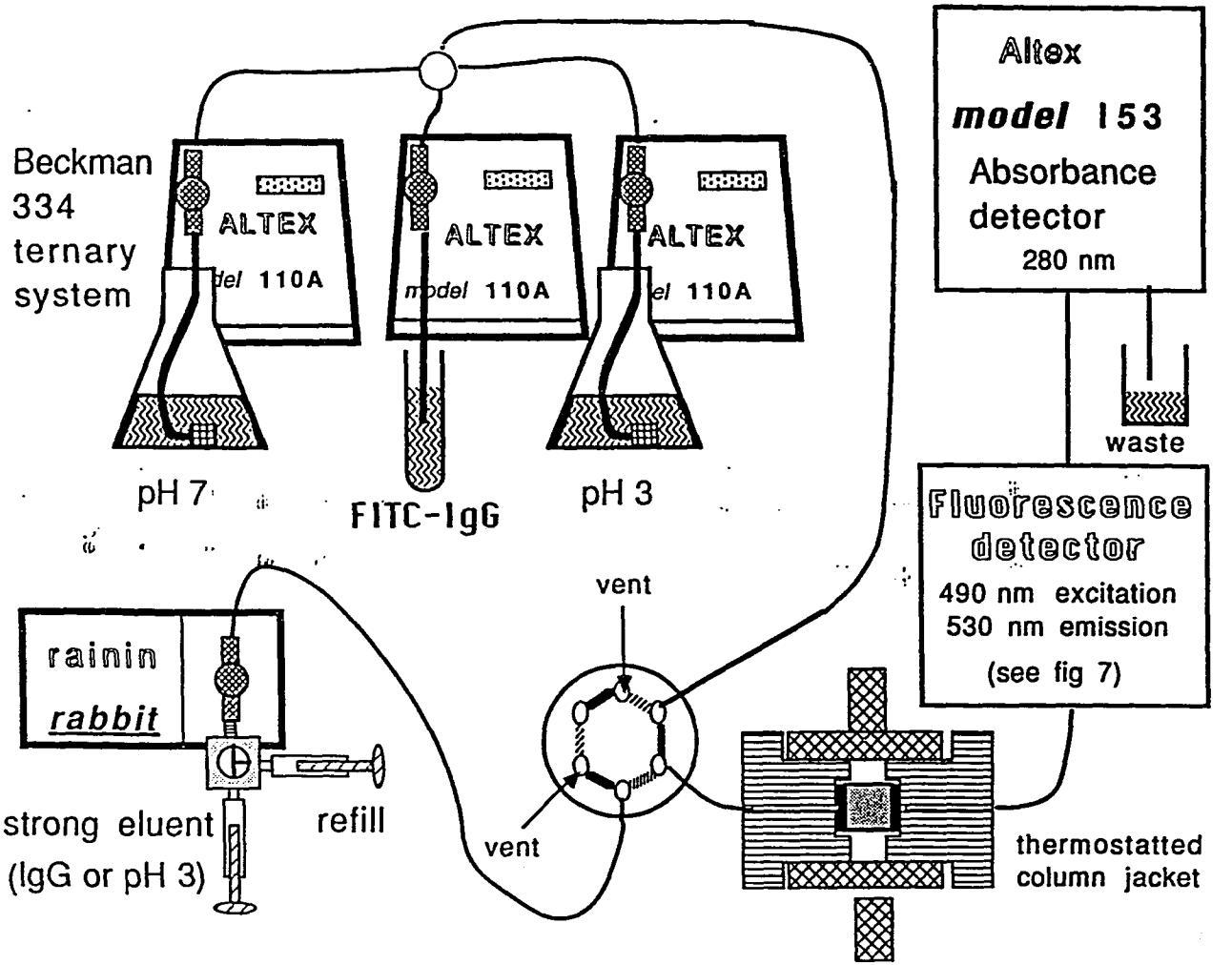
Beckman
334
ternary
system
ALTEX
model 110A
ALTEX
model 110A
ALTEX
model 110A
pH 7
FITC-IgG
pH 3
Altex
model 153
Absorbance
detector
280 nm
waste
Fluorescence
detector
490 nm excitation
530 nm emission
(see fig 7)
rainin
rabbit
strong eluent
(IgG or pH 3)
refill
vent
vent
thermostatted
column jacket

were thermostatted at 25°C, except during the temperature studies where the appropriate temperatures were used. To preserve bioactivity the columns were stored at 4°C while not in use.

To monitor column effluent, a two detector system was used. The initial detector was a fluorometer optimized for detection of the fluorescein label and used to obtain the PD profile as the FTIC labeled analyte IgG eluted from the column. To monitor total IgG (both the analyte and inhibitor IgG), an Altex model 153 absorbance detector with a biochemical flow cell and 280 nm filter was used. This detector was connected in series after the fluorometer and was used to monitor the completion of the various saturation and washing procedures. Outputs from both the fluorescence and absorbance detectors were recorded simultaneously. The fluorescence signal was also monitored with a computer data acquisition system (9,13) and stored on disc for later analysis of the PD elution profile.

The fluorometer detector was an extensively modified SPEX 1670 minimate double monochromator fluorometer equipped with a DPC-2 photon counting device (SPEX, Metuchen, NJ). The final configuration of this instrument is presented in Figure 7. The fluorescence flow cell used with this instrument was adapted from a Kratos (Ramsey, NJ) model FS 980 filter fluorometer and mounted into the SPEX sample compartment. The final focusing lens served to focus the excitation beam into the flow cell for maximal intensity and minimal illuminated volume. Although the cell had a total volume of 35 μL, only the initial seven μL of this volume were illuminated, minimizing the contribution of the

Figure 7. Illustration of the fluorometric detector modified in our lab and used in obtaining the PD profiles

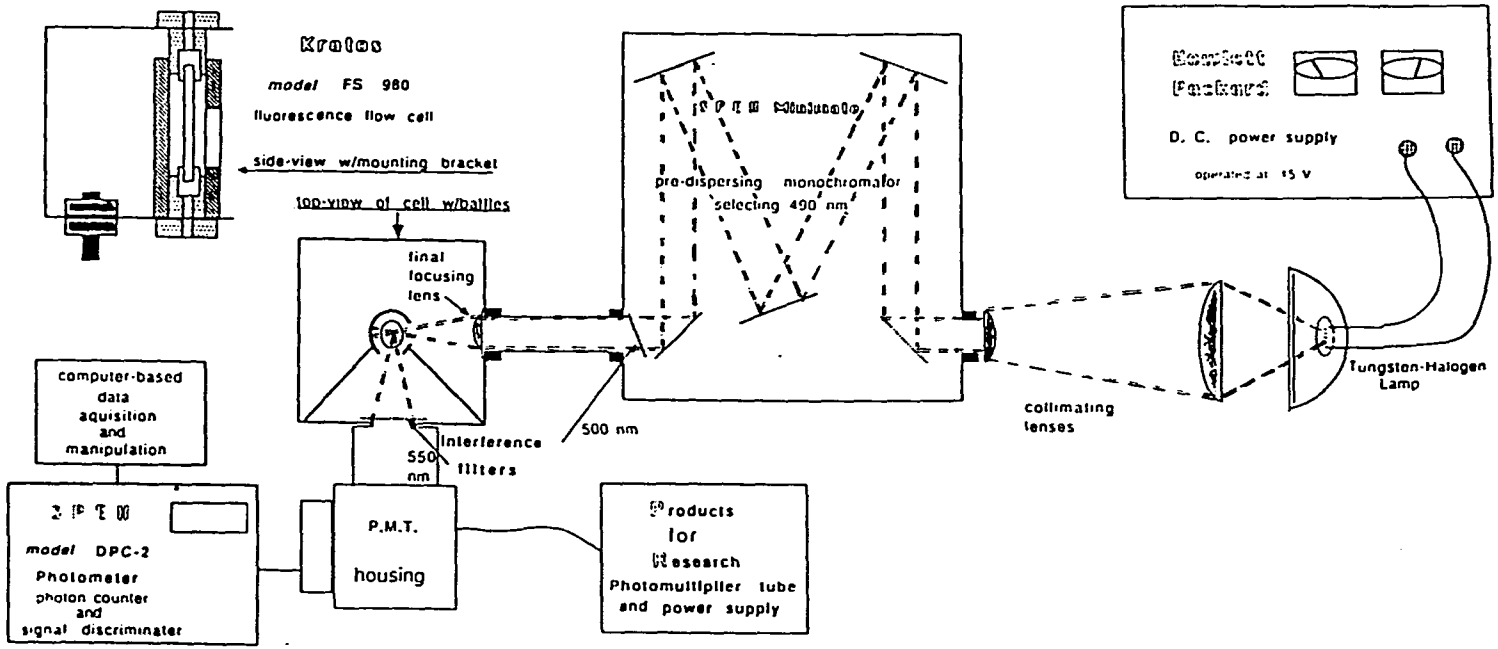
Kratos
model FS 980
fluorescence flow cell
side-view w/mounting bracket
top-view of cell w/baffles
final focusing lens
pre-dispersing monochromator selecting 490 nm
D. C. power supply
Tungsten-Halogen Lamp
collimating lenses
500 nm
Interference filters
550 nm
computer-based data aquisition and manipulation
model DPC-2
Photometer
photon counter and signal discriminater
P.M.T. housing
Products for Research
Photomultiplier tube and power supply

large cell volume to the broadening of the detected band.

Several modifications were made to maximize the throughput of both the exciting and emitted radiation. On the excitation side, the slits were removed from the monochromator. This component thus served only to predisperse the radiation prior to the final excitation wavelength selection by an interference filter. The emission monochromator was removed and the PMT housing was directly attached to the sample compartment. A second interference filter was used to discriminate the fluorescent radiation from the background. Both of these interference filters were from Melles Griot (Rochester, NY) and were bandpass filters with a 10 nm FWHM. These filters were angle tunable over a 50 nm range about the central wavelength of 500 nm and 550 nm for the excitation and emission filters, respectively. Prior to the final mounting these filters were tuned by maximizing the detector response to a solution of fluorescein in the flow cell. The voltage of the PMT was adjusted to 650 V for the optimal S/N ratio using this instrument configuration. A tungsten halogen lamp model 7001 from General Electric (Albany, NY) was operated with a Hewlett Packard power supply at 15 V with 63 watts DC drawn by the lamp. This was found to be sufficiently intense and stable.

The analytical capability of this instrument was determined with fluorescein dye solutions. The column was removed and the dye sample was applied to the system as a flow injection bolus. Alternatively, the dye solution was continuously applied to the detector in a static technique. The limit of detection at a signal-to-noise ratio of three

was found to be 2 x 10^{-12} moles injected and 1 x 10^{-8} M for the flow injection and static techniques, respectively. Using the static technique with the seven μL cell, an absolute detection limit of 7 x 10^{-14} moles of dye was indicated. This compares favorably with the determination of fluorescein by laser fluorescence methods (27).

Procedures

Preparation of Material

Diol-bonded LiChrospher SI4000 was prepared and Protein A was immobilized by the Schiff's base method as previously described (9). The yield of total immobilized Protein A was determined with the BCA protein assay from Pierce (Rockford, IL) (28). The yield of active Protein A was determined by breakthrough analysis (9). This assay technique measures only the active Protein A ligands. The columns were packed by the upflow slurry technique at 3000 psi with a Micromeritics slurry packer (Norcross, PA) and a Haskell pneumatic pump (Deerfield, IL).

FITC-labeled IgG was prepared by the method of The and Feltkamp (29,30,31) using FITC adsorbed on celite as the dye source. The celite was removed by filtration and the FITC-IgG conjugate purified on the preparative chromatographic system built in our lab and described in Figure 8. This system was composed of a Sephadex size exclusion column, with an exclusion limit of 20 kD, coupled with a DEAE cellulose anion exchange column. Initially, the excess label was separated from the IgG reagent on the Sephadex column with the green band of labeled

Figure 8. Low performance preparative dual column chromatograph. This system was used to prepared FITC-IgG. Additionally, it may be used for other such applications. Either column may be used individually or in the switching mode as described. The entire system was assembled from simple components and built entirely in our lab. This chromatograph proved to be very durable in over one year of use

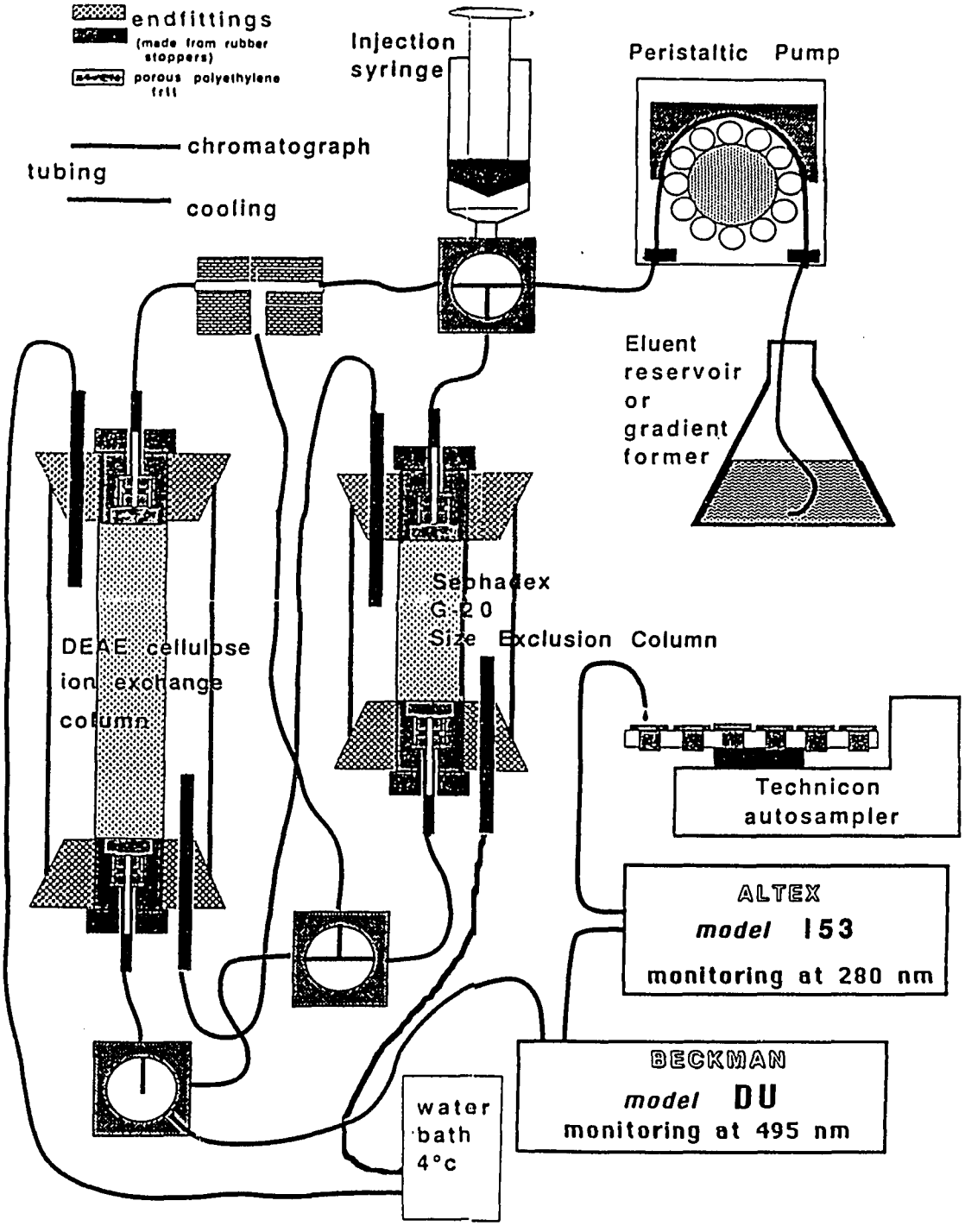
endfittings
(made from rubber stoppers)
porous polyethylene frit
chromatograph tubing
cooling
Injection syringe
Peristaltic Pump
Eluent reservoir or gradient former
Sephadex G-20 Size Exclusion Column
DEAE cellulose ion exchange column
Technicon autosampler
ALTEX
model 153
monitoring at 280 nm
BECKMAN
model DU
monitoring at 495 nm
water bath 4°c

IgG eluting at the void volume. Unreacted IgG was removed from the conjugated IgG with a salt gradient on the DEAE column. Column effluent was monitored for the fluorescein label at 495 nm with a Beckman DU spectrophotometer equipped with a flow cell and for total IgG protein with the Altex detector.

The eluent was collected in five mL fractions and the degree of FITC labeling of the IgG molecule determined using the nomogram of The and Feltkamp (30). Typical values of the degree of labeling were 1.8 to 4.5 dye labels per IgG molecule. The fractions containing the IgG conjugate were pooled to obtain a sufficient quantity for experimental use. After pooling, typical values obtained for IgG concentration were 0.3 mg IgG/mL, with a degree of labeling of three.

Acquisition of the Peak Decay Elution Profile

The experimental generation of a PD profile with the chromatographic system described in Figure 6 was a multistep procedure. Initially, the immobilized Protein A was saturated with FITC-IgG by recycling this solution through the column. A small amount of the FITC-IgG reagent was required to saturate the column; this allowed the FITC-IgG solution to be reused several times. The excess FITC-IgG was then washed from the column with pH 7 buffer until a stable fluorescent baseline was obtained. The flow rate of this washing buffer and that of the strong eluent from the Rainin pump, either an IgG solution or pH 3 buffer, were then matched. The switching valve was activated and the strong eluent applied to the column. This initiated the computer data

acquisition and the output of the DPC-2 was monitored for approximately two half-lives of the decay process. While the PD profile was eluting from the column, the ternary chromatograph eluent was changed from the pH 7 buffer to the pH 3 buffer. After the PD profile had been collected, the valve was returned to the initial position and all of the retained IgG was flushed from the Protein A column. When the baseline stabilized, the ternary system was returned to the pH 7 buffer and the Protein A column re-equilibrated. During this re-equilibration, the Rainin pump was restarted and, when completed, the valve again actuated so that the strong eluent once again saturated the column. At this point a sufficient amount of data was collected to describe the strong eluent baseline and data collection stopped. Finally, the column was flushed with the pH 3 buffer to again remove all of the IgG from the column. The column was then re-equilibrated with pH 7 buffer and the system was again ready to repeat the sequence. An example of the data obtained with the procedure is presented in Figure 9A.

Calculation of the Peak Decay Rate

The data acquisition procedure described above was designed to simplify the extraction of the PD kinetic rate from the experimental PD profile. The simplest treatment of first order kinetic data for extracting the rate is to linearize the data with a logarithmic transformation (11). The kinetic rate is then expressed as the slope of this line. This treatment assumes that the reaction is complete or

that an infinite reaction time has passed and that the analytical signal at this time is measurable. Accurate linearization of the data requires that the infinite time signal be included in the mathematical treatment of the kinetic data.

Often, the analytical signal at infinite time cannot be approximated experimentally. Data treatments have been described to allow for the estimation of kinetic rates where the sampling time is limited. Examples of such treatments are the Guggenheim (32) and Kezdy-Swinbourne (33,34) methods. Unfortunately, these data techniques amplify noise in the data. This limits the applicability of these methods when the detection limit of the instrument is approached by the experiment (35).

In addition to the mathematical treatments of the data, the PD chromatographic model allows for the experimental simulation of the infinite time signal. The initial step in the data reduction for the experimental approximation is the determination of the infinite time baseline value. Using Figure 9a as an example, this would be the region from 902 to 1068 sec obtained when the IgG solution was reapplied to the column after the initial flushing. The baseline signal was averaged over this region. The exponential decay region was then selected as 72 to 308 sec and the baseline value subtracted from this decay region to correct for the infinite time instrument component of the signal. These corrected data were then linearized by log transformation, as demonstrated in Figure 9b. The linear portion of this plot was then selected as 84 to 248 sec and the best fit line

calculated with the linear least-squares technique. The slope of this line is taken as the best estimate of the apparent PD rate.

After using each of the techniques, it was decided that the experimental infinite time approximation and linearization of the data was the most reproducible of the data reduction methods used. All of the data presented have been obtained using this method.

RESULTS AND DISCUSSION

Characterization of the Affinity Support

The properties of the affinity support are important for the design of the actual experiment. The coverage of Protein A ligand was selected to be 0.5 mg Protein A/g silica. This coverage was chosen because a capacity factor of 1.15 could be predicted for a 0.5 mg/mL IgG inhibitor solution and thus minimize consumption of the inhibitor reagent. The support actually prepared for this work had a total Protein A coverage of 0.61 mg protein/g silica. Using a breakthrough assay technique (9), an active ligand density of 2.9×10^{-6} mole protein A/L was found. This represents an activity of 1.5 mg IgG/mg Protein A or about a 20% retention of activity by the immobilized ligand. When compared with similar preparations of immobilized Protein A (9), this represents a typical retention of activity. This support was calculated to produce a k' of 0.94 with an IgG inhibitor solution of 0.5 mg/mL. When this material was packed in the 4.2 mm x 25 mm column, a total column loading of 2×10^{9} moles of IgG could be expected to be retained by the column.

Determination of Chromatographic Parameters

Biospecific Elution

The experimental determination of the residence time and inhibitor concentrations required to produce the PD effect was required. It was necessary to fix either the t_m or inhibitor concentration at a value sufficient to produce the PD effect and vary the other parameter over the region where the PD assumptions become valid. This "break" region where the PD rate becomes independent of the experimental parameter demonstrates that the assumptions have been met. As the affinity support was well defined experimentally, it was decided to initially estimate the necessary inhibitor concentration and then to experimentally determine the residence time required to produce the PD effect.

The estimation of the experimental parameters with the computer simulations was complicated by the varying kinetic and thermodynamic data available for the Protein A-IgG system. The initial step in this process was the estimation of the k_{-1}/k_{-3} rate ratio. The diffusion kinetic rate k_{-1} was calculated by substituting values of 4.7×10^{-7} cm^2/sec and 0.1 for the diffusion coefficient and tortuosity, respectively, into Eq. 2. A k_{-1} value of 2.4 sec^{-1} resulted. Values of k_{-3} for both the primary and secondary adsorptions can be determined from independent work. Under low IgG conditions the k_{-3} was estimated to be 2.3×10^{-5} sec^{-1} and with high IgG concentrations the k_{-3} was estimated as 5.5×10^{-4} sec^{-1} as described by Mayhre (6) and O'Keefe (5), respectively.

Alternatively, k_{-3} may be estimated with k_3 and affinity constant (K_3) considerations. The association rate of the Protein A IgG complex (k_3) has been estimated as 2.4×10^5 M^{-1} sec^{-1} using split peak affinity chromatography with immobilized Protein A (9). Using these data, Protein A IgG complex dissociation rates (k_{-3}) were estimated for the primary and secondary adsorptions as 6.1×10^{-4} sec^{-1} and 3.75×10^{-2} sec^{-1}, respectively.

Each of these dissociation (k_{-3}) rates and conditions under which they were generated results in a unique set of parameters required to produce the PD effect. These are summarized in Table I. The estimation of inhibitor concentration was done with Figure 4. The most rigorous inhibitor concentration requirement was $k' = 1$ with a normalized slope of 0.9. This should be capable of demonstrating the PD effect for each of the possible experimental models presented in Table I.

The estimation of the flow rate required to produce the PD effect is shown with Figure 5. This estimation is complicated because the appropriate subplot must be determined. For the high performance support used in this work, V_p was equal to V_e. Unfortunately, this series of plots does not extend to the 10,000 range estimated for the Protein A IgG rate ratio. Extrapolation of the trends in Figures 4 and 5 would produce a plot similar in form to Figure 5c with the $k' = 1$ line shifted to approximately the position of the $k' = 0.1$ line and the $k' = 0.01$ line for rate ratios of 100 and 1000, respectively. Using this approach, it was estimated that values of $t_m \times k_{-3} < 0.3$, corresponding to residence times of < 480 sec, would be appropriate to

produce the PD effect with the primary adsorption. Similar treatment for the secondary adsorption indicates that a maximum residence time of eight seconds would be required, as shown in Table I.

The initial set of experimental studies involved the determination of the flow rates required to meet the assumptions of the PD model. For this work the long column was used with flow rates from 0.05 to 0.75 mL/min and an inhibitor concentration of 0.6 mg IgG/mL, corresponding to column residence times of 278 to 18.5 sec and a k' of 0.8, respectively.

An example of the data obtained with the biospecific elution is presented in Figure 9. The various regions of the data collection process are noted. The linearized form of the data from which the "apparent" PD rate was determined is also presented.

The results of this study are presented in Figure 10 where the measured PD rate is plotted against the flow rate. The measured PD rate decreased with flow rates below 0.5 mL/min and was independent of flow rate above this value. The plateauing at a flow rate above 0.5 mL/min indicates that column residence times smaller than 27.5 sec were required to meet the PD model assumptions. This value is intermediate with respect to the column residence time of 480 sec and 8 sec predicted for the primary and secondary adsorptions, respectively. This discrepancy arises from an error in the estimation of the actual k_{-3} rate. The best estimate of the k_{-3} rate for primary adsorption was 6×10^{-4} sec^{-1}, while the experimentally measured values presented in Figure 10 are closer to 8×10^{-3} sec^{-1}. Using this experimental k_{-3} rate, a rate ratio of 300 was calculated. If the experimental rate

Figure 9. Example chromatogram of biospecific elution of analyte IgG with inhibitor IgG. An eluent flow rate of 0.6 mL/min and an IgG inhibitor concentration of 0.6 mg IgG/mL were used. The peak decay region was selected as 72-308 sec and logarithmically transformed as shown in B). The region from 84-248 sec was selected as the best linear portion and the k_{-3} calculated as 0.0068 sec^{-1} with a regression coefficient of 0.96

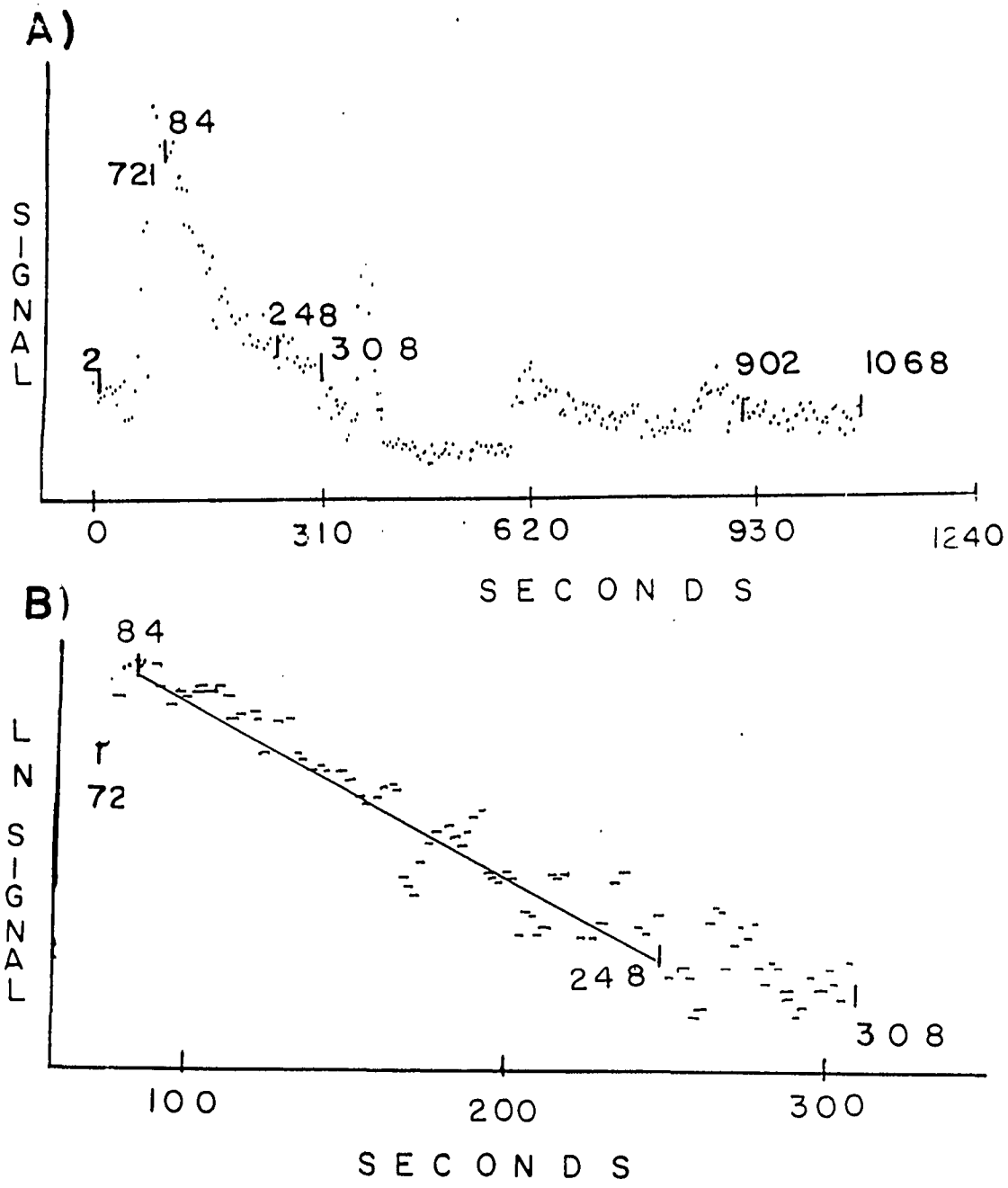
A)
84
721
248
308
2
902
1068
SIGNAL
0
310
620
930
1240
SECONDS
B)
84
72
LN SIGNAL
248
308
100
200
300
SECONDS

Figure 10. Plot of the experimental PD rate versus eluted flow rate used in obtaining the PD profile. All data were taken at 25°C with the 25 mm column and an inhibitor concentration of 0.6 mg IgG/mL. Error bars are ± one standard deviation

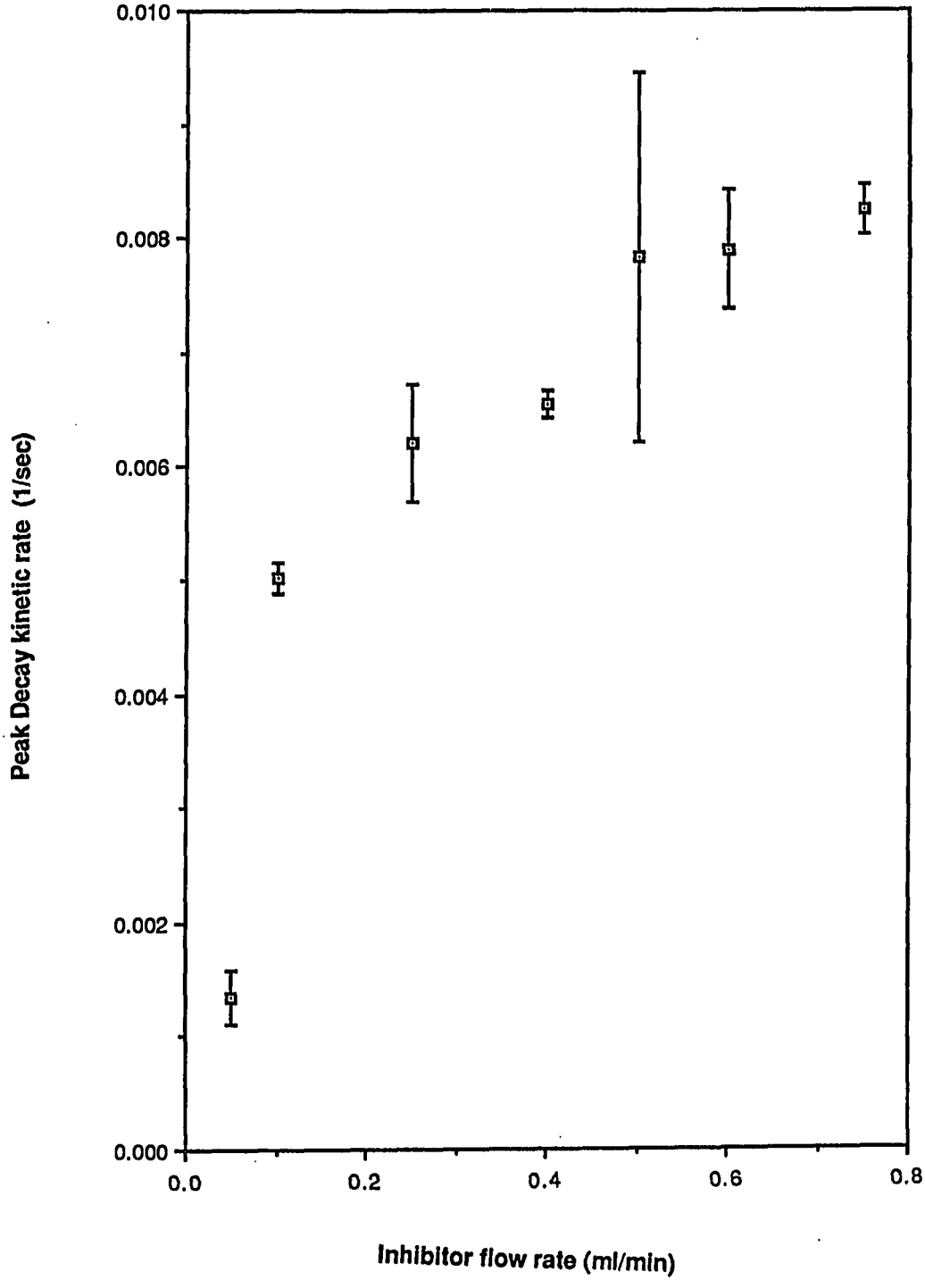
0.010
0.008
0.006
0.004
0.002
0.000
0.0
0.2
0.4
0.6
0.8
Peak Decay kinetic rate (1/sec)
Inhibitor flow rate (ml/min)

constant were used to estimate the residence time, assuming the same k' approximation as above, a residence time of 37.5 sec is predicted by Figure 5. This value is close to the experimental value of 27.5 sec and demonstrates the ability of the computer simulation to approximate the residence time requirements. The original error was in the estimation of the k_{-3} rate and affirms our assumption regarding rate ratio and k' conditions used in interpreting Figure 5c. This also illustrates the importance of the estimation of the kinetic rate in the prediction of the experimental parameters needed to produce the PD effect. The initial region of the decay was used to calculate the PD kinetic rate. At later times curvature was observed in the linearized plot and is indicative of heterogeneities in the desorptive sites (8).

Upon completion of the flow rate study it is necessary to determine the validity of the inhibitor concentration used in this study. The internal consistency must be verified by comparing the inhibitor concentration used for the flow rate study with the plateau values obtained with the inhibitor concentration study. If the initial inhibitor concentration was found to be out of the plateau region, it would be necessary to repeat the flow rate study at a higher inhibitor concentration. For this work IgG concentrations between 0.05 and 1.0 mg/mL corresponding to k' values of 9.2 to 0.47 were studied at a flow rate of 0.6 mL/min (t_m = 23 sec). The apparent PD rates were determined and are plotted versus IgG concentration in Figure 11.

The break region is shown in Figure 11 to be about 0.5 mg/ml (k' = 0.94), with measured PD rates being independent of inhibitor

Figure 11. Plot of the experimental Peak Decay kinetic rate versus the inhibitor concentration used in obtaining the rate. All data were taken at 25°C with the 25 mm column and a flow rate of 0.6 mL/min. Error bars are ± one standard deviation

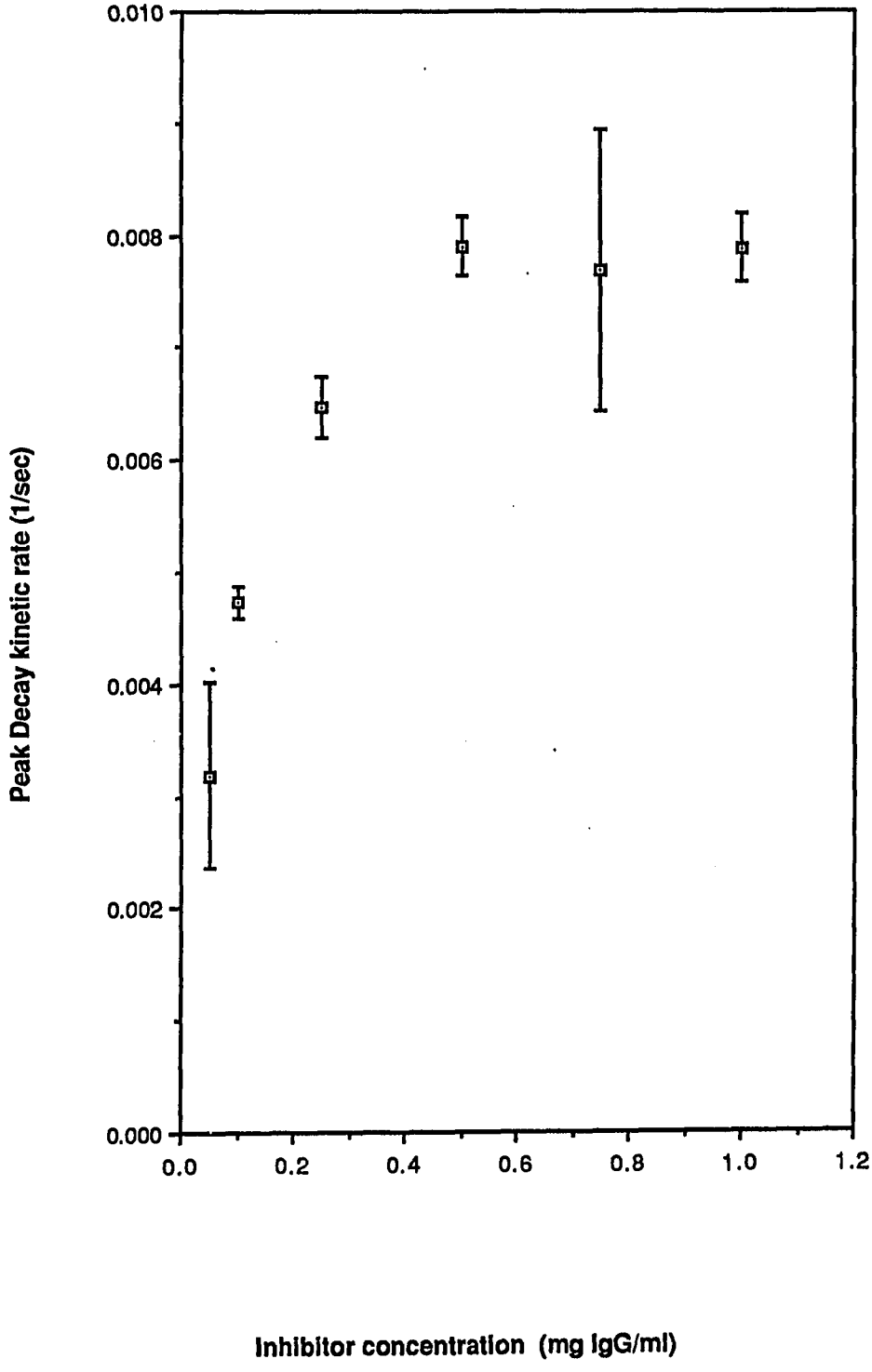
0.010
0.008
0.006
0.004
0.002
0.000
0.0
0.2
0.4
0.6
0.8
1.0
1.2
Peak Decay kinetic rate (1/sec)
Inhibitor concentration (mg IgG/ml)

concentration above this value and decreasing at our inhibitor concentration. The kinetic rate measured in the plateau region was 8.2 x 10^{-3} sec^{-1}, which is consistent with the flow rate study. The IgG inhibitor concentration of 0.6 mg/mL predicted with the simulations and used in the flow rate study was thus found to be sufficient to meet the PD assumptions. Thus, the experiments were found to be internally consistent.

The k_{-3} value of 0.008 sec^{-1} was faster than both the primary adsorption (k_{-3}) calculated rate of 6 x 10^{-4} sec^{-1} and the experimental k_{-3} rate of 5.5 x 10^{-4} sec^{-1} (5). This discrepancy in the experimental k_{-3} values may be an artifact of the experimental design. This latter high IgG work was performed in free solution and the effect of diffusion was not controlled.

Biospecific elution may also be studied with electrophoretic desorption where once the analyte has dissociated, the electric field moves the analyte through the support (36). The dissociation of the Protein A IgG affinity complex has also been studied with electrophoretic desorption of IgG from the support by Haff (37). A k_{-3} rate of 9.11 x 10^{-5} sec^{-1} was estimated from this work. Unfortunately, this work was performed with no IgG inhibitor and is thus indicative of the primary adsorption. Haff's desorption rate is, however, in good agreement with the k_{-3} value of 2.3 x 10^{-5} sec^{-1} obtained by Mayhre and Kronvall (6). Consideration of these results indicates that the secondary adsorption (high IgG) has a faster k_{-3} rate than the primary adsorption by about one order of magnitude. The selection of the

initial decay region further emphasizes this faster secondary k_{-3} value as any slower heterogeneous sites are expected to affect the latter regions of PD profile (8). This further corroborates the presence of two cooperative adsorption sites for IgG on Protein A as has been previously reported (20).

Nonspecific Elution

The concentration of urea and ammonium thiocyanate has been shown by Chervenka (38) and Eveleigh and Levy (39) to directly affect biocomplex dissociation kinetic rates. The pH of the eluent has also been shown to affect the dissociation of the IgG-Protein A complex with the selective elution of the human IgG subclasses on immobilized Protein A columns (40,41). These studies demonstrate the importance of quantitative study of denaturing dissociation processes.

Rather than determining the effect of strong eluent pH on the dissociation rate, the step change of eluent pH from seven to three was selected for the denaturing elution studies. Once this elution scheme was selected, the column residence time could be estimated with Figure 5c by assuming a k' of 0.01 for the strong eluent. This permits t_m x k_{-3} values as large as 1 to be valid for the estimation of the PD kinetic rates. A value of 2.4 sec^{-1} was chosen for the k_{-3} dissociation rate. This is the fastest process that can be determined by the PD method with diffusion as the limiting case, and faster flow rates would be futile. With these assumptions, a residence time of 0.42 sec was calculated for pH elution. To achieve this, small columns and rapid flow rates were required.

Similar flow rate experiments were thus undertaken for the estimation of the pH elution PD kinetic rate. Rather than the rigorous estimation of column dimensions, the smallest available column was used for this study. This column permitted a maximum of cross-sectional area with a minimum of column length, producing the lowest backpressure at a given flow rate. With this design it was possible to simply increase the flow rate until the plateau region was observed.

The kinetic rate of the pH dissociation technique was much faster than the biospecific dissociation kinetic rate. The pH elution profile decayed to the baseline or the infinite time approximation in less than one min. This eliminated the need to experimentally simulate the infinite time situation. Data collection was stopped after the baseline had stabilized, simplifying both data collection and evaluation. An example of the data obtained with the nonspecific elution technique is presented in Figure 12 along with the linearized form from which the apparent kinetic rate was determined.

The effect of flow rate on the measured peak decay rate with nonspecific elution was determined. The plot of flow rate versus the "apparent" kinetic rate is presented in Figure 13 and demonstrates the plateau effect at high flow rates. The kinetic rate obtained for this region was 1.2 sec^{-1}, or approximately a hundredfold increase in the apparent PD kinetic rate with pH elution. As expected, the plateau effect occurred at much higher flow rates than observed with the biospecific elution. Flow rates above 4.0 mL/min or, for the column used, residence times below 0.89 sec were required to demonstrate the

Figure 12. Example chromatograms of pH elution of analyte IgG from the 6.25 mm column. For this study an eluent flow rate of 2.0 mL/min was used. The baseline region was taken as 29.1-33.0 sec and the peak decay region was selected as 19.5-26.8 sec and logarithmically transformed. The best fit linear region of 21.0-24.2 sec was chosen and the slope determined. A k_{-3} rate of 0.54 sec_{-1} was calculated from a line with a regression coefficient of 0.99

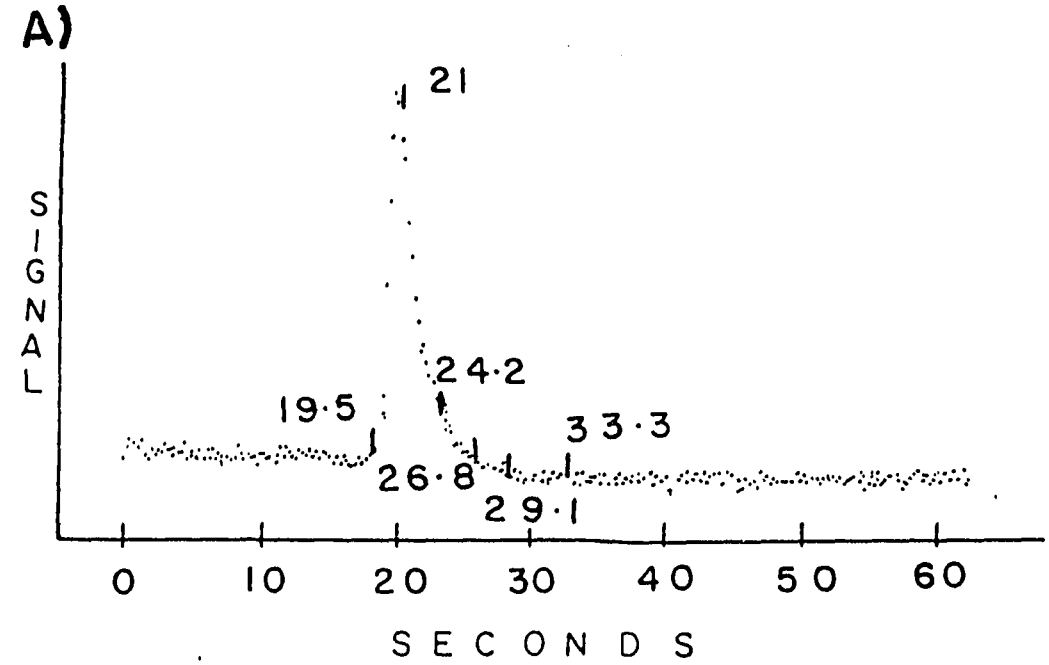
A)
SIGNAL
21
24·2
19·5
33·3
26·8
29·1
0
10
20
30
40
50
60
SECONDS

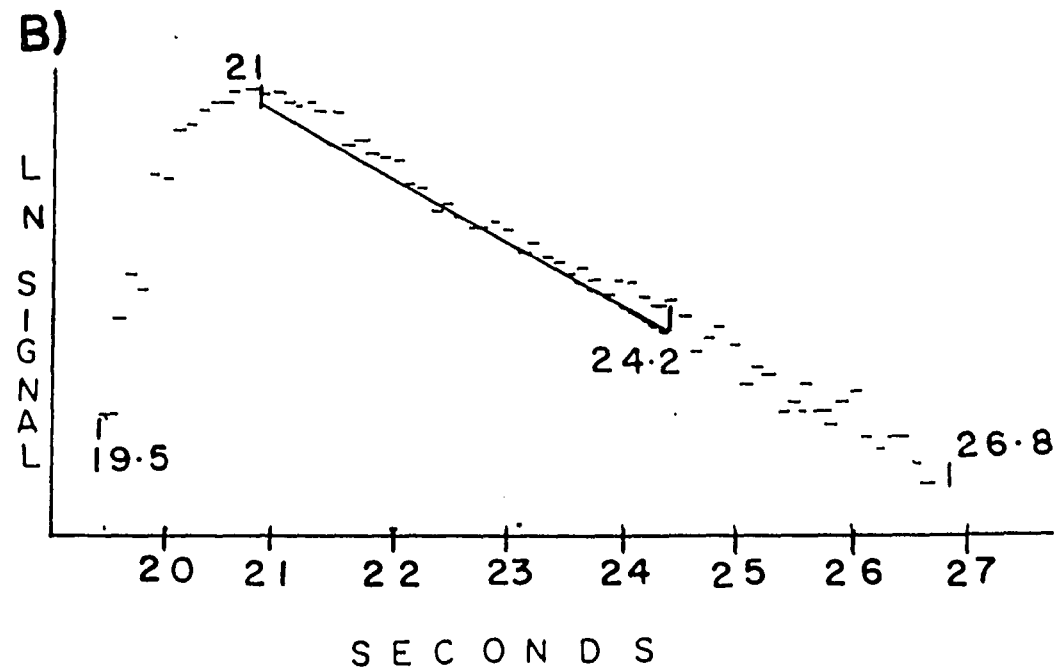
B)
LN SIGNAL
21
24·2
19·5
26·8
20
21
22
23
24
25
26
27
SECONDS

Figure 13. Plot of the Peak Decay kinetic rate (k_{-3}) for pH elution versus the flow rate used in the experiment. The independent plateau region was demonstrated at flow rates above 4.0 mL/min. Error bars are ± one standard deviation

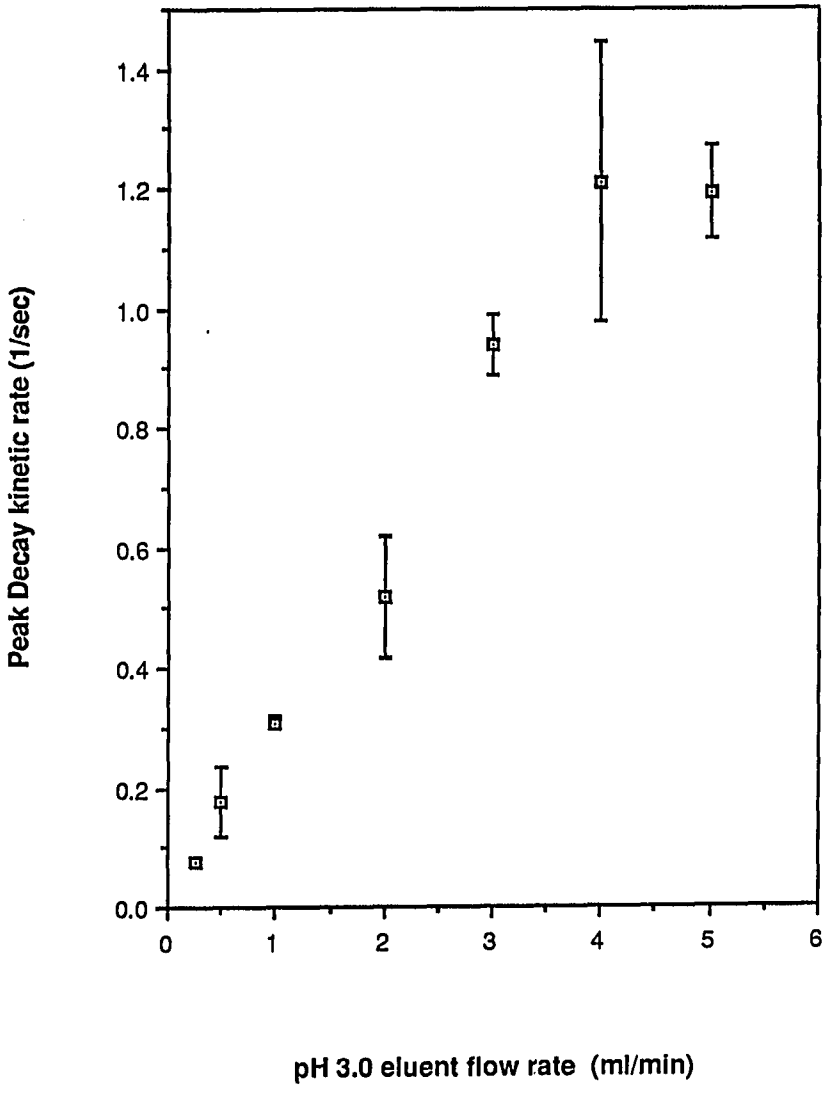
Peak Decay kinetic rate (1/sec)
1.4
1.2
1.0
0.8
0.6
0.4
0.2
0.0
0
1
2
3
4
5
6
pH 3.0 eluent flow rate (ml/min)

PD effect with pH elution. The computer simulation had indicated a residence time of 0.42 sec, which is in reasonable agreement with the experimental data.

Unfortunately, this work demonstrates one of the shortfalls of the PD model. As illustrated in Figure 4, the PD model fails to accurately estimate either k_{-3} or k_{-1} if $0.1 < k_{-1}/k_{-3} < 10$. The k_{-1} value has been calculated to be 2.4 sec^{-1} and, with substitution of the experimentally determined k_{-3}, a rate ratio of 1.9 can be estimated. This was only a rough estimate of the rate ratio, as 2.4 was only an estimate of k_{-1}.

It is possible to infer that the denaturation rate constant was not significantly different from the diffusion-limited rate constant. Another possibility is that the nonspecific elution actually is diffusion-limited, with a k_{-1} rate of 1.2 sec^{-1}, and the estimated diffusion rate constant (k_{-1}) was a poor estimate with much faster denaturation/dissociation kinetics. The data obtained with these techniques are not capable of differentiating these cases.

The kinetic rate studies presented above indicate significant differences between the biospecific elution and nonspecific elution techniques. These results are not surprising in that these elution schemes proceed along fundamentally different mechanisms. With the biospecific elution schemes the tertiary and quaternary structures are preserved and dissociation of the biocomplex occurs through interactions of the native molecule. The various nonspecific elution schemes operate under fundamentally different mechanisms at the

molecular level. Reagents such as urea and guanidinium HCl break the hydrogen bonds responsible for complex formation so that denaturation induces the dissociation (12). Chaotropic salts affect the water structure, although they do not denature the affinity complex. Rather, these elution techniques undergo native dissociation whereupon the chaotropic salts eliminate the reformation processes. This unique property is caused by the tight association of the biocomplex which precludes the reagent from reaching the binding site until native dissociation occurs (12). Other examples of denaturing elution techniques are extremes of pH which affect the protonation of the protein and, thus, the hydrogen bonds forming the complex; the addition of organic solvent such as ethylene glycol to affect the hydrophobic interactions; and the use of anionic salts such as citrate affect salt bridge formation (21). These examples demonstrate the differences in the denaturing desorption techniques and the importance of the selection of desorption method in the design of the experiment. Kinetic analysis of the desorption phenomenon is required to delineate the mechanism of the dissociation.

An example of this type of study was illustrated with the pH elution of IgG. Rather than focusing on the dissociation or diffusion limitation of IgG desorption with low pH elution, the relative magnitude of the native and denatured dissociation rates is important. These values indicate that the pH elution is similar to the H bond breaking dissociation rather than the chaotropic dissociation of IgG. Had the opposite been true the denaturing dissociation rate would have

been several orders of magnitude slower and similar to the biospecific elution PD rate.

Determination of Activation Parameters

A classical technique for comparing various kinetic processes is the comparison of the activation parameters of the processes. The estimation of these parameters involves the determination of kinetic rates over a range of temperatures and calculation of the enthalpy (ΔH^*) and entropy (ΔS^*) of activation by various plotting techniques (11). The PD rate constant for the Protein A-IgG complex was estimated over a temperature range of 5-25°C. Other experimental parameters were used as determined above for the biospecific and pH elution techniques. The "apparent" PD kinetic rate was determined in triplicate for each of the temperatures studied.

The kinetic data obtained at the various temperatures are plotted as ln (k_{-3}) versus 1/T(°K) and are presented in Figures 14 and 15 for the biospecific and pH elution, respectively. From these plots, the ΔH^* and ΔS^* parameters were calculated to be 14 ± 6 Kcal/mol and -38 ± 21 cal/mol °K for biospecific elution, and 4.6 ± .3 Kcal/mol and -16 ± 1 cal/mol °K for pH elution. Comparison of these values indicates that the biospecific elution process has larger energy requirements.

Of more significance than the magnitude of the quantitative results was the qualitative shape of the activation energy plots. The pH elution plot appears linear over the temperature range studied,

Figure 14. Arrhenius activation energy plot for biospecific elution. All chromatograms were obtained at a flow rate of 0.6 mL/min and a concentration of 0.6 mg IgG/mL. Error bars are ± one standard deviation

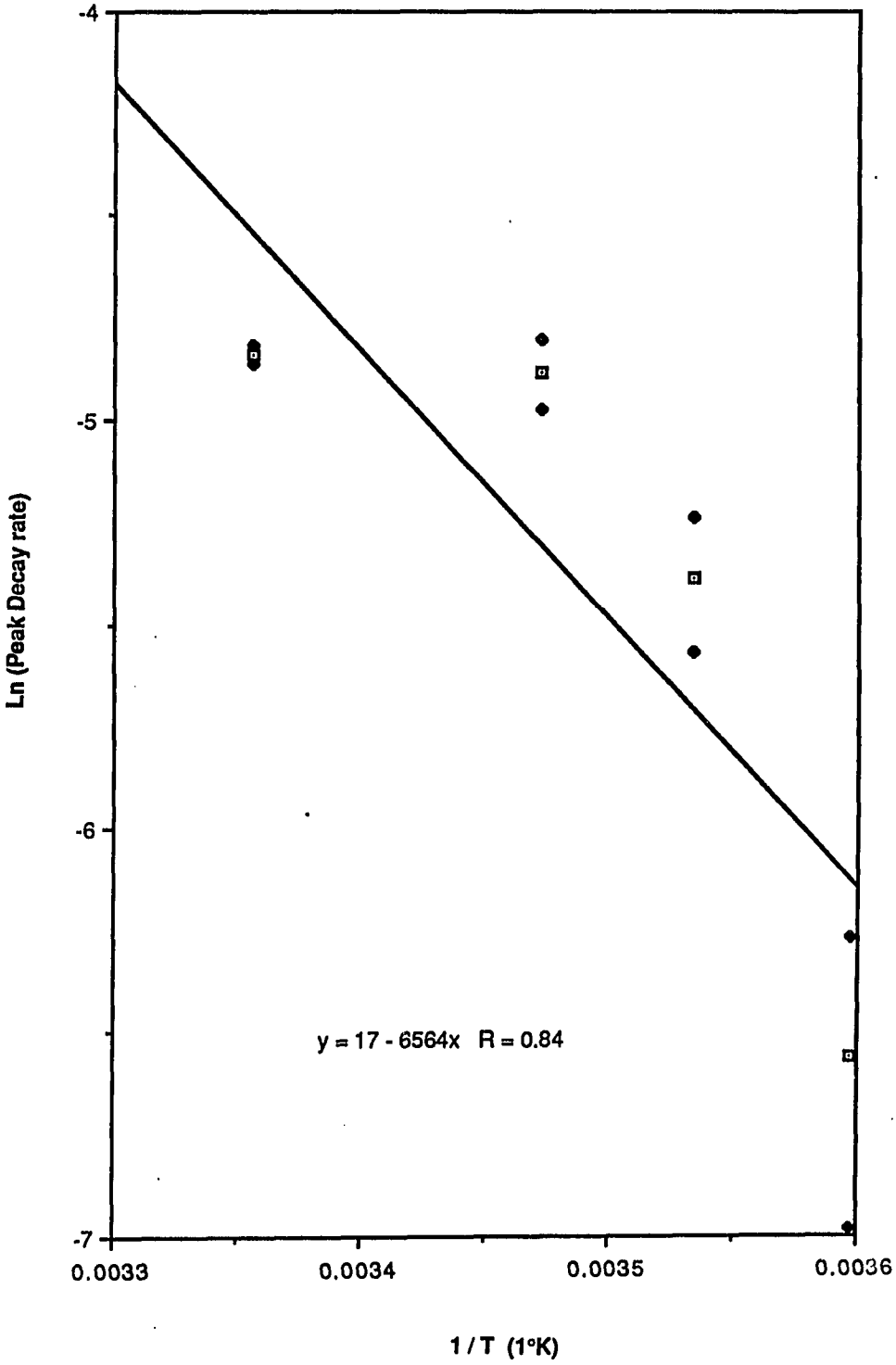
-4
-5
-6
-7
Ln (Peak Decay rate)
y = 17 - 6564x R = 0.84
0.0033
0.0034
0.0035
0.0036
1 / T (1°K)

Figure 15. Arrhenius activation energy plot for pH denaturing elution. All chromatograms were obtained at a flow rate 5.0 mL/min. Error bars are ± one standard deviation

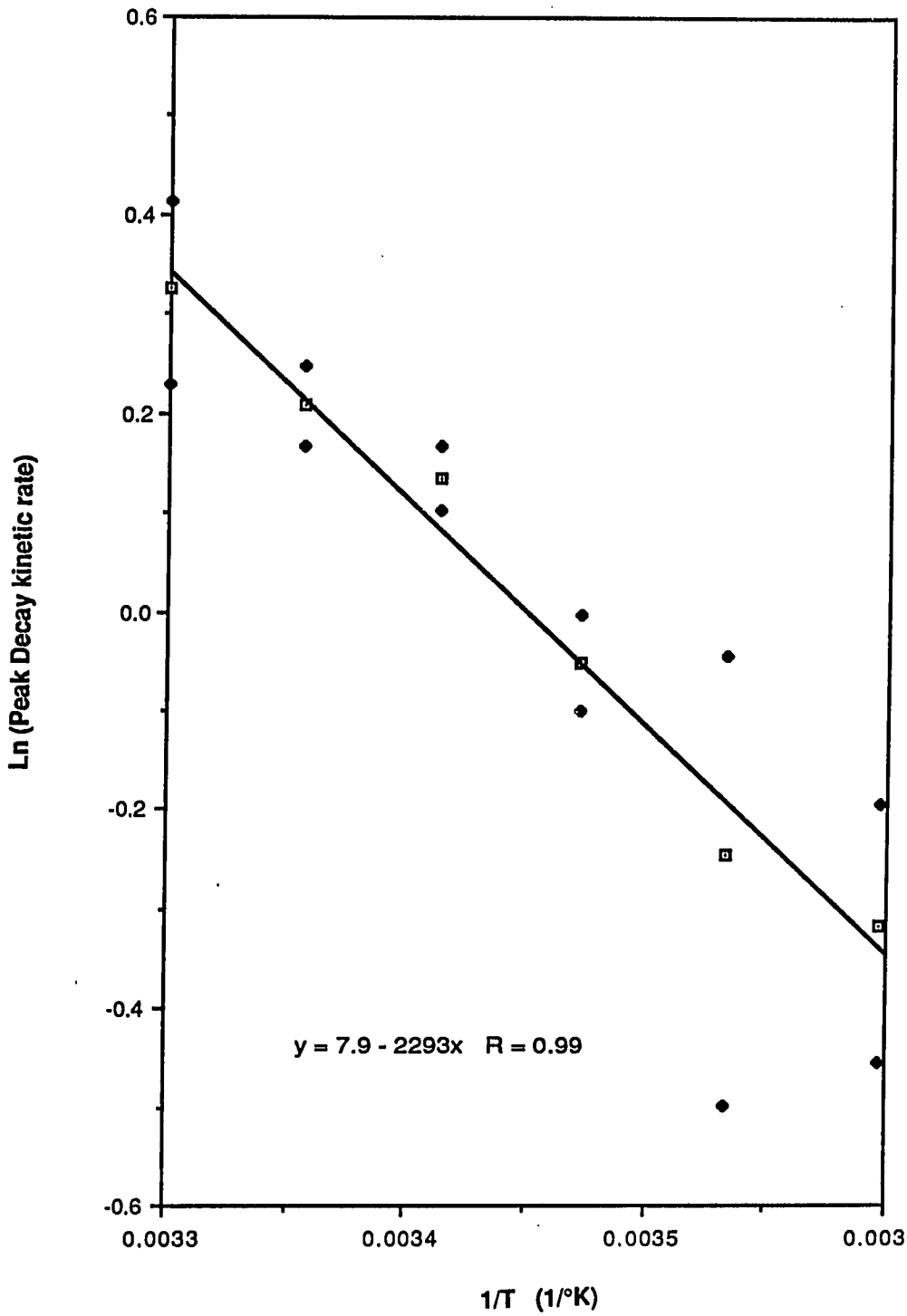
0.6
0.4
0.2
0.0
-0.2
-0.4
-0.6
0.0033
0.0034
0.0035
0.0036
Ln (Peak Decay kinetic rate)
1/T (1/°K)
y = 7.9 - 2293x R = 0.99

while the biospecific elution plot exhibits a downward curvature, indicative of a more complex interaction. This curvature could arise from the more complex biochemical dissociation or as a result of the experimental method.

For the initial evaluation of these data, the complex behavior of the biospecific elution was assumed to arise from the native dissociation process. From the magnitude of the dissociative (k_{-3}) and diffusive (k_{-1}) rates reported for the pH elution, it was not possible to determine whether the limiting case was diffusion- or dissociation-controlled as was previously described. The activation data, however, indicate a simple mechanism for pH elution and could simply reflect the activation parameters for a diffusion-controlled process. Biocomplex dissociation control of the pH elution process would be expected to be a complex pattern as with the biospecific elution. The absence of this complex behavior would support the diffusion control of the pH elution. Diffusion control of the IgG pH elution is also indicated by the magnitude of enthalpy value. A ΔH^* value of 4 Kcal/mol has been reported for a kinetic process under diffusion control (42) due to the effect of temperature on aqueous solvent viscosity.

Complicating this simple analysis of the activation parameters is work by O'Keefe and Bennett (5). As previously described, these workers studied the dissociation of the Protein A IgG complex with high IgG inhibitor concentrations. In addition to the determination of the dissociation rates, the effect of temperature on these rates was also

studied. These data permit the calculation of the dissociation activation parameter under conditions similar to the biospecific elution experiments. The activated complex plot of their work was linear from 4-37°C with a correlation coefficient of 0.95. Values of $\Delta H^* = 8.95$ Kcal/mol and $\Delta S^* = -39.4$ cal/mol were found. These results are well above the diffusion-limited case and demonstrate excellent linearity. These results indicate that the curvature of the PD biospecific dissociation plot of Figure 4 was a result of the experimental method and not a fundamental property of the biocomplex. Downward-curved activation energy plots are common for immobilized biochemicals (43). These curved plots are generally interpreted to imply the occurrence of a pore diffusion problem at the high end of the temperature range studied. Rather than a limitation of the PD method, this would be a problem with all porous support-immobilized biochemicals. Additionally, the immobilization processes can affect the ΔH^*, complicating the comparisons of the results (1).

It is also possible that the curvature of the activation energy plot was an artifact of the PD experimental method. The experimental process assumed that the conditions sufficient to produce the PD effect at 25°C were also sufficient to produce the effect at 5°C. This would require a similar dependence upon temperature for both the diffusion and dissociation phenomena. Both processes demonstrate approximately a doubling of rate with a 10°C temperature increase, as is typical with many reactions (11). If both rate processes were similarly affected by temperature, the PD assumptions would apply over the entire temperature

range. It would be expected that any change in the temperature dependence would be most obvious with the biospecific elution where the lower temperatures would slow the diffusion rate. This slowed diffusion would result in longer within-pore residence times for dissociated analyte IgG. This increased time would enhance the possibility of a second adsorption and require higher IgG inhibitor concentrations to meet the PD assumptions.

This proposed behavior is analogous to the failure of the PD method at rate ratios less than 1 as illustrated in Figure 4 and described earlier. When covering a range of temperatures with the PD method, it may be necessary to determine the flow rate and inhibitor concentration required to produce the PD effect over the entire range of temperatures to be studied.

CONCLUSIONS

The PD model has been theoretically described and a computer simulation of this model reviewed. A mid-affinity system, the Protein A IgG interaction, was used as a model to study the application of the PD model to the higher affinity biocomplexes. The application of the PD model to the fundamental studies of these biocomplexes has also been demonstrated.

Critical to the success of obtaining the PD effect are the experimental conditions of the analyte residence time in the column and the inhibitor concentration. The use of the computer simulations to estimate the initial experimental conditions was described and can simplify the early design of the experiments. The simulation was proven to be capable of predicting the required experimental conditions to produce the PD effect. The use of the simulations in this manner can save much experimental effort.

This work has demonstrated the need to accurately estimate the thermodynamic and kinetic data describing a system and the effect of the various situations on the predicted feasibility of the PD experiment.

As immobilized biochemicals attain wider use, their fundamental properties will become increasingly important to experimental design. In addition to kinetic rates, factors such as the activation energy parameters can be used to describe thse systems. The PD model has been shown to be suitable for determining these kinetic and thermodynamic parameters for immobilized biochemicals. Unfortunately, ambiguities in

the data limit the quantitative evaluation of the biospecific and pH elution schemes studied. However, the differences demonstrated qualitatively that the two elution schemes were fundamentally different. The PD method has been demonstrated to be appropriate for the estimation of the apparent dissociation rates as well as evaluation of the fundamental activation parameters allowing comparison of different elution techniques.

ACKNOWLEDGMENTS

The authors gratefully acknowledge the support of the National Science Foundation under Grant No. CHE-8305057.

REFERENCES

1. Guilbault, G. G. "Analytical Uses of Immobilized Enzymes"; Dekker: New York, 1984.

2. Monroe, D. Anal. Chem. 1984, 56, 921A.

3. Scouten, W. H. In "Chemical Analysis," Elving, P.J.; Winefordner, J. D.; Kolthoff, I. M., Eds.; Wiley: New York, 1982, Vol. 59.

4. Larsson, P. O.; Glad, M.; Hansson, L.; Mansson, M. O.; Ohlson, S.; Mosbach, K. Adv. Chromatogr. 1983, 21, 41.

5. O'Keefe, E.; Bennett, V. J. Biol. Chem. 1980, 355, 561.

6. Mayhre, E. B.; Kronvall, G. Molec. Immunol. 1980, 17, 1563.

7. Denizot, F. C.; Delaage, M. A. Proc. Natl. Acad. Sci. USA 1975, 72 4840.

8. Walters, R. R. In "Analytical Affinity Chromatography"; Chaiken, I. M., Ed.; CRC Uniscience: Boca Raton, FL, 1987.

9. Hage, D. S.; Walters, R. R.; Hethcote, H. H. Anal. Chem. 1986, 58, 274.

10. Anderson, D. J., Ph.D. Dissertation, Iowa State University, 1986.

11. Espenson, J. H. "Chemical Kinetics and Reaction Mechanisms"; McGraw-Hill: New York, 1981.

12. Chase, H. A. Chem. Engin. Sci. 1984, 39, 1099.

13. Moore, R. M., Ph.D. Dissertation, Iowa State University, 1987.

14. Sjodahl, J. Eur. J. Biochem. 1977, 78, 471.

15. Sjodahl, J. Eur. J. Biochem. 1977, 73, 343.

16. Goding, J. W. J. Immunol. Meth. 1978, 20, 241.

17. Langone, J. J. Adv. Immunol. 1982, 32, 157.

18. Mota, G.; Ghetie, V.; Sjoquist, J. Immunochem. 1978, 15, 639.

19. Sjoquist, J.; Meloun, B.; Hjelm, H. Eur. J. Biochem. 1972, 29, 572.

20. Lindmark, R.; Biriell, C.; Sjoquist, J. Scand. J. Immunol. 1981, 14, 409.

21. Bywater, R.; Eriksson, G. B.; Ottosson, T. J. Immunol. Meth. 1983, 64, 1.

22. Dandliker, W. B.; Levison, S. A. Immunochem. 1967, 5, 171.

23. Levison, S. A.; Dandliker, W. B. Immunochem. 1969, 6, 253.

24. Goding, J. W. J. Immunol. Meth. 1976, 13, 215.

25. Giddings, C. "Dynamics of Chromatography"; Marcel Dekker: New York, 1965.

26. Hage, D. S., Ph.D. Dissertation, Iowa State University, 1987.

27. Ishibashi, N.; Ogawa, T.; Imasaka, T.; Kunitake, M. Anal. Chem. 1979, 51, 2096.

28. Smith, P. K.; Krohn, R. I.; Hermanson, G. T.; Mallia, A. K.; Gartner, F. H.; Provenzano, M. D.; Fujimoto, E. K.; Goeke, N. M.; Olson, B. J.; Klenk, D. C. Anal. Biochem. 1985, 150, 76.

29. The, T. H.; Feltkamp, T. E. W. Immunol. 1970, 18, 865.

30. The, T. H.; Feltkamp, T. E. W. Immunol. 1970, 18, 875.

31. Rinderknecht, H. Nature 1962, 193, 167.

32. Guggenheim, E. A. Phil. Mag. 1926, 2, 538.

33. Kezdy, F. J.; Kaz, J.; Bruylants, A. Bull. Soc. Chim. Belges 1958, 67, 687.

34. Swinbourne, E. S. J. Chem. Soc. 1960, 2371.

35. Hobey, W. D.; Shen, W. H.; Gouin, D. A. American Laboratory, 1986, 18, 97.

36. Morgan, M. R. A.; George, E.; Dean, P. D. G. Anal. Biochem. 1980, 105, 1.

37. Haff, L. A. Electrophoresis 1981, 2, 287.

38. Chervenka, C. H. J. Amer. Chem. Soc. 1961, 83, 473.

39. Eveleigh, J. W.; Levy, D. E. J. Solid Phase Biochem. 1977, 2, 45.

40. Duhamel, R. C.; Schur, P. H.; Brendel, K.; Meezan, E. J. Immunol. Meth. 1979, 31, 211.

41. Martin, L. N. J. Immunol. Meth. 1982, 52, 205.

42. Levison, S. A. Biochem. Fluoresc. Concepts 1975, 1, 375.

43. Pritcher, W. H.; Havewela, N. B. In "Immobilized Enzymes, Antigens, Antibodies and Peptides. Properties and Characterization"; Weetall, H. H., Ed.; Marcel Dekker: New York, 1975, p. 116.

GENERAL SUMMARY

The work described in this thesis involves many aspects of the design and use of High Performance Affinity Chromatography. HPAC combines the speed, convenience and separation efficiency of HPLC with the selectivity of biological recognition. With affinity chromatographic separations, the ligand is immobilized and may be easily reused, unlike other bioaffinity-based analytical methods such as immunoassay (11). An additional advantage of the HPAC technique is the automation of the analysis which is possible with available autosampling and signal integration equipment. This approach could simplify many separation methods and lead to new methods for the study of biomolecular interactions (37). Both practical and theoretical aspects of HPAC were studied and the implications on the experimental design discussed.

The quantitation of IgG from human serum with HPAC was demonstrated in Section I. For this work the affinity adsorbent was Protein A from the S. aureus bacteria immobilized on diol-bonded silica using CDI. Sample preparation was negligible, with only filtration of the serum performed. Small sample volumes, usually less than 10 µL of serum, were required for the analysis. The stability of the Protein A affinity ligand was excellent, with little loss of activity after several hundred analyses over a two year period. Analysis times were quite rapid, with a complete cycle of pre-equilibration, injection, elution of nonsorbed components, low pH elution of IgG and re-

equilibration in pH 7 buffer possible in four minutes. The diol bonding minimized nonspecific adsorption of protein, and column plugging was not observed over this use.

Limitations of an affinity separation are also evident in this HPAC method for IgG. With this type of application, the affinity ligand must be very selective since the low pH buffer will elute all of the retained species as a single band. If the support retained multiple sample components, the purity of the analyte would be compromised (2). This is a problem with the use of Protein A as an affinity ligand. Protein A retains most IgG and some IgA and does not retain IgG3, IgM or some IgA. These binding anomalies ultimately limit the ability of the retained immunoglobulins to accurately profile the actual immunoglobulin concentration in serum. However, the HPAC method was shown to be of comparable accuracy to radial immunodiffusion for IgG analysis. This could result from the fortuitous correction for loss of IgG3 with the retention of some IgA.

In addition to this fundamental bioactivity limitation, the activity of the CDI immobilized Protein A ligand was low. In Sections II and III the activity of immobilized Protein A was reported as 10% and 20% for CDI and Schiff's base immobilized Protein A, respectively. Not only was the binding activity of Protein A for IgG affected by the immobilization method, the kinetics of the adsorption process have been shown to be affected as well. In a study by Hage, the adsorption kinetics of CDI-immobilized Protein A were shown to be much slower than those of the Schiff's base-immobilized Protein A using Split Peak

affinity chromatography (24). The slower IgG adsorption kinetic rate of CDI-Protein A requires longer column residence times for the IgG analyte to fully bind with the ligand. Thus, CDI-Protein A is unsuitable for very small column dimensions, as have been used with Schiff's base Protein A (33). This latter case of a kinetic limitation illustrates a specific restriction of the immobilization chemistry and column dimensions for a particular situation as opposed to the fundamental specificity limitations described above. These latter problems may be minimized by proper design of the experiment.

The immobilization of various ligands on diol-bonded high performance silica supports using the 1,1'-carbonyldiimidazole reagent was studied in Section II. This CDI immobilization chemistry was used to attach protein macromolecular ligands and glucosamine to diol-bonded silica supports. This reagent was selected because of the non-ionic and stable urethane linkage through which the ligand is held to the solid support (33,65-67).

To fully optimize the yield of immobilized ligand, both the activation of the support and the actual coupling of the ligand were shown to be important. The activation studies reported in Section II represent dramatic increases in the yield of the imidazole carbonate reactive intermediate. It was found that longer CDI activation reaction times and sonication were responsible for this increase. With these synthetic techniques it was possible to approach monolayer coverage of imidazole carbonate active intermediate sites on the diol support. The ability to control the degree of support activation was

also demonstrated with the CDI reagent. Unfortunately, proteins must be kept in aqueous solution and the imidazole carbonate active site is subject to rapid hydrolysis in aqueous solution. Previous workers had observed this hydrolysis and stopped the ligand coupling reaction after only a few hours (66,68,69). This was further studied in Section II and evidence for two populations of active sites presented. Approximately 90% of the active sites were hydrolyzed in several minutes of exposure to aqueous neutral buffers, but the remaining sites were stable for several days. Thus, the yield of CDI immobilized ligand was easily increased with longer reaction times.

Other factors important for the immobilization of proteins in high yield were determined. The pH of the ligand coupling buffer was found to be a factor in the yield of immobilized protein ligand. Neutral and slightly acidic (pH 7-4) buffers were found to be capable of immobilizing protein ligands in high yield. The maximal yield of immobilized protein was found to be at approximately the isoelectric point of the protein. However, the optimal coupling pH for maximal yield must be determined empirically for each protein ligand. Once these coupling reaction parameters were described, it was possible to reproducibly prepare immobilized protein supports. This was demonstrated specifically with BSA, where a relative standard deviation of 13% was found with repetitive immobilization experiments. Where required, very high yields of immobilized proteins are possible. As was shown in Section II with the 10% by weight coverage of IgG on diol-bonded silica.

The preparation of a highly active ligand is more important than just immobilizing a high yield of a low activity ligand. The effect of immobilization conditions on the activity of the ligand was also investigated in Section II. As the coupling solution pH was changed, the population of neutral amines capable of binding protein also changed. This effect may then affect the orientation of the immobilized protein ligand and thus the activity of the protein ligand (8). Studies were undertaken to demonstrate the effect of solution pH on the activity of the immobilized protein. The results were unpredictable, though differences were observed, illustrating the importance of optimizing the immobilization conditions for each protein ligand immobilized with a given immobilization chemistry.

Many chromatographic techniques require the preparation of suppports of a known and reproducible ligand density. Examples are ion chromatography, ion-exchange chromatography, and hydrophobic interaction chromatography. The importance of ligand density to the ion-exchange chromatographic behavior of proteins has been demonstrated by Landgrebe, Wu and Walters (70). These workers have reported the "ester-amide" synthesis technique for the preparation of supports with a reproducible and controllable degree of activation. Unfortunately, the preparation of activated supports using this chemistry is a rigorous procedure.

An interesting application of the CDI immobilization chemistry would be the preparation of supports of various ligand densities for these techniques. In Section II it was shown that the imidazole

carbonate reactive intermediate could be reproducibly prepared over a wide range of active site densities. The inability to control final ligand density with the active site coverage arose from the hydrolysis of the active site in aqueous buffers. The immobilization of the ligands used with these relatively nonspecific types of chromatography would be amenable to nonaqueous reaction conditions. The reactive site hydrolysis would then not be a factor, so that final ligand density could be controlled through the activation. Other advantages of using CDI for this type of support preparation would be the inertness, stability and ease of preparation inherent in the CDI chemistry.

In the final section, the use of HPAC methods, specifically the Peak Decay model, for the determination of fundamental biocomplex dissociation kinetics was demonstrated. The Peak Decay model and a computer-simulation of this model were described in Section III. The simulation was used to estimate the suitability of the Peak Decay method to the study of the Protein A-IgG affinity system, as well as for the estimation of the chromatographic parameters required to produce the Peak Decay effect.

In the Peak Decay model all adsorptive processes are minimized through the use of high concentrations of competitive inhibitor and rapid eluent flow rates. Once the analyte dissociates, it should elute from the column without further interactions. The validity of using the Peak Decay model to describe the dissociation of analyte from the affinity support was demonstrated both qualitatively and quantitatively in Section III. Both the shape of the actual Peak Decay elution

profile (Figure III-9) and the shape of inhibitor concentration and residence time plots (Figures III-10 and III-11) were as predicted with the computer simulation.

Using sufficient chromatographic parameters to meet the Peak Decay assumptions, an experimental Peak Decay kinetic rate (k_{-3}) of 0.008 sec^{-1} was observed. The parameters required to produce accurate desorption rate values using the Peak Decay effect for the Protein A-IgG affinity system using experimentally determined rate values were estimated with the computer-simulation and were found to be a column residence time of 37 sec and an inhibitor concentration of k' equivalent to 0.94. For the support and column chosen this represented an inhibitor concentration of 0.5 mg IgG/mL and a flow rate of 0.540 mL/min. The actual values of these parameters required to produce plateau values of the desorption rate constants from the Peak Decay effect were then experimentally determined. Values of 0.6 mL/min and 0.5 mg IgG/mL were required. Expressed as the reduced parameters, these represented a residence time of 27 sec and a k' = 0.94. This indicated that the computer simulation was appropriate for the estimation of the chromatographic parameters required to produce the Peak Decay effect. Similarly, the appropriateness of the Peak Decay model has been shown for the Con-A sugar system (64).

The study of Protein A-IgG biocomplex dissociation with the Peak Decay model demonstrates many fundamental properties of the Protein A-IgG interaction. As was described in Section III, evidence for a

negative cooperativity between the two adsorption sites has been shown (62). The results of the Peak Decay experiments clearly favor the negative cooperativity argument since the other models do not fit with the experimental results.

The magnitude of the Protein A-IgG native dissociation rate (k_{-3}) (0.008 sec^{-1}) provides insight into the biocomplex interaction. The half-life for this first-order dissociation process is 87 sec. Rather than the very stable biocomplex imagined when the affinity constant of 4×10^8 M^{-1} is considered, the Protein A-IgG interaction is a dynamic process of association and dissociation events. This relatively rapid turnover would be significant for competitive binding assay techniques. This indicates that shorter incubation times (minutes rather than hours) could be suitable for competitive binding assays, as has been observed by de Alwis and Wilson (71).

Studies of low pH nonspecific elution were also performed. A diffusion-limited dissociation rate of 1.2 sec^{-1} was found for this type of IgG elution from Protein A supports. This was much faster than the 0.008 sec^{-1} found for the native dissociation of the Protein A-IgG complex. The Peak Decay effect was also shown to be capable of determining the activation parameters for the dissociation of the affinity complex with both the naturing and denaturing elution techniques. The Peak Decay method should be useful for studying the various types of nonspecific elution for comparison and selection of the optimum elution technique for a particular affinity system. The Peak Decay method should also provide information on the fundamental

denaturation/dissociation processes as was described in Section III.

Many aspects of High Performance Affinity Chromatography have been studied. An actual application was described in Section I. This work demonstrated the advantages of HPAC for the quantitation of biological substances. The development of an affinity separation requires the immobilization of the affinity ligand. This was studied in Section II with techniques for the optimization of immobilized ligand yield and activity. Once the affinity support is prepared and packed in the column, the separation is performed. Assuming analyte retention, the method of elution is important. The eluent strength should suffice to elute the analyte yet not damage the activity of the ligand. This was addressed in Section III where methods for the optimization of the elution technique were described using the Peak Decay kinetic model.

REFERENCES

1. Hearn, M. T. W. Trends Anal. Chem. 1983, 2, 263.
2. Scouten, W. H. "Affinity Chromatography"' John Wiley and Sons: New York, 1981.
3. Karger, B. L.; Synder, L. R.; Horvath, C. "An Introduction to Separation Science"; John Wiley and Sons: New York, 1973.
4. Kopaciewicz, W.; Regnier, F. E. Anal. Biochem. 1983, 129, 472.
5. Regnier, F. E. Anal. Chem. 1983, 55, 1298A.
6. deMontigny, P. Ph.D. Dissertation, University of Kansas, 1986.
7. Kristjansson, F. K. Ph.D. Dissertation, University of Kansas, 1987.
8. Guilbault, G. G. "Analytical Uses of Immobilized Enzymes"; Marcel Dekker: New York, 1984.
9. Monroe, D. Anal. Chem. 1984, 56, 921A.
10. Sundaram, P. V. J. Solid Phase Biochem. 1976, 1, 101.
11. Walters, R. R. Trends Anal. Chem. 1983, 2, 282.
12. Emlen, U.; Burdick, G. J. Immunol. Meth. 1983, 62, 205.
13. Eveleigh, J. W.; Levy, D. E. J. Solid Phase Biochem. 1977, 2, 45.
14. Chase, H. A. Chem. Engin. Sci. 1984, 39, 1099.
15. Parikh, I.; Cuatrecasas, P. In "Immunochemistry of Proteins"; Atassi, M. Z., Ed.; Vol. 2; Plenum: New York, 1977.
16. Cuatrecasas, P.; Wilchek, M.; Anfinsen, C. B. Proc. Natl. Acad. Sci. USA 1968, 61, 636.
17. Larsson, P.-O.; Glad, M.; Hansson, L.; Mansson, M. O.; Ohlson, S.; Mosbach, K. Adv. Chromatogr. 1983, 21, 41.

18. Regnier, F. E.; Noel, R. J. Chromatogr. Sci. 1976, 14, 316.

19. Anderson, D. J. Ph.D. Dissertation, Iowa State University, 1986.

20. Muller, A. J.; Carr, P. W. J. Chromatogr. 1984, 284, 33.

21. Hearn, M. T. W.; Bethel, G. S.; Ayers, J. S.; Hancock, W. S. J. Chromatogr. 1979, 185, 463.

22. Nilsson, K.; Mosbach, K. Biochem. Biophys. Res. Commun. 1981, 102, 449.

23. Larsson, P.-O. Meth. Enzymol. 1984, 104, 212.

24. Hage, D. S.; Walters, R. R.; Hethcote, H. H. Anal. Chem. 1986, 58, 274.

25. Nilsson, R.; Mayhre, E.; Kronvall, G.; Sjogren, H. O. J. Immunol. Meth. 1983, 62, 241.

26. Denizot, F. C.; Delaage, M. A. Proc. Natl. Acad. Sci. USA 1975, 72, 4840.

27. Starkenstein, E. Biochem. Z. 1910, 24, 210.

28. Campbell, D. H.; Luescher, E.; Lerman, L. S. Proc. Natl. Acad. Sci. USA 1951, 37, 575.

29. Lerman, L. S. Proc. Natl. Acad. Sci. USA 1953, 39, 232.

30. Hjerten, S. Arch. Biochem. Biophys. 1962, 99, 446.

31. Axen, R.; Porath, J.; Ernback, S. Nature (London) 1967, 214, 1302.

32. Dean, P. D. G.; Lowe, C. R. "Affinity Chromatography"; Wiley-Interscience: New York, 1974.

33. Hage, D. S.; Walters, R. R. J. Chromatogr. 1987, 386, 37.

34. Alltech catalog #100, Alltech Associates, 2051 Waukegan Road, Deerfield, IL, 1987, p. 511.

35. Ohlson, S.; Hansson, L.; Larsson, P.-O.; Mosbach, K. FEBS Lett. 1978, 93, 5.

36. Walters, R. R. Anal. Chem. 1983, 55, 1395.

37. Walters, R. R. In "Analytical Affinity Chromatography"; Chaiken, I. M., Ed.; CRC Uniscience: Boca Raton, FL, 1987.

38. Sportsman, J. R.; Wilson, G. S. Anal. Chem. 1980, 52, 2013.

39. Phillips, T. M. Liq. Chromatogr. 1985, 3, 962.

40. Sjoquist, J.; Meloun, B.; Hjelm, H. Eur. J. Biochem. 1972, 29, 572.

41. Goding, J. W. J. Immunol. Meth. 1978, 20, 241.

42. Miller, T. J.; Stone, H. D. J. Immunol. Meth. 1978, 24, 111.

43. Hjelm, H.; Hjelm, K.; Sjoquist, J. FEBS Lett. 1972, 28, 73.

44. O'Keefe, E.; Bennett, V. J. Biol. Chem. 1980, 355, 561.

45. Mayhre, E. B.; Kronvall, G. Molec. Immunol. 1980, 17, 1563.

46. Langone, J. J. J. Immunol. Meth. 1978, 24, 269.

47. Kronvall, G.; Quie, P. G.; Williams, R. C. J. Immunol. 1970, 104, 273.

48. Bywater, R.; Eriksson, G. B.; Ottosson, T. J. Immunol. Meth. 1983, 64, 1.

49. Richman, D. D. In "New Developments in Diagnostic Virology"; Bachmann, P. A., Ed.; Springer-Verlag: Berlin, 1983, Chap. 3.

50. Cantor, C. R.; Schimmel, P. R. "Biophysical Chemistry, Part II"; Freeman: San Francisco, 1980.

51. Bjork, I. Eur. J. Biochem. 1972, 29, 579.

52. Sjodahl, J. Eur. J. Biochem. 1977, 73, 343.

53. Mota, G.; Ghetie, V.; Sjoquist, J. Immunochem. 1978. 15, 639.

54. Barret, J. T. "Textbook of Immunology"; C. V. Mosby: St. Louis, MO, 1970, Chap. 5.

55. Langone, J. J. Adv. Immunol. 1982, 32, 157.

56. Fasman, G. D., Ed. "CRC Handbook of Biochemistry and Molecular Biology"; CRC Press: Cleveland, OH, 1976, 3rd ed., Vol 2, p. 452.

57. Vidal, M. A.; Conde, F. P. J. Biochem. Biophys. Meth. 1981, 4, 155.

58. Balint, J.; Ikeda, Y.; Nagai, T.; Terman, D. S. Immunol. Comm. 1982, 11, 283.

59. Johansson, S. G. O.; Inganas, M. Immunol. Rev. 1978, 41, 248.

60. Duhamel, R. C.; Schur, P. H.; Brendel, K.; Meezan, E. J. Immunol. Meth. 1979, 31, 211.

61. Martin, L. N. J. Immunol. Meth. 1982, 52, 205.

62. Lindmark, R.; Biriell, C.; Sjoquist, J. Scand. J. Immunol. 1981, 14, 409.

63. Lindmark, R.; Thoren-Tolling, K.; Sjoquist, J. J. Immunol. Meth. 1983, 62, 1.

64. Moore, R. M. Ph.D. Dissertation, Iowa State University, 1987.

65. Hage, D. S. Ph.D. Dissertation, Iowa State University, 1987.

66. Bethell, G. S.; Ayers, J. S.; Hancock, W. S.; Hearn, M. T. W. J. Biol. Chem. 1979, 254, 2572.

67. Hearn, M. T. W.; Harris, E. L.; Bethell, G. S.; Hancock, W. S.; Ayers, J. A. J. Chromatogr. 1981, 218, 509.

68. Hearn, M. T. W.; Bethell, G. S.; Ayers, J. S.; Hancock, W. S. J. Chromatogr. 1979, 185, 463.

69. Bethell, G. S.; Ayers, J. S.; Hearn, M. T. W.; Hancock, W. S. J. Chromatogr. 1981, 219, 353.

70. Landgrebe, M. E.; Wu, D.; Walters, R. R. Anal. Chem. 1986, 58, 1607.

71. de Alwis, P.; Wilson, G. S., Department of Chemistry, University of Kansas, personal communication.

ACKNOWLEDGMENTS

The last few pages have proven the most difficult to write. This dissertation represents the completion of my formal education; a process requiring some 23 years and the efforts of an untold number of teachers. Without their much appreciated early efforts, this manuscript and all that it represents would not have been possible.

Throughout this process my parents have been an unending source of wisdom and encouragement. To them and to my great-aunt Lora Uhl, I dedicate this dissertation. This remarkable trio provided a very unique environment where both book and practical experience were easily obtained and highly valued. Finally, the most deserving of praise is Melissa, my wife, who has played the unfortunate role of "lab widow" so well for so long. For her support and encouragement, this degree is as much hers as mine.

I also wish to express a special thanks to Dr. R.R. Walters for his advice and assistance throughout my graduate career. During my sojourn at ISU under his tutelage, I matured as an individual and became well-rounded as a scientist. A special mention must be included for my cohorts in Dr. Walters' research group, Dave Anderson, Rob Moore, John Graham, Dave Hage, Danlin Wu, Larry Larew, Jackie Larew, King Chan, Mary Landgrebe and Steve Gilles. This group was the source of many valuable discussions and suggestions. Additionally, Harvey Burkholder must be included in this group for his many kind thoughts and ideas.

The experimental contributions of many must also be included. Firstly, a special thanks to King Chan for his efforts in preparing and characterizing many of the silicas described in Section II. For the work described in Section III, the Kurtz group contributed the preparative LC packings as well as the use of the power supply. The Ames Lab environmental group provided the basic fluorometer; a special thanks to Rob Moore for his help in converting this instrument.

I would like also to acknowledge the contributions of the people involved in the preparation of this manuscript. Both Dave Anderson and Dave Hage have made many excellent suggestions involving Section III and the General Introduction and Summary sections. Nancy Harmony has done an excellent job of taking my "scrolls," many of which were handwritten, and turning them into a dissertation. Her efforts are much appreciated. A special thanks must be extended to Larry and Jackie Larew for their efforts to complete my paperwork at ISU.

Finally, Dr. John Stobaugh and Dr. Ted Kuwana at the University of Kansas must be included. They have proven more than understanding of my situation. Dr. Stobaugh especially has been very cooperative during my efforts to complete this manuscript. Without his consideration, this effort would have proven very difficult.